7.º CONGRESO INTERNACIONAL DE CORROSIÓN MARINA E INCRUSTACIONES

7th INTERNATIONAL CONGRESS ON MARINE CORROSION AND FOULING

7ème CONGRES INTERNATIONAL DE LA CORROSION MARINE ET DES SALISSURES

UNIVERSIDAD POLITÉCNICA
Valencia, 7-11 Noviembre, 1988
ESPAÑA

SECCION I

Corrosión marina
Corrosion marine
Corrosion marine

The unpublished manuscripts have been reproduced as received from the authors. The Scientific Committee takes not responsability for any error or omission.

Las ponencias no han sido publicadas y están reproducidas tal y como se han recibido de sus autores. El Comité Científico no se responsabiliza de cualquier error u omisión.

SESSION I Corrosion marine
Wednesday 9th November

THE EFFECT OF HYDROSTATIC PRESSURE ON THE ELECTROCHIMICAL BEHAVIOUR OF SOME COPPER ALLOYS
A M Beccaria and D Festy

CHARACTERIZATION OF CONDENSER TUBE COATINGS BY ELECTROCHEMICAL IMPEDANCE
A Colombo, G Rocchini and P Spinelli

OXYGEN REDUCTION ON "PASSIVE" METALS AND ALLOYS IN SEAWATER. EFFECT OF BIOFILM
Ragnar Holthe, Per Olav Gartland and Einar Bardal

CORROSION OF THE BRAZED JOINT BETWEEN Cu90Ni10Fe PIPES
P Vassiliou and V J Papazoglou

CATHODIC PROTECTION OF STEEL IN PURE CULTURES OF THE MARINE BACTERIA *VIBRIO NATRIEGENS*
L Fiksdal and J Guezennec

ON THE BARNALCE-INDUCED CREVICE CORROSION PHENOMENON IN STAINLESS STEEL
M Eashwar, G Subramanian and P Chandrasekaran

THE EFFECT OF HYDROSTATIC PRESSURE ON THE ELECTROCHIMICAL BEHAVIOUR OF SOME COPPER ALLOYS

A.M BECCARIA, Istituto per la Corrosione Marina dei Metalli Genova, Italia
D.FESTY, Institut Français de Recherche pour l'Exploitation de la Mer, Brest, France

ABSTRACT

The hydrostatic pressure effects on the electrochemical behaviour of Cu-Al and Cu-Zn alloys has been studied by ICCM and IFREMER joint-working. The average corrosion rates of both alloys increases with increasing hydrostatic pressure, the anodic process of alloy 1 and both anodic and cathodic processes of alloy 2 being enhanced. The increase of the alloys corrodibility seems to be linked to the less hydrated nature of the corrosion products formed at high pressure.

RESUME

Les effets de la pression hydrostatique sur le comportement électrochimique d'alliage Cu-Al and Cu-Zn ont été étudiés conjointement par l'ICCM et l'IFREMER. La vitesse moyenne de corrosion des deux alliages augmente avec la pression hydrostatique, cela se traduisant par une modification des tracés potentio-cinétiques : augmentation des densités de courant anodique pour l'alliage 1 et anodique et cathoqique pour l'alliage 2. Ce comportement semble être lié à la nature différente des produits de corrosion (moins hydratés) formés sous hautes pressions.

RESUMEN

Los efectos de la presion hidrostatica sobre el comportamiento electroquimica de los aliages Cu-Al y Cu-Zn fueron estudiados conjutamente por el ICMM y IFREMER. La velocidad media de corrosion de los dos aliages aumenta con la presion hidrostatica, tradusiendose en una modificacion de las trazas potenciocineticas : aumento de las pensidades de corriente anodica en el aliage 1 y anodica y catodica en el aliage 2. Este comportamiento parece estar en relacion con la naturaleza diferente de los productos de la corrosion (menos hidratados) formados bajo altas presiones.

INTRODUCTION

A series of experiments carried out by Reinhart (1,2,3) in natural sea water at the surface and at depths of 760 m and 2100 m, on some copper alloys, showed that the average corrosion rate of brasses was unaffected by the depth change while the bronzes corrodibility decreases with increasing depth, their average corrosion rate at 760 m and 2100 m depth was lower than at surface, (1 mpy and 0.5 mpy respectively). This decrease was attributed to the effect of decreasing temperature and D.O (Dissolved Oxygen) content and excluded the effect of the depth (i.e. of the hydrostatic pressure).

Another experiment showed that pure copper and brass (alloy LS-59-1) exposed in the subarctic zone of the Pacific Ocean (4), (where D.O and temperature remain constant with depth), have behaviours influenced by the depth (the most dangerous depth value was 3000 to 5000 m for brass alloys and 100 m for Cu).

Therefore the change of D.O and temperature cannot explain alone the variation of corrosion rate with depth.

Laboratory experiments, carried out in vessels at pressures ranging from 1 to 300 bar, D.O and temperature values remaining constant with pressure, showed on the contrary that hydrostatic pressure influences the corrosion behaviour of various metals, as copper (5,6), nickel (7,8) and aluminium (9). This effect was attributed to the changing values of some parameters (hydratation degree, ionic radius, diffusion coefficient (10), etc.) that influences both the transport phenomena of different ions and the reaction kinetic at the solution/oxide and oxide/bare metal interfaces, to wich the nature of the passivation layer and the metal corrodibility can be correlated.

Previous work (5-9) showed that with increasing the hydrostatic pressure the average corrosion rate and the susceptibility to pitting of nickel decreases, while the corrodibility of copper and aluminium increases. The different behaviours of these elements can influence the dealloying mechanism when the pressure increases, for example by decreasing the preferential dissolution of the most active element of the alloy (Zn, Al or Ni) with respect of Cu, modifying therefore the phenomenon towards homogeneous dissolution.

In order to investigate if the different behaviour of the alloying elements (Zn and Al) affect the dealloying phenomena when hydrostatic pressure increases, some experiments were carried out at various pressures, temperature and D.O concentration remaining constant.

It is know that the dealloying is enhanced by a large grain size structure. Therefore the grain size of specimens was increased by annealing and water quenching treatment, to emphasise the dealloying and enhance the different behaviour of alloying elements.

EXPERIMENTAL

Experiments were carried out by using Cu-Al and Cu-Zn alloys with the following compositions.

Cu-Al (alloy 1) 95 Cu 5 Al

Cu-Zn (alloy 2) 88 Cu 10 Zn 2 Sn

By thermal treatments, annealing in nitrogen atmosphere (alloy 1 : 900 °C, 30 mn, alloy 2 : 600 °C, 90 mn) and water quenching, a monophasic structure (phase α) of both alloys was obtained with average grain size dimensions of 4-6 mm and 25 μm respectively. Specimens were polished with grade 600 abrasive paper and degreased with petroleum before being immersed in sea water at 8.2 pH, 15 °C and 6.5 to 7 ppm D.O. Experiments were carried out in two pressure vessels, one of 3.5 l quiescent sea water (vessel A) and the other of 125 l continously renewed sea water (vessel B), with 1 l/mn flow rate. Both above described vessels (5,6)(11) were pressurized by a hydro-pneumatic pump with sea water as working fluid. Free corrosion and electrochemical tests were performed at various pressures (1, 150, 300 bar) by using specimens of different dimensions. In the vessel A flat specimens (10x100x2 mm) were exposed for 144 h, while in vessel B specimens (100x100x10 mm) were immersed for 144 and 720 h. The volume of corrosive solution per exposed surface were higher than 200 ml/cm² and avoided any appreciable modification of the sea water composition due to the formation of soluble corrosion products.The total weigth loss of specimens corroded in renewed sea water was measured by gravimetric method followingg the ASTM G 1 specification.

The total weight loss of specimens exposed in quiescent sea water was evaluated by adding the amount of the oxidated metals both as soluble corrosion products and as corrosion products adhering to the metallic surface. The latest compounds were analysed by X-ray diffractometry (Cu α radiation) and by analytical chemical methods that permitted the selective dissolution of various oxidation compounds with suitable solvents while the metallic matrix was dissolved to a negligable extent. The specimens, washed with distilled water and treated with methanol, were immersed in aqueous glycine solution in order to remove the bivalent metals compounds and in aqueous diluted ammonia solution to dissolve cuprous and aluminium compounds following a method described in ref.12,13. Cations and anions of the dissolved corrosion products were measured by atomic-absorption flame-less spectrophotometry (Cu^{++},Cu^{+}, Al^{+++}, Zn^{++}, Sn^{++}), by atomic absorption flame atomization (Na^{+}, Ca^{++}, Mg^{++}), by ionic chromatography (Cl^{-}, $SO4^{--}$) and by gaschromatography (CO_3^{--}). All methods had an accuracy and precision better than 8 %.

The electrochemical tests were performed by using flat specimens (64 cm² of surface) in renewed sea water (vessel B) and cylindrical specimens (10 cm² about of surface) in quiescent sea water (vessel A).

Polarization potentiodynamic curves were carried out at a scanning rate of 250 mV/h on specimens exposed 2, 144 and 720 h at various (1, 150, 300 bar) pressures. The electrochemical impedance was measured by setting the electrode, exposed 2 and 144 h at 1 and 300 bar in quiescent sea water, to its free corrosion potential and perturbing it by a 10 mV a.c. potential. A wide frequency range (10 mHz - 10 KHz) was covered by using five points per decade and displaying the data as a Nyquist plots (ImZ versus -YReZ). From these measurements the corrosion current density and polarization resistance was calculated.

RESULTS AND DISCUSSIONS

Fig.2 shows that the weight loss values obtained from experiments in renewed and in quiescent sea water extrapoled to 720 h, increase with increasing hydrostatic pressure. The weigth losses on specimens exposed in renewed sea water are higher than values obtained from specimens corroded in static conditions probably because in this case a precipitation of solid corrosion products is promoted. The interface metal/solution reaches a higher concentration of oxidation products and a protective film is formed that inhibits the corrosion process. Also, the i_{corr} values, calculated from polarization potentiodynamic curves after 144 h of exposure in renewed (table 1) and in quiescent (table 2) sea water confirm the greater corrodibility of the alloys in dynamic conditions and their different behaviour with the change of hydrostatic pressure, alloy 2 being more influenced. The average corrosion rate (see weight loss values, fig.2 and i_{corr}, tables 3 and 4) of this alloy is almost doubled when the pressure reachs 300 bar, while the corrosion rate of the alloy 1 increases with about 25%.

The i_{corr} values of electrochimical tests are in good agreement with the i_{corr} values calculated from weigth losses (table 3). The electrochemical results obtained with polarised specimens can sometimes be different from those obtained in free corrosion.

Polarization curves (fig.3,4) at 1, 150, 300 bar explain the greater influence of the hydrostatic pressure on the alloy 2, that presents an acceleration of both anodic and cathodic processes. The acceleration of the anodic process of alloy 1 is the same than alloy 2 but cathodic process is almost unchanged in the potential domain of Tafel region, this for the whole pressure range. Alloy 2 shows an increase in i_d (diffusion current) between -700 to -850 mV/AgAgCl (potential domain of oxygen diffusion limit current), that does not influence the kinetic of the corrosion process. This process is under mixed control as shown by similar values of the anodic and

cathodic Tafel slopes (tables 1-3) so results are unaffected, by i_{corr} change. The anodic curve of alloy 1 at atmospheric pressure displays, in the range -200 to -100 mV/AgAgCl, a hump probably indicating the coprecipitation of Cu-Al compounds. This hump decreases with increasing hydrostatic pressure and has disappeared at 300 bar. The cathodic curve at 1 bar also shows the presence of oxidation compounds. The first peak can be due to the reduction reaction : $Cu^{+} + e^{-} \rightarrow Cu$ (14). These peaks have disappeared at 300 bar. The cathodic curve of the alloy 2 (fig.4) corroded at atmospheric pressure shows two reduction peaks, at -300 and -450 mV/AgAgCl, corresponding to the reduction of Cu^{+} and Cu^{++} compounds. With increasing the hydrostatic pressure the peak at -450 mV/AgAgCl disappears, while the peak at -300 mV/AgAgCl becomes less evident. The feature of the anodic curve reveals, that the anodic process is stimulated by the hydrostatic pressure, it increases since the Tafel slopes decrease and the anodic current shifts towards higher values. This shift can be explain by a decrease of the corrosion layer thickness with increasing pressure. Chemical analysis confirms this suggestion, as shows fig.5 that plots metal under the form of corrosion products adhering to metallic surface. The main variation of the composition of the corrosion layer formed on both alloys is the decrease of copper compounds amounts (tables 5,6) with increasing pressure. CuO, Cu_2O, CuCl, copper oxychlorides, oxycarbonates or oxysulphates are present at atmospheric pressure, while at 300 bar only hydrated copper compounds are present (table 7). The formation of hydrated copper compounds can perhaps be inhibited by the lowest hydratation degree of various ions at high pressure.

The change of the Al/Cu and Zn/Cu atomics ratio (Al/Cu from 0.20 to 0.40 and Zn/Cu from 0.06 to 0.02) in corrosion layers, with increasing pressure, do not seems to influence noticeably the passivation ability of the corrosion layer, the Al or Zn concentrations are too small. That the covering power of the passivation layer is greater at 1 bar has to be attributed to the presence of hydrated copper compounds precipated on the primary corrosion layer constitued by CuO and CuCl.

The lower corrodibility of the alloys at atmosphere pressure is confirmed by the impedance spectra carried out on specimens exposed 2 h and 144 h at various pressures in quiescent sea water. The R_{ct} values (transfer charge resistance) (fig.6,7), highest at atmospheric pressure, fairly agree with R_p values (linear polarization resistance)(table 2), as expected, because R_{ct} and R_p may be considered equivalent. Theses values determine the rate of corrosion reaction and are related to the electron transfer through the surface.

The impedance spectra in the low frequencies domain regarding the electron transfer through the passivation film due to the adsorption-desorption reactions on the film itself, clearly shows that the films formed at 1 and 300 bar are different. The impedance spectra suggests only one relaxation process for the specimens corroded at 300 bar regarding the adsorption of an intermediate species for example : $Cu(Cl)^{+} + e^{-} \rightarrow Cu(Cl)_{ads}$, wich forms copper chloride. The two semicircles in the low frequencies domain of the impedance spectra of specimens corroded at 1 bar suggest at least two relaxation processes. The first appears in the same frequencies domain as for specimens corroded at 300 bar , and is due to the adsorption-desorption reactions on oxide or chloride copper compounds,the second suggests the formation of hydrated compounds such as hydroxycarbonates, hydroxysulfates with greater passivating power (15).

The increase of the corrosion rate of the alloys with increasing pressure is probably linked to the different natures of the corrosion layers, that also seem to enhance the partial dissolution of copper, as shows fig.8 and affect the alloy dissolution mechanism. It is also linked to the kinetic of the partial dissolution of the alloying elements (Al or Zn). The pressure increase can influence the solubility rate of these elements (fig.8), that displays the amount of Al and Zn at different pressures. The increase of Al solubility with increasing pressure may be explained by the dealloying mechanism proposed by Kerr and Pryor (16) according to which the selective dissolution of the most active element (Al) takes place until this element reaches the potential value of the most passive element (Cu). The increase of Cu dissolution also enhances the Al dissolution, as confirmed by fig.8 and by dealloying of alloy 1 (fig.9). The factor Z of this figure is described by the relationship :

$$Z = (Al_{exp}/Cu_{exp}) \times (Cu_x/Al_x)$$

where : - Al_{exp},(Cu_{exp}) = total amount of oxidated Al,(Cu), experimently determined.
- Cu_x,(Al_x) = Average percentage of Cu,(Al) in the alloy.

It is less obvious to explain the behaviour of alloy 2 because a preferential copper dissolution takes place, with increasing pressure (fig.9).

The potential equilibrium values of pure elements (about -200 mV/AgAgCl for Cu and -900 mV/AgAgCl for Zn) suggest a preferential dissolution of Zn, avoided by the presence of Sn as confirmed by the dealloying factor value of Z=1, at atmospheric pressure.

With increasing pressure the amount of Cu oxidated increases while the Zn amount remains unchanged (fig.8). This can be explained only by the formation at high pressure of less hydrated corrosion products, with lattice

dimensions more similar to metallic Zn, that can therefore inhibits its dissolution.

CONCLUSIONS

- Experiments in renewed and quiescent sea water show a good agreement in spite of different exposure times (144 h and 720 h).
- The average corrosion rates of alloy 1 (Cu-Al) and alloy 2 (Cu-Zn) increase with increasing hydrostatic pressure, the anodic process of the 1 and both anodic and cathodic processes of alloy 2 being enhanced.
- The increase of alloys corrodibility seems to be linked to the less hydrated nature of corrosion products formed at high pressure.
- A dealloying factor Z has been calculated to verify a preferential dissolution phenomenon of the alloys. This factor is different to 1 when preferential dissolution of alloying elements takes place. For alloy 1, Z is >1 in the whole pressure range and increases with increasing pressure. For the alloy 2, Z is <1 at atmospheric pressure and >1 at 150 and 300 bar, thus revealing a copper preferential dissolution at high pressures.

CAPTIONS OF TABLES

1 - θ_a, β_a, i_{corr}, R_p^{-1}, R_p values from polarisation curves in quiescent sea water (144 h exposure).
2 - β_a, β_c, i_{corr}, R_p^{-1}, R_p values from polarisation curves in renewed sea water (144 h exposure).
3 - Comparison between i_{corr} values from weigth loss and polarization curves.
4 - β_a, β_c, i_{corr}, R_p^{-1}, R_p values from polarisation curves in renewed sea water (720 h exposure).
5 - Corrosion products ($\mu g.cm^{-2}$) of specimens exposed in renewed sea water (720 h exposure).
6 - Corrosion products ($\mu g.cm^{-2}$) of specimens exposed in quiescent sea water (144 h exposure).
7 - Corrosion products X ray diffractometric analysis.

CAPTIONS OF FIGURES

1 - Specimens exposure in renewed sea water apparatus.
2 - Weight losses values in renewed and quiescent sea water.
3 - Polarization curves of alloy 1 in renewed sea water at 1, 150 and 300 bar.
4 - Polarization curves of alloy 2 in renewed sea water at 1, 150 and 300 bar.
5 - Corrosion products weight and Cu amount in renewed and quiescent sea water at different pressures.
6 - Impedance spectra of alloy 1 at 1 and 300 bar.
7 - Impedance spectra of alloy 2 at 1 and 300 bar.
8 - Cu, Al and Zn oxidated amount at various pressures.
9 - Dealloying factor Z as a function of hydrostatic pressures.

REFERENCES

1 - F.M.Reinhart - Corrosion of materials hydrospace. Technical report 504-11-12-107 U.S Naval Civil Engineering. Laboratory Cal 1966 Alexandra-Virginia.
2 - F.M.Reinhart - Rep 834, U.S Naval Civil Engineering Laboratory Port Hueneme. Corrosion of metals and alloys in the deep ocean - 1976 - Alexandra-Virginia.
3 - J.J.De Luccia - Mater.Prot. 1966,6,(5),49
4 - Yu.M.Korivin - A.V.Ledenev- Yu.F.Lukashev- Zashch.Met. 1984,20,(6),919
5 - E.D.Mor - A.M.Beccaria - Br.Corros.J. 1978,13,142.
6 - E.D.Mor - A.M.Beccaria - Werst.Korros. 1979,30,551.
7 - A.M.Beccaria - G.Poggi - G.Capannelli - G.Castello - 37th Int.Congress of ISE - Vilnius 1986 USRR
8 - A.M.Beccaria - G.Poggi - Euroccor'87 - Karlsruhe April - Dechema ed. 627,1987.
9 - A.M.Beccaria - G.Poggi - British Corros.Jr. 1985,20,4,183
10 - R.A.Home - Marine Chemistry - Wiley Interscience - John Wiley e Sons - New York 1969.
11 - D.Festy -Euroccor'87 - Karlsruhe April - Dechema ed. 641,1987.
12 - A.M.Beccaria - G.Poggi - Anal letters 1985, 18(A), 2259.
13 - A.M.Beccaria - G.Poggi - Anal letters 1986, 19(A), 1205.
14 - A.M Shams El Din - F.M Abd El Wahals - Corr Sci. 1977, 11, 49.
15 - G.Bianchi - P.Longhi - Corros Sci - 1973, 13, 853.
16 - D.S. Kerr - M.J.Pryor - J. Electrochem.Soc 1980, 127, 2138.

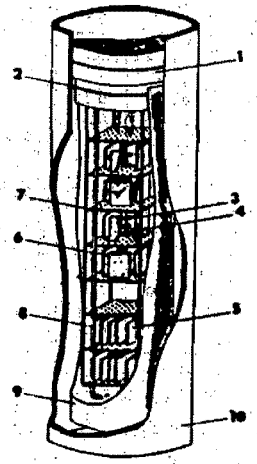

Figure 1 - Specimens exposure in renewed sea water apparatus.
1.Titanium plug
2."O" ring
3.Counter electrode
4.Reference electrode
5.Samples for weigth loss
6.Samples for polarization curves
7.Samples support
8.Sea water inlet
9.Titanium tube
10.High pressure vessel main body

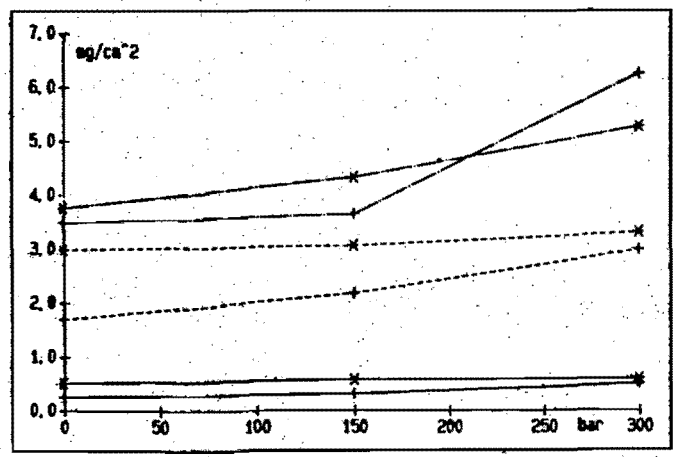

Figure 2 - Weight losses values in renewed and quiescent sea water. --*--* Alloy 1, --+--+ Alloy 2. _____ quiescent sea water, 144 h; ------ quiescent sea water; 144 h, extrapoled to 720 h; __.__. renewed sea water. 720 h.

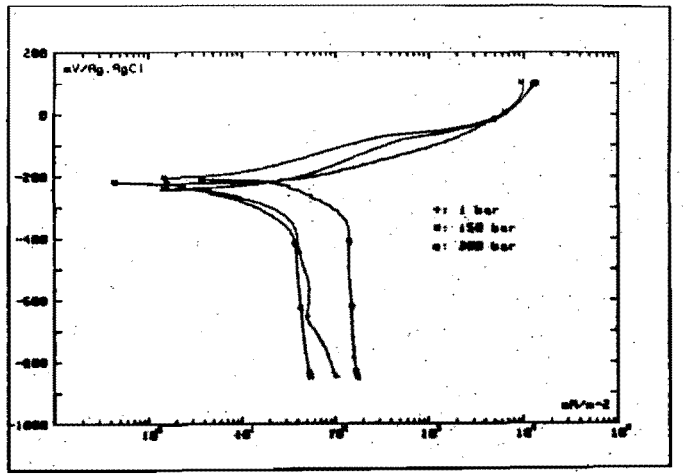

Figure 3 - Polarization curves of alloy 1 in renewed sea water at 1, 150 and 300 bar.

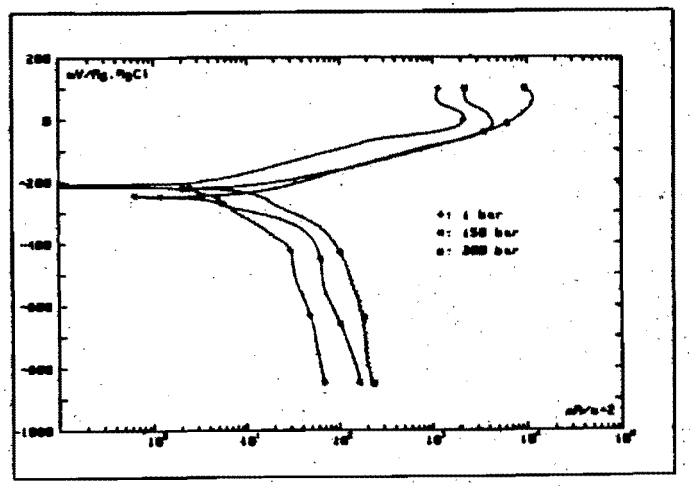

Figure 4 - Polarization curves of alloy 2 in renewed sea water at 1, 150 and 300 bar.

Alloy	P bar	βa mV/dec	βc mV/dec	icorr mA/m²	Ecorr mV	Rp-1 mA/Vm²	Rp KΩcm²
1	1	58.0	-174	15.6	-203	830	12.00
	150	27.0	-307	16.0	-89	1430	6.99
	300	22.0	-270	19.0	-100	2152	4.65
2	1	56.6	-70	9.4	-234	690	14.49
	150	56.6	-66	15.1	-230	1142	6.76
	300	25.3	-50	17.3	-225	2372	4.21

Table 1 - βa, βc, icorr, Rp-1, Rp values from polarisation curves in quiescent sea water (144 h exposure).

Alloy	P bar	βa mV/dec	βc mV/dec	icorr mA/m²	Ecorr mV	Rp-1 mA/Vm²	Rp KΩcm²
1	1	62.5	-206	19.4	-207	933	10.7
	150						
	300						
2	1	62.5	-109	17.7	-209	1027	9.7
	150						
	300						

Table 2 - βa, βc, icorr, Rp-1, Rp values from polarisation curves in renewed sea water (144 h exposure).

Alloy	P bar	icorr from polar	icorr from W.L
1	1	15.6	17.1
	150	16.0	17.8
	300	19.0	20.6
2	1	9.4	9.3
	150	15.1	11.7
	300	17.3	16.5

Table 3 - Comparison between icorr values from weigth loss and polarization curves.

Alloy	P bar	βa mV/dec	βc mV/dec	icorr mA/m²	Ecorr mV	Rp-1 mA/Vm²	Rp KΩcm²
1	1	75.0	-68	2.1	-241	133	75.2
	150	57.5	-68	2.1	-222	155	64.5
	300	52.8	-71	26.1	-214	1829	5.5
2	1	86.0	-210	3.8	-213	145	68.7
	150	40.8	-74	4.2	-250	379	26.3
	300	43.3	-32	5.9	-224	737	13.6

Table 4 - βa, βc, icorr, Rp-1, Rp values from polarisation curves in renewed sea water (720 h exposure).

Alloy	P bar	βa mV/dec	βc mV/dec	icorr mA/m²	Ecorr mV	Rp-1 mA/Vm²	Rp KΩm²
1	1	58.0	-174	15.6	-203	830	12.00
	150	27.0	-307	16.0	-89	1430	6.99
	300	22.0	-270	19.0	-100	2152	4.65
2	1	56.6	-70	9.4	-234	690	14.49
	150	56.6	-66	15.1	-230	1142	6.76
	300	25.3	-50	17.3	-225	2372	4.21

Table 1 - βa, βc, icorr, Rp-1, Rp values from polarisation curves in quiescent sea water (144 h exposure).

Alloy	P bar	βa mV/dec	βc mV/dec	icorr mA/m²	Ecorr mV	Rp-1 mA/Vm²	Rp KΩm²
1	1	62.5	-206	19.4	-207	933	1.07
	150						
	300						
2	1	62.5	-109	17.7	-209	1027	0.97
	150						
	300						

Table 2 - βa, βc, icorr, Rp-1, Rp values from polarisation curves in renewed sea water (144 h exposure).

Alloy	P bar	icorr from polar	icorr from W.L
1	1	15.6	17.1
	150	16.0	17.8
	300	19.0	20.6
2	1	9.4	9.3
	150	15.1	11.7
	300	17.3	16.5

Table 3 - Comparison between icorr values from weigth loss and polarization curves.

Alloy	P bar	βa mV/dec	βc mV/dec	icorr mA/m²	Ecorr mV	Rp-1 mA/Vm²	Rp KΩm²
1	1	75.0	-68	2.1	-241	133	7.52
	150	57.5	-68	2.1	-222	155	6.45
	300	52.8	-71	26.1	-214	1829	5.46
2	1	86.0	-210	3.8	-213	145	6.67
	150	40.8	-74	4.2	-250	379	2.63
	300	43.3	-32	5.9	-224	737	13.56

Table 4 - βa, βc, icorr, Rp-1, Rp values from polarisation curves in renewed sea water (720 h exposure).

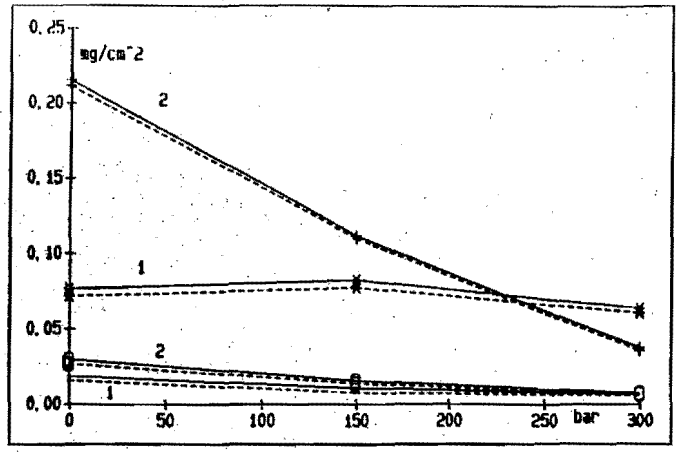

Figure 5 - Corrosion products weight and Cu amount in renewed and quiescent sea water.------ Cu^{+} + Cu^{++}, _____ Cu^{+} + Cu^{++} + Al (or Zn)

	Alloy 1			Alloy 2.		
P bar	1	150	300	1	150	300
Cu+	57.02	52.00	7.30	13.40	29.00	2.00
Cu++	15.51	27.00	54.10	200.00	66.00	35.60
Al+++	4.58	6.20	2.50	-----	-----	-----
Mg++	6.67	11.40	23.70	11.40	1.20	3.20
Ca++	-----	-----	2.50	-----	-----	1.50
Zn++	-----	-----	-----	3.64	1.70	0.60
Sn>2+	-----	-----	-----	-----	-----	-----
Cl-	20.93	50.00	8.52	20.10	24.00	1.50
SO42-	13.30	27.00	9.90	25.0	5.4	1.0
CO32-	4.50	5.50	-----	6.5	3.0	-----

Table 5 - Corrosion products (µg.cm^{-2}) of specimens exposed in renewed sea water (720 h exposure).

	Alloy 1			Alloy 2		
P bar	1	150	300	1	150	300
Cu+	6.35	2.95	2.95	17.66	12.25	6.80
Cu++	9.62	5.49	4.10	3.57	3.10	2.00
Al+++	1.58	0.32	1.20	-----	-----	-----
Mg++	1.26	1.10	1.40	-----	0.80	0.95
Ca++	-----	-----	-----	-----	-----	-----
Zn++	-----	-----	-----	1.11	0.47	0.20
Sn>2+	-----	-----	-----	0.87	2.80	-----
Cl-	0.04	-----	-----	3.58	0.09	1.20
SO42-	-----	-----	-----	0.15	-----	-----
CO32-	-----	0.20	0.35	-----	0.20	0.20

Table 6 - Corrosion products (µg.cm^{-2}) of specimens exposed in quiescent sea water (144 h exposure).

Alloy	P bar	Compounds identified
1	1	CuCl, CuO, Cu2O, CuSO4.5H2O, CuCO3.Cu(OH)2, Mg6Al2CO3(OH)16.4H2O, Al(OH)3
	150	CuCl, CuO, Cu2O, AlO(OH) Mg6Al2CO3(OH)16.4H2O
	300	CuCl, CuO, Cu2O
2	1	CuCl, CuO, Cu2O, CuSO4.5H2O, CuCO3.Cu(OH)2
	150	CuCl, CuO, Cu2O, CuSO4.5H2O
	300	no compounds

Table 7 - Corrosion products X ray diffractometric analysis.

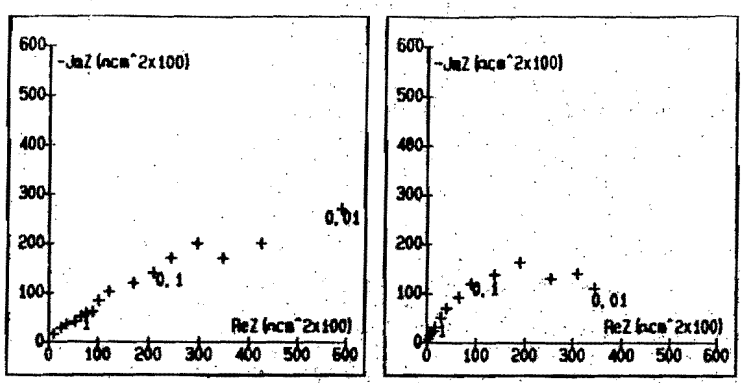

Figure 6 - Impedance spectra of alloy 1 at 1 and 300 bar.

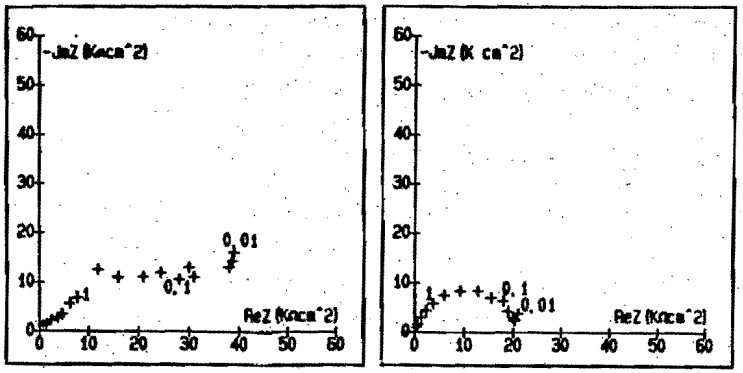

Figure 7 - Impedance spectra of alloy 2 at 1 and 300 bar.

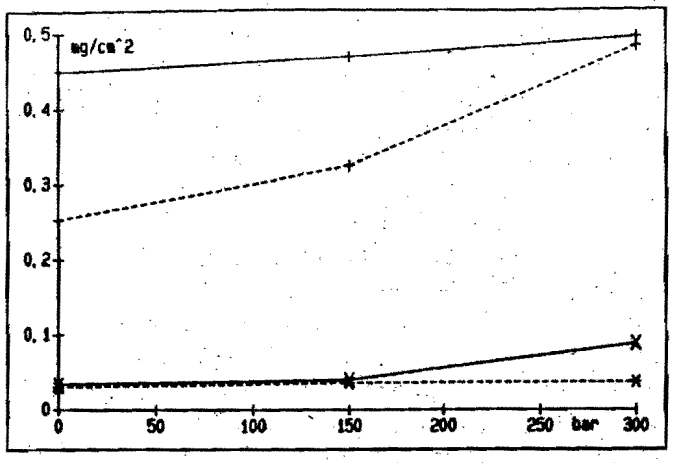

Figure 8 - Cu, Al and Zn oxidated total amount. Quiescent sea water, 144 h.--+--+ Cu,--x--x Al or Zn, _____ Alloy 1, ------ Alloy 2.

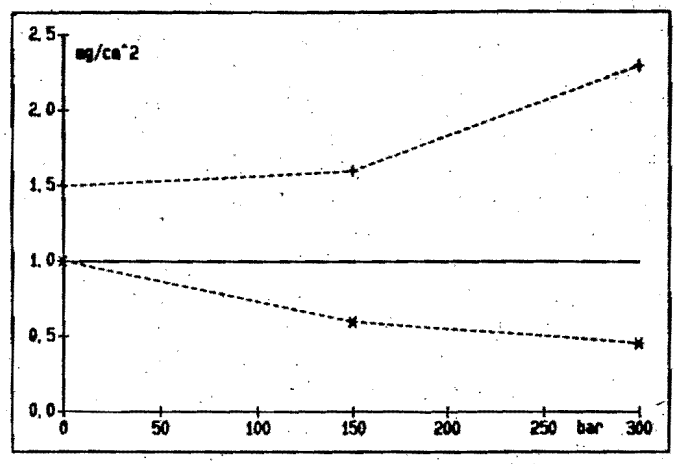

Figure 9 - Dealloying factor Z as a function of hydrostatic pressures. --+--+ Alloy 1, --x--x Alloy 2.
Z = (Al_{max} or Zn_{max})/Cu_{max} x Cu_x/(Al_x or Zn_x)

CHARACTERIZATION OF CONDENSER TUBES COATINGS BY ELECTROCHEMICAL IMPEDANCE

A. Colombo, G. Rocchini, ENEL/DSR-CRTN, Milano, Italy
P. Spinelli, Politecnico di Torino, Italy

ABSTRACT

Long term testing to evaluate the protective effectiveness of organic coatings of condenser tubes has been performed on aluminium brass, Cu90Ni10 and Cu70Ni30 in a circulating loop using a 3.5% sodium chloride solution. Surface characterization was obtained by means of impedance measurements. The results indicated that the electrical capacity is a good parameter for evaluating the effectiveness of the coating. A discussion on the interpretation of impedance data for practical systems is reported.

INTRODUCTION

Corrosion prevention of copper alloys tubes of thermal and nuclear power plants condensers and of heat exchangers operated in sea water, may be obtained both by the addition of inhibitors to the operating fluid and by internal coating of the tubes.

In the first case the cooling liquid is treated by addition with a ferrous salt (1) or by dissolution of iron anodes (2), another possibility is given by the addition of corrosion inhibitors such as benzotriazole (3). In both cases the scope is to obtain a compact film on the internal surface of the tube so that a barrier is formed between the metal and the aggressive environment, which in turn would not reduce heat transfer.

The addition of ferrous salts to the cooling water is very common in power plants. Experience showed that a more compact film can be obtained by means of "Taprogge" system. The principal drawback, which is encountered when inhibitors are employed, is due to the fact that normally the protective film is not completely compact over the whole surface, thus favouring the possible formation of localized attacks.

In the second case the protective action consists in applying an organic product on the tube surface which allows a very good electrical insulation between the base metal and the cooling fluid. It is known that an organic coating protects the the underlying metal basically behaving as a barrier against water, oxygen, and ions. In some cases the coating serves as an inhibitor source, thus improving its protective effectiveness. Protection of such barrier is enhanced by increasing the coating thickness and by the addition of pigments and additives which lengthen the diffusion path for water and oxygen. However, the use of organic coatings does not completely eliminate corrosion phenomena and sometimes it only represents a temporary remedy with the possibility of potential corrosion problems.

The most common under coating forms of corrosion are: blistering, early rusting, flash rusting, anodic undermining, filiform corrosion, cathodic delamination. Another drawback of coatings which may be related to corrosion is the lack of adhesion.

Internal coatings are generally preferable compared to the treatment of the cooling fluid because in principle they allow more controlled surface films with a very low porosity. From an economical point of view an advantage of organic coating, respect to ferrous salt or inhibitors addition, is that the coating may be associated with less noble metals, at least for heat exchangers, thus obtaining a saving of resources and decreased costs for subsidiary plants.

Due to the remarkable industrial interest of the organic coatings and also to the presence of erosion-corrosion phenomena on the internal surface of the tubes in a small region of the condenser of some ENEL plants, some coated tubes were operated (5) in order to evaluate the behaviour of commercial products and their effectiveness in preventing such problems. That preliminary investigation showed the rise of specific problems of protective coatings outlined above. Thus a research program was initiated with the aim of characterizing the porosity of commercial products for coating and developing an electrochemical technique for on-line monitoring of the effectiveness of the coating.

Due to the high electric resistance value of a good organic coating, we choose to employ a.c. techniques. So it is possible to investigate the behaviour of the metal-coating-solution interphase and to estimate the protection effectiveness of the coating by employing the mathematical technique of equivalent circuit simulation. It must be noted that a.c. techniques, though less known than the methods based on polarization-resistance (6), are encountering wide spread applications for this kind of problems, particularly in the case of passive films (7) and corrosion inhibiters both for iron base materials (8) and for copper alloys (9). A comprehensive review of possible application of a.c. techniques to the monitoring of corrosion processes is given in (10).

EXPERIMENTAL

General remarks

In the present work the behaviour of three copper alloys: aluminium brass, cupronickel 90/10, and cupronickel 70/30 was investigated. These alloys are normally employed in the condensers cooled with sea water of ENEL thermal power plants.

All the examined specimens were obtained from condenser tubes stock. The internal diameter of the tubes was 19 mm and the thickness was 2 mm.

The coating has been carried out by SECAPHEN with Corrodex 7156. This product was chosen both because it was previously applied to a small number of condenser tubes of unit 4 of the Fusina power plant, and for its availability in Italy. The product was manually applied because the specimens length (55 mm) did not allow the use of automatic process developed by SECAPHEN for plant application when the whole tube length is concerned.

The coating, the average thickness of which is 200 μm, generally did not present microporosity leading to the formation of preferential paths.

Two series of tests have been carried out under the following operating conditions. The electrolyte was a 3.5 wt% NaCl solution, the temperature was 35 °C and the flow rate was 1 m/s in all the three branches of the loop. The first series of tests gave rise to some difficulties relating to coating deposition, which was limited to the internal surface of the tube and to the two bases. During cell assembly, the non perfect adherence of the organic product to the base, caused in some cases local detachment of the coating. This was firstly realized by the comparison of the different a.c. responses and it was subsequently confirmed by visual inspection which clearly indicated that the responses close to those of an ideal capacitor corresponded to the undamaged specimens, whereas marked shifts from such behaviour referred to specimens the coating of which had been mechanically damaged during mounting.

After realizing that coating of the tube bases was rather critical, we tried to eliminate problems coming from mounting by partially extending the coating to the external surface for about 1 cm, in order to assure a continuity of the film. These kind of specimens were employed in the second series of tests. As a result we eliminated the drawback of electrical coupling of the internal and external surface of the tube caused by non perfect sealing of the cell. This is by no means a minor problem because in the case of long term tests a mechanical settling of the cells may occur with the possibility of electrolyte solution leakage, even if at the beginning the sealing system did not leak at all. The increase in concentration of the leaked solution, due to evaporation, may damage for long exposures the protective coating. In this work a overhead seal system was initially used, which was changed for the second series of tests to lateral surface sealing. This system has been tested for some months proving to be very reliable, in fact no leakage was observed.

The effect of electric coupling between the internal and external surface is reported in table 1, which shows how important is the need for a very good electric insulation of the external surface of the specimen when quantitative evaluation of the behaviour of the coating is required. By observing the 4th column in table 1, it can be seen that the phase angle is markedly shifted from the behaviour of an almost ideal capacitor which should give -90°. We can also add that micrographic examination of internal zone of the tube did not present any damage and the metal surface did not undergo any corrosion process.

Electrochemical measurements

Electrochemical impedance measurements were carried out by means of the EG&G computerized system including mod. 173 potentiostat with mod. 276 interface and mod. 5206 lock-in amplifier. The potentiostat had been modified to perform long distance measurements by the four wires technique according to the manufacturer indications. This was required because the conncting cables were about 5 m long.

All the measurements were carried out under potentiostatic configuration as required by mod. 368 AC software of EG&G, written in "Pascal" for Apple IIe computers. Two version of this software were employed, the first one for operation at the maximimun frequency of 100 kHz, the second one at the maximum ferquency of 20 kHz.

Generally the frequency range [20, 5] kHz was used. The signal amplitude (= 4 mV) was fixed before the tests for all the frequencies. This was necessary because for the above described equipment it is not possible to change by software the output level of the oscillator signal. Some tests were performed starting from the upper frequency of 60 kHz. Some other tests were run at the lower frequency of 10 Hz. These tests pointed out that the computerized system properly operates down to the lower frequency of 300 Hz. Below this value the increase in the impedance modulus drastically reduces the current flowing through the system, bringing up some difficulties in the measurement probably due to non optimum selection of the potentiostat current range. This has been verified by employing the Frequency Response Analyser Solartron mod. 1152 and by varying the current range. The best results were obtained when the measurements were performed starting from the 1 mA range. This fact indicates that the above outlined problems, which must be seriously taken into account for a correct interpretation of the experimental data, are only apparent and must be reported to the non specificity of the available software which has been developed for general use. Moreover such software does not allow an effective organization of the experimental data files and their subsequent efficient numerical processing. For these reasons, we decided to develop a software more adequate to our experimental conditions, particularly with the aim of a more efficient data organization.

In the first series of tests some impedance measurements in the range [11, .1] Hz were carried out by means of the Fast Fourier Transform (FFT) technique as implemented in EG&G mod. 368 AC software. The results were not very encouraging because the real part of the impedance, in contrast with its physical meaning, casually took negative values, as shown in table 2. This could be attributed to the very low value of the electric current (less than 1 nA) and to the numerical processing of the response. However, this kind of measurements gives useful information on the d.c. resistance of the coating. For the EG&G system the FFT technique employs a d.c. voltage within the range [-10, 10] mV and carries out the analysis of the current I(t), due to the fact that the applied voltage is the sum of fixed number of alternating signals having selected frequencies. One fact to be pointed out in our experiments is that it is practically impossible to polarize the sample at the corrosion potential, because this potential is not well defined.

The circulating loop

Every cell, fig. 1, holds five specimens of the same material and a saturated calomel reference electrode. In the present work two of the five specimens were coated. The internal surface of the uncoated specimens has been mechanically polished up to n. 200 emery paper before the tests. The uncoated samples at the two ends of the cell were connected to improve the current density distribution, and were employed as counterelectrode. The third uncoated specimen was used for evaluating the protective effectiveness of the organic coating.

The circulating loop in polipropilene is illustrated in fig. 2. It incorporates three parallel branches, a by-pass, a pump, some membrane and on-off valves. We chose a magnetically driven pump to eliminate the sealing problems. The pump capacity was 10 m^3/h with a dynamic head of 7.5 m. It allows a maximum flow rate of 3 m/s on the three branches.

An external thermostat having a volume of 30 l served for temperature control through a glass heat exchanger. Under these conditions we could eliminate the heat generated by the pump allowing a minimum operating temperature of 30 °C. At the highest point of the loop a resistivity level control was inserted for protecting the entire

system. Flow-meters on every branch indicated the flow rate, which required a very low degree of adjustment over the time.

INTERPHASE ELECTRIC EQUIVALENT

It is known that the characterization of the behaviour of the coating and therefore the interpretation of the experimental results require a schematization of the metal/coating/electrolyte interphase for taking into account the response to a sine wave modulation of the electrode voltage. To this aim a number of models have been proposed in the literature (11), which should account for the electrochemical mechanism of the corrosion process. Particularly, for a protective coating or for a passive layer, by considering that these films always present a certain microporosity, it should seem a good approach the line-transmission model based on a continous distribution of the parameters. However, in the present case, on the basis of considerations regarding the thickness value of the coating, microscopic examination of the specimens, and the results of the impedance measurements, we chose the electric equivalent circuit reported in fig. 3. The impedance Z of the dipole shown in fig. 3 is composed of three elements, R_s (electrolyte resistance), C (capacitance of the coating), and R (leak resistance). The leak resistance R accounts for the fact that on an electrical basis, the capacitor C exhibits a phase value slightly different from the ideal -90° value.

All the measurements concerning specimens without electric coupling between the internal and external surface, gave phase values very close to -90°. It is so very difficult to state if the slight difference from the ideal trend corresponds to a real behaviour of the electrochemical system or must be attributed to some measurement errors. However, we can affirm that such situation does not depend on the non simultaneous recording of the current and voltage signals, because the electrochemical system does not undergo any change on polarization in the absence of corrosive processes as previously outlined.

We can say qualitatively, also on the base of some d.c. measurements which evidenced the extremely low value of the current density in spite of the high polarization value, of the order of 1 V, that the higher is the leak resistance value the most satisfying results the coating behaviour. This point is confirmed by the fact that it is not possible to determine a unique open circuit electrode potential in the absence of electrolyte leakage. In fact a high porosity value favours due to the formation of preferential paths, an extended contact between the base metal and the electrolyte solution, thus increasing the contribution of the bare metal to the overall impedance. Under these conditions a defined value of the open circuit potential is obtained. The impossibility of measuring the open circuit potential for coated specimens does not consent to employ the interrupter method for evaluating the differential capacitance of the interphase.

Such a situation can be physically representd by two real parallel capacitors (12). In fact the bare metal is characterized by a very low value of the transfer resistance (13). When the coating porosity is such that no preferential path is formed or when the extent of surface porosity is negligible respect to the total surface, it is by no means an easy task to reveal the presence of defects by means of impedance measurements only, because they contain a global response of the system.

It is our opinion that quantitative evaluation requires the definition of some standards at different degree of porosity to be able to indicate an electric equivalent of the electrochemical system for best fitting of experimental data. We are also convinced that the simple electric scheme of fig. 3 is very useful for the practical need of defining a non ambiguous parameter for characterizing the protective coating.

RESULTS AND DISCUSSION

A typical trend of the Z'=Z'(-Z") curves, Z' being the real part and Z" the imaginary part of the impedance Z, concerning the three different materials Albrass, cupronickel 90/10, and cupronickel 70/30, is reported in fig. 4 which shows the Nyquist diagram on the Argand

plane Z',-Z". This figure indicates that in the frequency range [20, 5] kHz the real part of the impedance can be reasonably considered constant. This means that the electric current is completely non-faradaic, confirming the validity of the circuit reported in fig. 3. Moreover the very low values of the transfer resistance for the three uncoated materials suggest the correctness of the model chosen for coated specimens. This fact can be discussed on the basis of what previously reported on the presence of defects related to the porosity of the coating. We can therefore accept the general observation that at high frequencies no electrochemical process can be activated, because the process cannot follow the external modulation.

The purpose of the measurements performed on uncoated specimens was to compare the interphase capacitance values in order to evidence the effect of the protective coating and to determine the ohmic drop, which was obtained by the extrapolation method (14) as reported in fig. 5 showing three of the examined cases. It was experimentally verified, as illustrated in fig. 6, that it is not possible to obtain a good value of the ohmic drop on the coated specimens even for frequencies in the range [60, 20] kHz.

Curves 1,2, and 3 in fig. 7 show the Z'=Z'(-Z") trend for the three coated specimens and refer to measurements taken in the second series of tests after 30 days of loop operation.

Fig. 8 illustrates the difference between the behaviour of a specimen with no coupling of internal and external surface, curve 1, and the behaviour of a specimen on which such coupling occurred, curve 2.

An example of the evaluation of the interphase capacity by the estrapolation method, in the case of a coated specimen, is illustrated in fig. 9. For uncoated specimens the capacity has been evaluated by solving for every frequencies the two simultaneous equations given by the real and imaginary part of the impedance.

Figs. 10, 11, 12 compare the trend of the capacity values with time for coated and uncoated specimens.

Lastly figs. 13, 14, 15 report the values of the leak resistance and of the transfer resistance as a function of time.

It is of some interest to note that a lower value of the leak resistance does not reflect an important change of the capacity. This means that though the electric coupling with the external surface modifies both real and imaginary part of the impedance, does not change the capacity value.

This is a very important result because it indicates that the interphase capacity can be considered as a good parameter for characterizing the effectiveness of the coating. From an electrical point of view, the previous finding can be explained by considering that non-faradaic current of the region subjected to electric coupling is negligible respect to the non-faradaic current of the whole surface. Under these circumstances the behaviour normally results in a slight increase of the phase angle.

From the above discussion we can say that the evaluation of the protective effectiveness of a coating may be far from real situation if it is based on the module of the impedance or on the phase angle only.

Inspection of figs. 10, 11, and 12 reveals the important diference between the capacity values of a bare and of a coated specimen, indicating that possible experimental errors do not significantly alter the above picture. It is also evident that a gradual weakening of the protective effectiveness of the coating causes an increase of the capacity value.

The above consideration are a further point in favour of the choice of capacity as a physical parameter for characterizing the surface coating.

CONCLUSION

Analysis of the overall experimental results indicates that for large thickness coatings, a.c. impedance techniques consent a correct evaluation of the protective effectiveness of the surface film.

The high value of the real part of the impedance at low frequencies limits the use of d.c. techniques as indicated by FFT tests. On the other hand for low thickness coatings, a.c. techniques, made on the basis of a more complex interphase scheme, allow the assumption of a certain number of parameters which are useful to differentiate the coating behaviour and to make some quantitative classification.

Finally we can observe that for a correct approach to the problem, the measurements made on uncoated specimens were very useful because besides the determination of the ohmic drop, they allow to rapidly visualize the difference between the classes of specimens and the effect of the coating against corrosion as indicated for example by comparing the leak resistance and transfer resistance values.

REFERENCES

1. T. W. Bostwick, Corrosion, 17, n. 8, p. 12, 1961.
2. H. P. Hack, J. P. Gudas, Materials Performance, 19, p. 49, 1980.
3. K. H. Wall, I. Davies, J. Appl. Chem. (London), 15, p. 389, 1965.
4. ENEL/DPT-SPT di Venezia, Report n. DI-41/78.
5. ENEL/DPT-SPT di Venezia, private communication.
6. F. Mansfeld, in "Advances in Corrosion Science and Technology", Vol. 6, p. 163, Plenum Press, New York 1976.
7. W. Paatsch, W. J. Lorenz, Electrochemical Corrosion Testing, Dechema Monographs, Vol. 101, p. 221.
8. G. Rocchini, Corrosion/85, Paper n. 188, Boston 1985.
9. G. Brunoro, F. Zucchi, M. Maja, P. Spinelli, 5th European Symposium on Corrosion Inhibition, Ferrara 1980, Vol. 3, p. 997.
10. F. Mansfeld, CORROSION/87, Paper n. 481, San Francisco, USA, March 1987.
11. D. D. Macdonald, CORROSION/87, Paper n. 479, San Francisco, USA, March 1987.
12. A. Alberigi Quarante, B. Rispoli, Elettronica, Zanichelli, Bologna 1960, p. 169.
13. A.Caprani, I. Epelboin, Ph. Morel, H. Takenouti, 4th European Symposium on Corrosion Inhibition, Ferrara 1975, Vol. 3, p. 517.
14. G. Perboni, G. Rocchini, Corrosion/86, Paper n. 352, Houston 1986.

Frequency (Hz)	Z' (ohm)	-Z" (ohm)	phase angle °
5020	6137	7344	-50.1
5646	5688	6922	-50.6
6320	5261	6530	-51.1
7100	4865	6150	-51.7
7960	4498	5794	-52.2
8930	4150	5447	-52.7
10000	3799	5090	-53.3
11200	3472	4802	-54.1
12600	3197	4470	-54.4
14200	2910	4190	-55.2
15900	2630	3973	-56.3
17800	2320	3868	-59.0
20000	2052	3556	-60.0

Table 1. Z', Z" and phase angle values for a Cu70Ni30 coated specimen on which electric coupling with the external surface occurred.

Frequency (Hz)	Z' (Mohm)	-Z" (Mohm)
0.1001	-38.33	250.80
0.3003	-5.72	38.30
0.5005	6.30	20.30
0.7007	3.82	21.62
0.9009	16.46	17.13
1.1010	-4.66	22.30
1.3010	-1.71	3.10
1.5010	3.69	8.06
1.7020	7.01	9.08
2.1020	1.78	9.23

Table 2. Results of FFT measurements on a coated Albrass specimen.

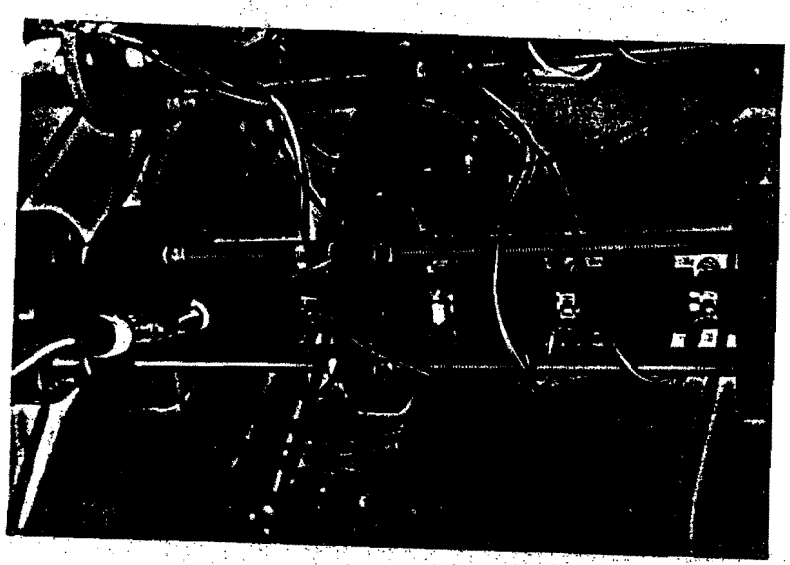

Fig. 1 - Test cell.

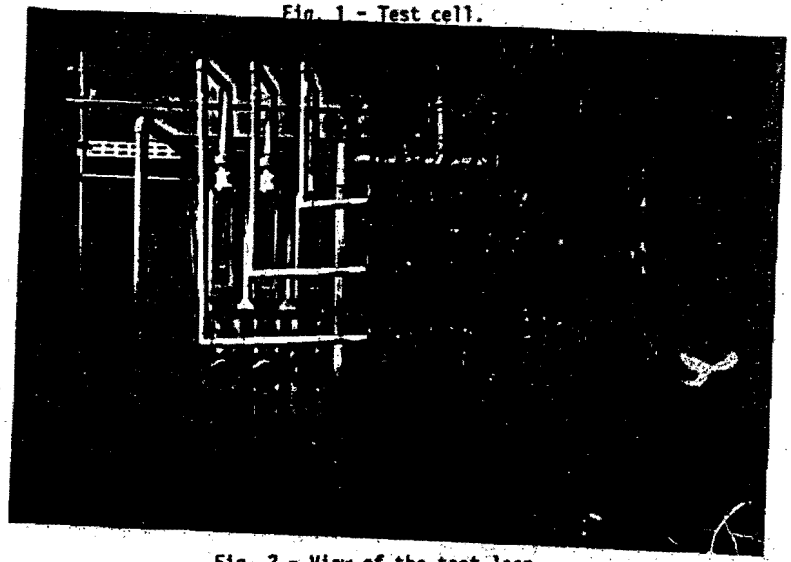

Fig. 2 - View of the test loop.

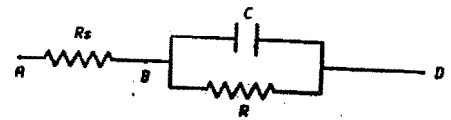

$Z = R_s + R/Q - i \cdot \omega \cdot C \cdot R^2/Q$

$Q = 1 + \omega^2 \cdot C^2 \cdot R^2$

$\lim_{\omega \to \infty} |Z| = R_s$

R_s = SOLUTION RESISTANCE

R = LEAKAGE RESISTANCE

C = INTERPHASE CAPACITANCE

Fig. 3 - Electric equivalent of the metal-coating-solution system.

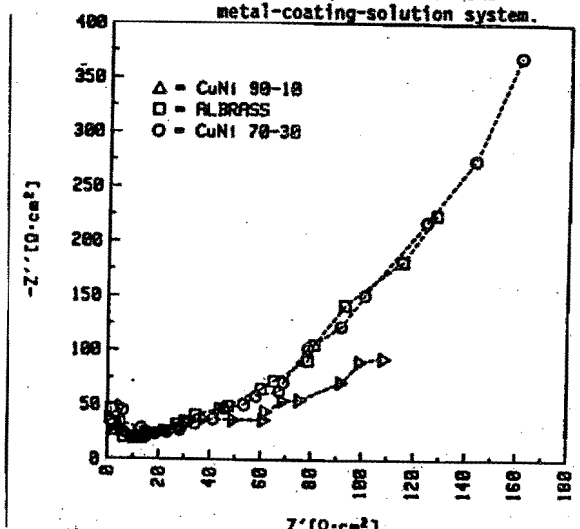

Fig. 4 - Nyquist plot for uncoated specimens. Frequency range [20, 0.02] kHz.

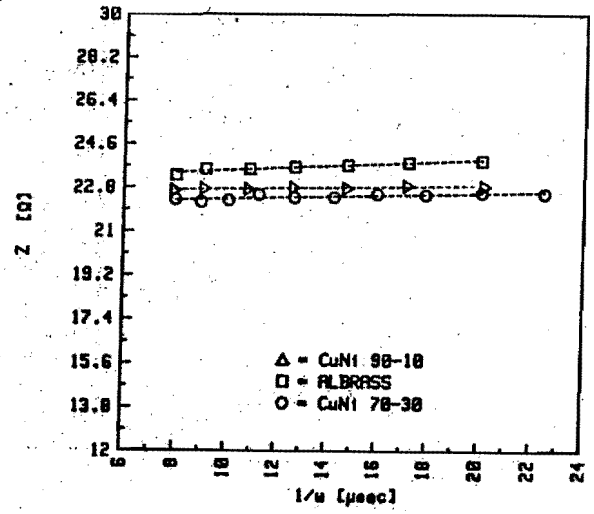

Fig. 5 - Ohmic drop determination for uncoated specimens. Frequency range [20, 7.1] kHz.

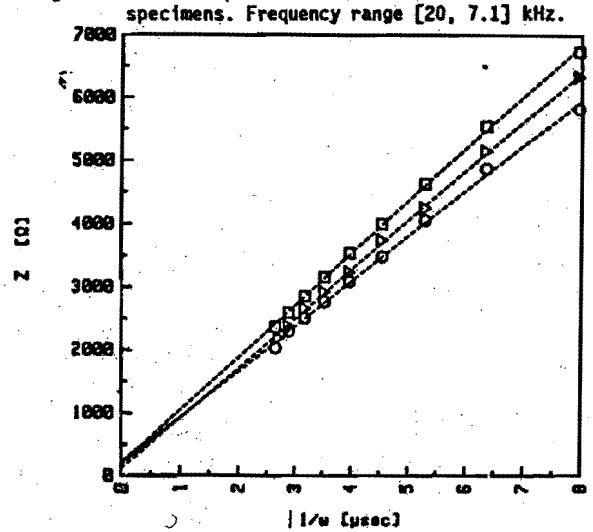

Fig. 6 - Ohmic drop determination for coated specimens. Frequency range [60, 20] kHz.

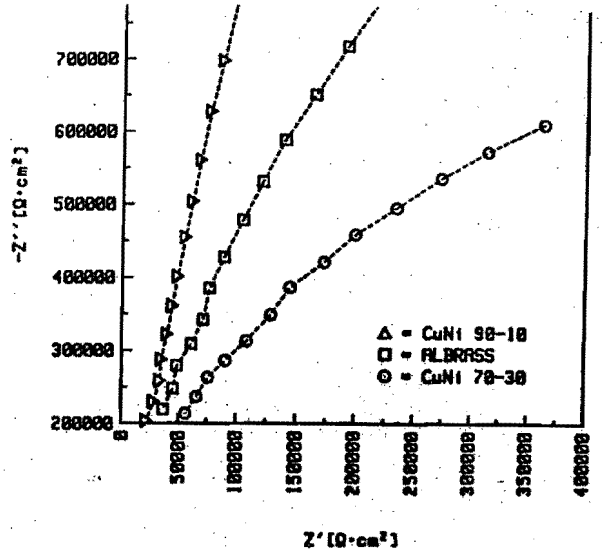

Fig. 7 - Nyquist plot for coated specimens. Frequency range [20, 5.02] kHz.

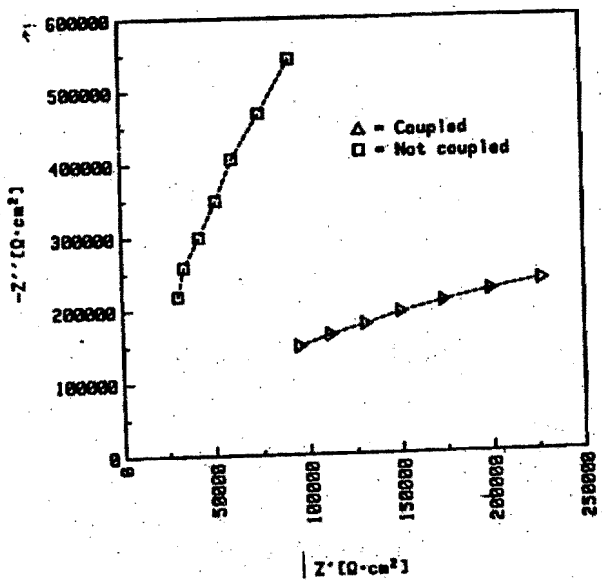

Fig. 8 - Nyquist plot for [illegible]

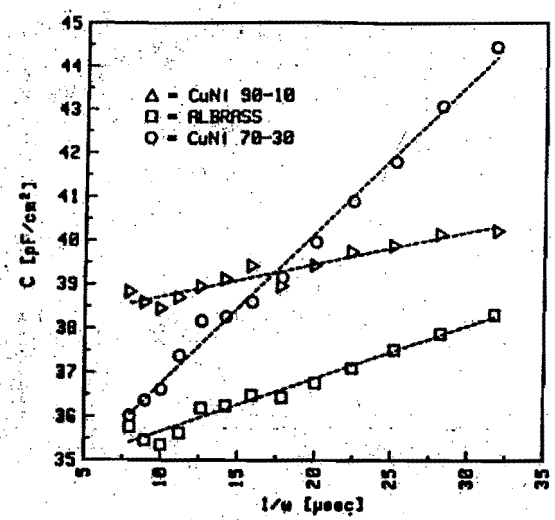

Fig. 9

Fig. 9 - Interphase capacity determination for coated specimens.

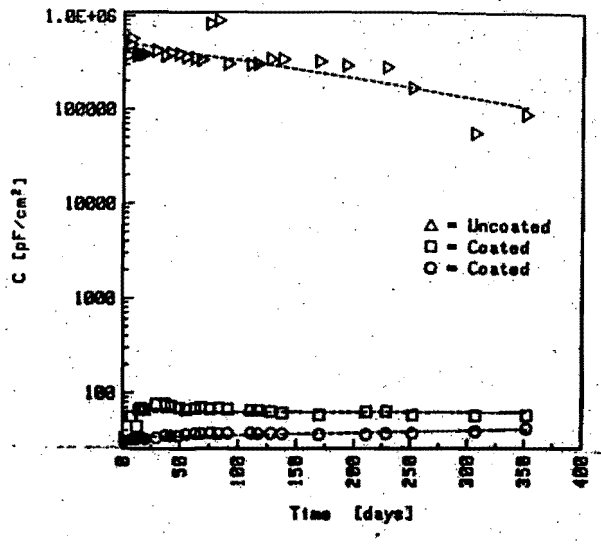

Fig. 11 - Capacity vs. time for coated and uncoated 70/30 copper-nickel specimens.

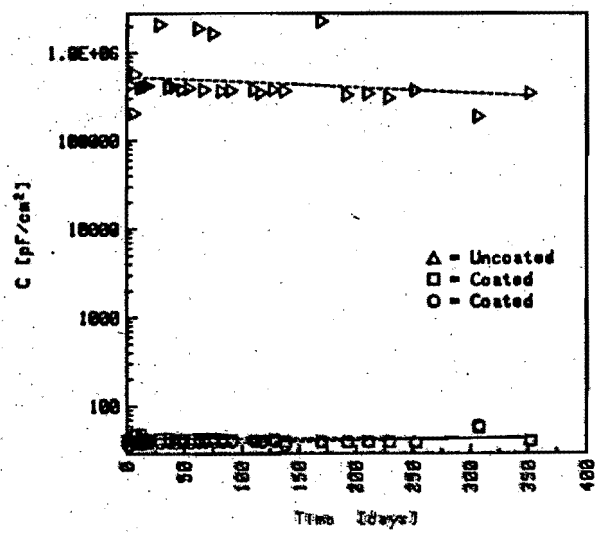

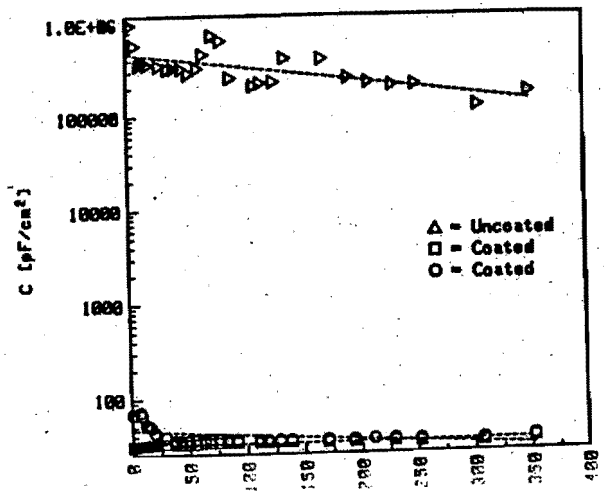

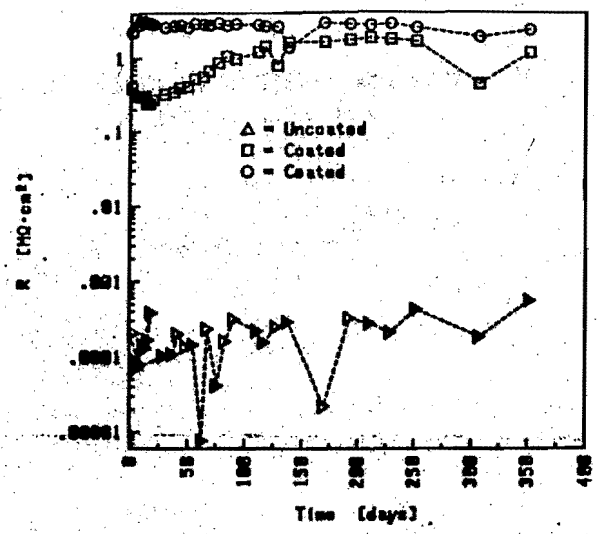

Fig. 13 - Leakage resistance vs. time for coated and uncoated 90/10 copper-nickel specimens.

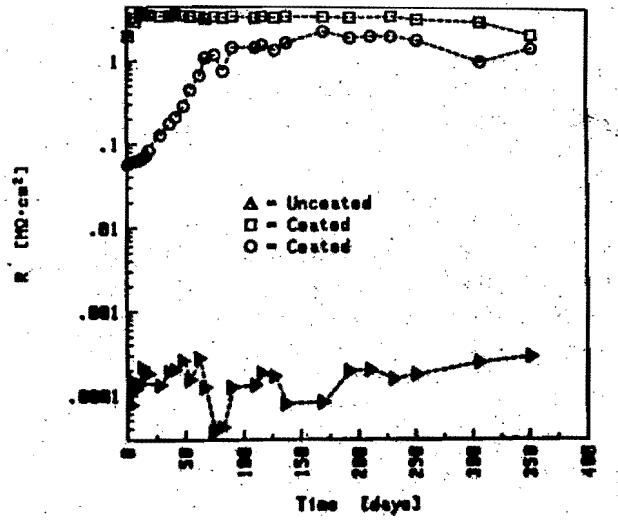

Fig. 15 - Leakage resistance vs. time for coated and uncoated Albrass specimens.

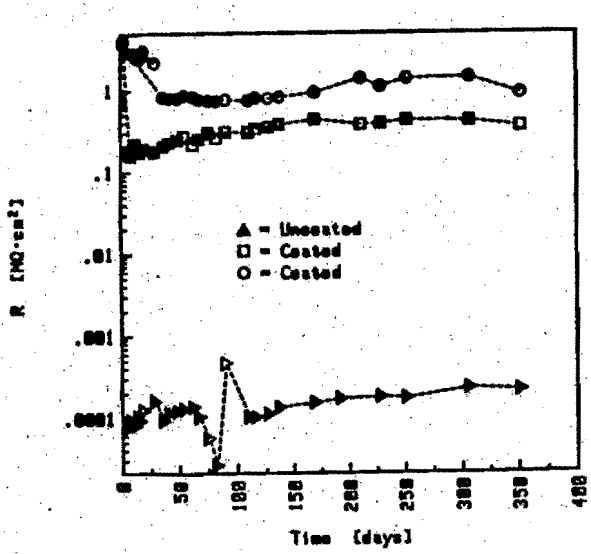

Fig. 14 - Leakage resistance

OXYGEN REDUCTION ON "PASSIVE" METALS AND ALLOYS IN SEAWATER. EFFECT OF BIOFILM.

Ragnar Holthe, Per Olav Gartland and Einar Bardal
The Corrosion Centre, SINTEF
7034 Trondheim, Norway

ABSTRACT

The oxygen reduction rate on passive metals and alloys in sea water is strongly enhanced due to a catalytic effect of the biofilm that forms on every substrate material immersed in sea water. The effect of the biofilm and its dependence of sea water flow rate and temperature is reviewed and some new results is added. The pH at the surface of stainless steel has been measured at free corrosion potential and during cathodic polarization. The maximum pH of 9.5 was reached at a maximum current density after about 2 weeks of exposure. At free corrosion there were no pH changes at the surface. A tentative model based on experimental observations that explain the time dependence of the cathodic properties of passive metals and alloys in seawater is presented. The model describes how the oxygen reduction rate increases due to the formation of super state microcathodes with a strongly enhanced exchange current for the oxygen reduction reaction.

INTRODUCTION

It has been pointed out that natural seawater is more corrosive than synthetic sea water. /1-2/. Concerning stainless steels it is agreed upon by several research groups that this increased corrosivity of natural seawater is due to the build up of a microbial slime layer or biofilm that forms on nearly every substrate material /1, 3, 20/. The biofilm formation leads to an ennoblement of the free corrosion potential and an increased cathodic efficiency that is quite similar on a wide range of passive metals and alloys in seawater. The enhancement of the free corrosion potential gives an increased tendency to crevice corrosion initiation on stainless steels, and the increased cathodic efficiency leads to high crevice corrosion rates experienced for activated crevices for a conventional stainless steel (AISI 316L) /4/. Furthermore it gives increased galvanic corrosion rates on less noble materials coupled [illegible] stainless steels, Ni-alloys and titanium in seawater /3-5/.

In previous reported tests /3-5/ the catalytic effect of the biofilm has shown to be only little dependent on the amount of light and surface roughness, a little more dependent on the depth of seawater inlet and the seawater velocity and finally very dependent on the seawater temperature.

In the present paper the effect of flow rate and temperature are reviewed and some new data added. On the basis of previously reported tests and some recent results presented herein, a tentative model that explains the time dependence of the cathodic properties of passive metals and alloys in seawater is discussed.

EXPERIMENTAL

Experimental conditions

The experiments were carried out with fresh seawater taken from depth of 60 m and the temperature was 9±2°C. The metals and alloys studied were an austenitic stainless steel UNS S31254 (Avesta 254 SMO), titanium, 90/10 CuNi and platinum. The chemical compositions are shown in table 1. All specimens were degreased and rinsed in acetone. The stainless steel specimen (except the rotating disk samples) were pickled in a solution composed of 17 vol % HNO_3 and 4 vol % HF for a period of 20 min and finally rinsed in water.

The experimental arrangements in the investigations referred to are shown in the original papers and reports and are not repeated in the present paper. The procedure for measurements by the rotating disk electrode technique and the surface pH measurements are given below.

Surface pH measurements

The pH near the surface was measured with a flat glass membrane microelectrode (Microelectrode Inc., model MI-404) referenced to a saturated calomel electrode (SCE) using a Radiometer model pH M82. The electrode was mounted in a PVC holder shown in Fig. 1. During the pH measurements the holder that had 4 legs (see Fig. 1) was placed or pressed onto the stainless steel surfaces, that brought the flat membrane electrode in a well defined distance from the surface. The sensing flat membrane was offset 25 µm (± 10 µm due to inhomo- [illegible] surface. The offset was adjusted by

viewing the flat membrane, mounted in the PVC holder, under a microscope equipped with a calibrated ocular recticle. The samples studied were stainless steel UNS 312254 sheet material cut to coupons with area 12.5x20 cm^2.

The samples were mounted in a fresh seawater containing PVC-cell both horisontically and vertically and the pH was measured at surface both at the up and down side of the horisontally mounted sample, and on the vertically mounted sample to see if there were any effects of the orientation of the sample. The pH at 25 μm was recorded at 5 different spots each time when its value stabilized after about 1 min at each position.

Rotating disk electrode measurements

The rotating disk electrode (RDE) technique was adpoted to study the effect of mass transport during cathodic polarization of stainless steel and platinum in seawater. This method ensures the establishment of uniform and well defined mass transfer conditions across the entire electrode surface. The mass flux J to the electrode surface is given by:

$$J = k_m C_b \qquad (1)$$

where C_b is the bulk concentration and k_m is the mass transfer coefficient. At an RDE under convective diffusion conditions k_m is given by /6/:

$$k_m = 0.62\, \nu^{-1/6} \cdot D^{2/3}\, \omega^{1/2} \qquad (2)$$

where, ν is the kinematic viscosity in cm/s, ω is the rotation rate in radians/s and D is the diffusion coefficient in cm^2/s.

The relationship derived for the RDE geometry can be extended to any hydrodynamic configuration, if the corresponding dimensionless number relationships are known /7/. The correlation between the convective diffusion conditions at the RDE and a smooth straight pipe wall in which fully developed turbulent flow previals, can be established trough the mass transfer coefficient. Sanchez and Schiffrin /8/ evaluated this quantity from empirical non-dimensional relationships and found:

$$Sh = 0.00165\, Re^{0.86} \cdot Sc^{0.33} \qquad (3)$$

Equation (3) was found to cover Re and Sc numbers of most situations encountered in practice /8/.

From (1) and (3) a relationship between rotation rate, pipe diameter and flow velocity can be obtained, i.e.

$$\omega = 7.08 \times 10^{-4}\, \frac{v^{1.72}}{d^{0.8}\, \nu^{0.72}} \qquad (4)$$

where d is the tube diameter v is flow rate. The use of equation (4) then allows the simulation of hydrodynamic conditions for turbulent flow inside tubes in service, in a simple laboratory RDE experiments.

Stainless steel and platinum samples studied were mounted with epoxy resin shown in Fig. 2. The samples were prepared with 1000 grit paper and polished after they had been mounted to the epoxy resin. The rotating disk assembly employed was supplied by Thompson Electrochem. LTD (Newcastle upon Tyne, UK).

RESULTS AND DISCUSSION

As stated above and shown in Fig. 3 the biofilm formation in seawater on passive metals and alloys (stainless steels, titanium and platinum) leads to an enhancement of the open circuit potential in the order 100 to 300 mV SCE during a period of 10-14 days of exposure.

Due to a catalytic effect of the biofilm the cathodic reaction is strongly stimulated upon weak cathodic polarization. Fig. 4 shows the increase in the cathodic CD as a function of time at +100 mV SCE for 254 SMO titanium and platinum. At -300 mV SCE in Fig. 5 platinum is replaced by 90/10 CuNi. Both Fig. 4 and 5 shows an increase in the cathodic CD between 1 and 3 orders of magnitude for a wide range of metals and alloys. The incubation periods for the increase in potential and cathodic reaction rate are about the same.

In previously reported tests for a series of different stainless steels /3/, the cathodic properties have shown to be quite independent of alloy composition. Furthermore as shown above the biofilm effect are quite similar on a wide range of materials e.g., titanium, platinum and Ni alloys.

As mentioned above the catalytic effect of the biofilm has shown to be very dependent of the seawater temperature. Fig. 6 shows the free corrosion potential for samples of stainless steel 254 SMO after 30 days of exposure at different temperatures and flow rates. The rise in potential observed on different materials vanishes at temperatures above 30°C. The same temperature sensitivity is evident for the cathodic CD on samples polarized to +100 mV SCE in nearly stagnant seawater. Fig. 7 shows that there is no increase in the CD at 32°C in opposi-tion to measurements at lower temperatures 9, 18 and 24°C. Measurements of the CD at potential -300 mV at different temperatures gave the same results (not shown). Above 30°C the increase in CD was only marginal.

Effect of flow rate

The rotating disk electrode technique was adopted to study the effect of flow rate on the biofilm catalysis of the cathodic reaction in seawater.

Fig. 8 shows the evolution of CD for samples of stainless steel 254 SMO polarized to -100 mV SCE at different rotation rates 0, 1000 and 2000 rpm. The incubation period for the increase in current is quite independent of rotation rate up to 1000 rpm. The incubation period at 2000 rpm is somewhat increased. The maximum CD values at different rotation rates is less dependent on the rotation rate than yield the diffusion limiting current for a film free surface. Fig. 9 shows the maximum CD as a function of rotation rate for stainless steel polarized to -100 mV compared to the limiting current for a film free Pt surface at -800 mV at different rotation rates.

The RDE measurements shown here are qualitatively similar to the results presented for plates in a tubular flow by Johnsen and Bardal /9/. The RDE tests have, however, not been run long enough to observe the marked decrease of the CD at long times shown in the previous paper /9/.

Fig. 10 shows dynamical polarization curves for platinum samples exposed at +100 mV at rotation rate 500 rpm in 21 days and without any preexposure respectively. The reduced limiting current for the sample preexposed at +100 compared to the film free Platinum electrode is possibly due to diffusion resistance of the biofilm.

In the case of stainless steel 254 SMO shown in Fig. 11 the situation is more complicated. Fig. 11 shows polarization curves for samples of 254 SMO exposed at -100 mV and at rotation rate 1000 rpm for 30 days and without any pre-exposure respectively. The limiting current for 254 SMO is much higher in the case with the biofilm than without. However, in both cases the limiting current density for 254 SMO is much smaller than the oxygen diffusion limiting current of the film free Pt surface at the actual rotation rate. The CD for the 254 SMO sample without biofilm is possibly limited by some charge transfer resistance in the oxide layer. This is concluded from the observation that the limiting current for stainless steel 254 SMO in the potential region -500 to -800 mV SCE is much less dependent of flow rate than should be expected for a mass transport controlled oxygen diffusion limiting current. This is shown in Fig. 12. Fig. 13 shows the limiting current at the same rotation rates for a Pt electrode that gives results in agreement with the oxygen mass transfer controlled curve shown in Fig. 8.

pH at the surface during free exposure and cathodic polarization

It has been reported by several authors that cathodic polarization retards biofouling at metal surfaces in seawater by increasing the interfacial pH due to the oxygen reduction reaction /10-12/. In the interfacial area of a cathodic polarized surface, the bacteria will experience a pH gradient that will change their surface charge, thereby affecting the interaction with the polarized surface. In addition one intermediate species in the oxygen reduction reaction is H_2O_2 that acts as a biocide /11/.

On the other side, different bacteria attached to metal surfaces modifies the interfacial environment by producing a wide range of different species e.g. acids, extracellullar polymers and enzymes. To get information about the effect of pH with respect to the catalytic effect of the biofilm a series of experiments has been performed. Fig. 14 shows pH as a function of time measured at distance 25 µm from the surface of stainless steel sample polarized to -100 mV SCE. The pH grows steadily from the bulk seawater value of 8.1 up to a maximum value of 9.5 after 14 days. The shape of the pH vs. time curve fits very well the plot of CD as a function of time for the same sample. After about 14 days the CD reach the limiting current. During the period when the pH increases there is a significant scattering of pH values over the surface, that indicates an inhomogeneous current and pH distribution over the surface. A stainless steel sample polarized to +100 mV reached a maximum pH value of 9.2 at maximum current 4 $\mu A/cm^2$ after 3 weeks of exposure. For samples exposed at free corrosion the surface pH (25 µm) remained at the bulk seawater pH during the test period of 6 weeks.

Engell and Forchhammer /13/ has calculated for seawater of normal oxygen concentration (8 ppm) that the pH in the boundary layer should rise to ~ 10.9 in the case of complete reduction of dissolved oxygen diffusing to a cathodically polarized surface. Due to the buffering capacity of seawater the pH value will not reach this theoretical value. The observed maximum pH at the surface of 9.5 at maximum CD may be due to either: Precipitation of $MgOH_2$ and $CaCO_3$ from the seawater at the metal surface /12/, or as will be discussed below, some pH limitation of the catalytic activity of the biofilm. From the shapes of the two curves shown in fig. 14 it seem like that the pH may increase further upon an increase in the maximum CD which indicates that the pH is not controlled by precipitation of salts from the seawater.

Visual inspection of the samples after the test showed that only the top side of samples mounted horisontally were covered by deposits. At the down side or at samples mounted vertically there were no precipitation of salts visible. Similarly the pH at the surfaces at the down side or at the vertically mounted samples were significantly lower than at the top aide of the horisontally mounted sample. The explanation to this may be that the biofilm and bacteria colonies do settle more efficient at the upside surface which gives a higher CD here.

The mechanism

The experiments described above show that the biofilm formation of different substrate materials in seawater more or less strongly affects the cathodic properties of a wide range of passive metals and alloys in seawater. The actual mechanism of the catalytic action of the biofilm is not known. In the literature there has been put forward several candidates for a catalytic specie e.g. enzymes /14/, heavy metal ions /3/ and calcium hydroxide modified by some organic matrix /15/. Scotto et al /16/ showed that an enzymatic inhibitor, sodium azide, that inhibits the respiratory activity of the bacteria eliminated the catalytic effect of biofilm. This supports a mechanism involving enzymatic biocatalysis, which is described in general by Tarasevic /17/.

We have made some efforts to establish a model that may explain the polarization properties of different passive metals and alloys in seawater. In the following this tentative model will be discussed.

The dominating cathodic reaction in seawater in the potential range +300 down to -800 mV is the oxygen reduction reaction.

$$O_2 + 2H_2O + 4e \rightarrow 4OH^-$$

To make sure that the reaction that is catalysed is the oxygen reduction reaction the effect of removing oxygen from the seawater was investigated. Samples of stainless steel 254 SMO and platinum was exposed in seawater at free corrosion and polarized to -100 mV SCE for one month at when the experimental cell was plugged and the oxygen was removed by purging nitrogen through the cell. Fig. 15 shows the oxygen concentration during the first 6 hours of nitrogen bubling. After 24 hour the oxygen level in the seawater was about 10 ppb. The CD for samples of Pt and stainless steel 254 SMO polarized to -100 mV, during the nitrogen bubling period are shown in Fig. 16. The CD decreases rapidly when the oxygen concentration decreases as shown in Fig. 15. After about 6 hours the CD shifts to the anodic direction. In the same manner the free corrosion potential for samples preexposed for 30 days drops from 350 mV down to -500 mV upon removing the oxygen from the seawater, shown in Fig. 17. Supply of fresh seawater saturated with oxygen shifted the potential nearly instantly (Fig. 17) from -500 mV up to about +100 mV, and up to 0 mV for 254 SMO. Removing the oxygen from seawater eliminated the effect of the biofilm and a new incubation period of 14 days was nessesary to let the potential increase above 300 mV and reestablish the catalytic effect of the biofilm.

Fig. 18 shows potentiodynamic curves for samples of stainless steel 254 SMO (the same effects are observed on other materials) exposed at free corrosion potential E_{corr} for 10 and 18 days and at +100 mV for 10 and 14 days respectively. There are only small changes of the polarization curves with time for samples exposed at $E = E_{corr}$. When exposed at $E < E_{corr}$, the polarization curve gradually adopts a shape with two limiting current densities of which the smaller one increases with time as shown in Fig. 18. The observations shown in Fig. 18 can be interpreted in terms of a two state model, where parts of the surface is in a normal activation controlled state and the rest consist of superstate of microcathodes with a strongly enhanced oxygen reduction exchange current due to an inhomogeneous build up of the catalytic biofilm. At these microcathodes the current density will not be activation controlled but reach a limiting current density even at rather positive potentials.

The dynamic behaviour of the polarization curves when $E < E_{corr}$ is then due to a gradual change in relative areas, going from a dominant normal state to a

dominant superstate. An inhomogeneous build up of the biofilm is evident from studies of the biofilm by optical and scanning electron microscopy at different stages during the formation process, Fig. 23-24. These micrographs will be discussed in more detail below.

The increase in exchange current until a limiting current at the highly effective microcathodes would account for the observed shape of the polarization curves for samples exposed at $E < E_{corr}$ in Fig. 18, showing an additional limiting current in the upper potential range that increases with time.

Tentatively, one would assume that the limiting current density of the superstate was due to diffusion limitations of O_2.

However, results from two independent tests show that the upper limiting current, Fig. 18, does not correspond to oxygen diffusion limitations at the microcathodes.

Firstly, Fig. 19 shows dynamic polarization curves recorded at different oxygen concentrations for samples of stainless steel 254 SMO prepolarized to -100 mV SCE in 14 days. If the upper limiting current did correspond to the oxygen diffusion limiting current at microcathodes, a reduction of the bulk oxygen concentration by 90 % should reduce this limiting current by the same amount. As shown in Fig. 19 the reduction in oxygen concentration gives a minor reduction in the upper limiting current while the limiting current in the lower potential range is reduced by about 90 % as it should be.

Secondly, rotating disk samples of steel 254 SMO were polarized to -100 mV SCE in seawater at a constant rotation rate. The instant effect of increasing the rotation rate was tested several times during the period of increase in the cathodic current (see Fig. 8). If the upper limiting current was an oxygen diffusion limiting current at the microcathodes the current at different stages of the increase period shown in Fig. 8 should be quite dependent of the rotation rate ω. No such dependence of the rotation rate was observed. An increase from 500 rpm up to 2000 rpm caused only minor increase in the current density (less than 10 %).

A possible limitation of the current density could be the pH at the surface. As discussed above the bacterial activity is reduced at high pH values. On the other hand, if species like $Ca(OH)_2$ are important for the catalytic activity, as suggested by some authors /15/, a weak alkalinization will be beneficial. From this, one should expect that the catalytic activity has a maximum at some pH value above the seawater pH, as illustrated schematically in Fig. 20.

Such a pH dependence can explain the observed limiting current density at the highest potentials as follows. When the specimen has been polarized to -100 mV SCE for some days, there will be a certain fraction of the area in the superstate, with a high exchange current density i_o. This value of i_o is, however, a function of the pH, when pH becomes very high (> 9.5) the value of i_o is much reduced. Upon dynamic stepwise polarization from -100 mV SCE and downwards, one would expect the current density to increase going along the activation controlled curve marked (1) in figure 21. An increase of the current density, however, leads to an increase of the pH at the surface which tends to reduce the i_o. So instead of sliding down a single activation controlled polarization curve like (1) in figure 21, the stepwise polarization jumps from one curve with $i_o = i_{o1}$ to another curve with $i_o = i_{o2}$, where $i_{o2} < i_{o1}$. The result is that we get a rather steep, diffusion controlled like curve where activation control is expected.

This model can also explain the poor sensitivity of the current density in this area to changes in the water flow (rotation speed) over short periods of time. When the rotation speed is increased for a specimen at e.g. -100 mV SCE, the surface pH will drop. This will allow a larger value of i_o and an increase in the current so that the "critical" pH is reached again. However, in contrast to the detrimental effect of increased pH the beneficial effect of lowering the pH has a slow response and no immediate current increase is observed.

Some aspects of the results in Fig. 16 can also be understood from the above model. For both platinum and 254 SMO there is no reduction of the current density during the first hour of oxygen removal. The reduction starts when the oxygen level is down to about 10 %. This is to be expected if the pH controlled current density is about one order of magnitude lower than the oxygen limiting current density.

The potential rise for freely corroding specimens is also a result of increased cathodic activity. The free corrosion potential is determined from the intersection of the anodic current density line and the cathodic current density line. Before a slime layer is formed a cathodic curve like C_o in Fig. 22 is observed. The anodic current density decreases with the time due to a thickening of the oxide layer and is indicated at 10^{-2} $\mu m/cm^2$ in Fig. 22. After some time this value is reduced to even lower values, e.g. 10^{-3} $\mu A/cm^2$ is

CONCLUSIONS

When "passive" metal and alloys such as stainless steels, titanium and platinum are kept in seawater at temperature below 30°C the microbial activity leads to an increase in the free corrosion potential. At cathodic polarization the same microbial activity leads to an dramatic increase in the oxygen reduction rate after a few days or couple of weeks of exposure. Both the increase in the open curcuit potential and the increased cathodic efficiency during cathodic polarization may be explained by an inhomogeneous biofilm formation, that is actually observed, containing clusters of bacteria colonies scattered around the surface. These bacteria colonies seem to form highly effective microcathodes where the exchange current for the oxygen reduction is strongly increased.

Due to the biofilm catalysis of the oxygen reduction reaction at weak cathodic polarization the pH at the surface increases to a maximum of 9.5 at a distance of 25 µm from the metal surface at maximum CD conditions. The maximum pH seems to be determined by the detrimental effect this increased pH has on the bacterial catalytic activity.

This critical pH limit proposed above fits several experimental observation, and gives an explanations to the typical shape of polarization curves recorded for samples preexposed at $E < E_{corr}$ that shows two limiting currents where the upper limiting current has shown not to be controlled by oxygen diffusion. The catalytic effect of the oxygen reduction reaction and its detrimental influence on corrosion tendency and rates does not exist at temperatures above 32°C for the sea water used in these experiments.

In the potential range -400 down to -800 mV the limiting current for stainless steel in sea water is quite independent of flow rate, also without a biofilm. The CD is possibly limited by some charge transfer resistance in the oxide layer.

RDE experiments shows that the catalytic effect of the biofilm on the increase in CD during cathodic polarization is only little dependent on flow rate. There seem to be a weak maximum CD at rotation rates between 500 and 1000 rpm. The maximum CD at potentials between +100 and -100 mV seem to be in the range 120-150 $\mu A/cm^2$.

ACKNOWLEDGEMENT

The presented results from work at The Corrosion Centre, SINTEF have been obtained in the research program "Corrosion resistant materials for process and sea water systems". The work has been financed by The Royal Norwegian Council for Scientific and Industrial Research (NTNF), Statoil, Avesta Jernverk AB and Sandvik AB.

REFERENCES

/1/ A. Mollica and A. Trevis, "The influence of the microbiological film on stainless steels in natural sea water". Proc. of the 4th Int. Cong. on Marine Corr. and Fouling. Juan-les-Pins, 351 1976.

/2/ J.M. Defranoux, Corr. Sci. 8, 245, 1968

/3/ R. Johnsen, E. Bardal: Corrosion, Vol 41, No 5, 296-302 1985.

/4/ R. Holthe, P.O. Gartland and E. Bardal: "Influence of the microbial slime layer on the cathodic properties of stainless steels in sea water". Proc. of EUROCORR '87, DECHEMA, Karlsruhe, April 1987.

/5/ R. Holthe, P.O. Gartland and E. Bardal: "Time dependence of cathodic properties of stainless steels, titanium, platinum and 90/10 CuNi in sea water". CORROSION 88, Paper no. 393, NACE, St. Louis, MO 1988.

/6/ V.G. Levich, Physicochemical Hydrodynamics, Pretice Hall 1962.

/7/ F.P. Berger and K.-F. F.-L. Hau, Int. J. Heat Mass Transfer, 20, 1185 1977.

/8/ S.R. Sanchez and D.J. Schiffrin, Corr. Sci., Vol. 22, No. 6, pp. 585-607, 1982.

/9/ R. Johnsen and E. Bardal: "The effect of microbiological slime layer on stainless steel in natural sea water". CORROSION 86 Paper no. 227, NACE Houston, Texas, 1986.

/10/ E. Littauer and D.M. Jennings: "The peventions of marine fouling by electrical currents". Proc. Int. Congr. on Marine Corr. and Fouling, 2nd pp. 527-536 1968.

/11/ H.P. Dhar, D.W. Howell and J. O'M. Bockris, J. Electrochem. Soc., Vol. 129, No. 10, p. 2178 1982.

/12/ A.S. Gordon, S.M. Gerchakov, L.R. Udey, Canadian J. of Microbiology, Vol. 27, p. 698 1981.

/13/ H.J. Engell and P. Forchhammer, Corr. Sci., Vol. 5, pp 479-488, 1965.

/14/ V. Scotto, R. DiCintio and G. Marcenaro: Corr. Sci., vol. 25, No. 3, p. 185 1985.

/15/ R. Nivens, P.D. Nichols, T.M. Henson, G.G. Geesey and D.C. White, Corrosion, Vol. 42, No. 4, 1986.

/16/ V. Scotto, G. Alabiso and G. Marcenaro: Bioelectrochemistry and Bioenergetics, 0 (1986) BEBO 0945, 1986

/17/ M.R. Tarasevic: Bioelectrochemistry and Bioenergetics, 6, 1979.

/18/ R. Holthe and P.O. Gartland: "Katodiske egenskaper til rustfrie stål i sjøvann. Effekt av marin biofilm". SINTEF report STF16 A87023, SINTEF, Trondheim, Feb. 1987.

/19/ A. Mollica, A. Trevis, E. Traverso, G. Ventura, V. Scotto, G. Alabiso, G. Marcenaro, U. Montini, G. De Carolis and R. Dellepiane, Proc. of the 6th Int. Congr. on Marine Corr. and Fouling, Athen, p. 269 1984.

/20/ S.C. Dexter and G.Y. Gao: "Effect of seawater biofilms on corrosion potential and oxygen reduction of stainless steel". Corrosion 87, paper no. 377, NACE, San Fransisco, California 1987.

/21/ W.A. Corpe: Marine Technology Society Journal, 13, 21-25 1979.

TABLE 1
CHEMICAL COMPOSITION OF THE METALS AND ALLOYS (WT %).

Material	C	Cr	Ni	Mo	Cu	Mn	N	Ti	Pt
Avesta 254 SMO	<0.02	20	18	6.1	0.7	0.5	0.2		
90/10 CuNi			10		90				
Titanium, pure								99.4	
Platinum, pure									99.9

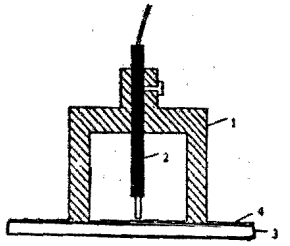

FIGURE 1 - Flat membrane pH electrode mounted in a PVC holder. (1) PVC holder. (2) pH electrode with a flat membrane sensing tip. (3) Sample materials. (4) Biofilm at the surface.

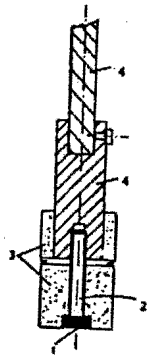

FIGURE 2 - Diagram of rotating disk electrode holder. (1) Sample material. (2) Stainless steel screw. (3) Epoxy resin holder. (4) Rotating disk holder shaft.

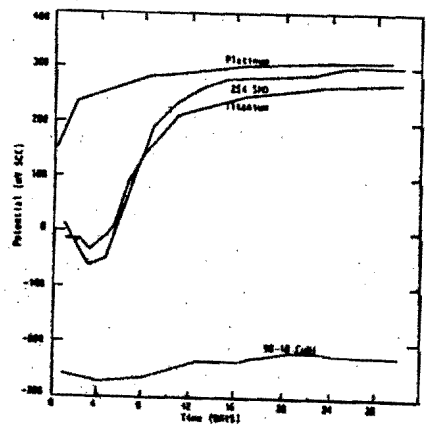

FIGURE 3 - The potential development on stainless steel 254 SMO, platinum, titanium and 90/10 CuNi in sea water at flow rate 1 m/s and temperature 12°C.

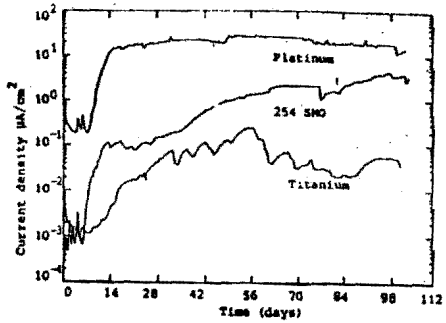

FIGURE 4 - Current density as a function of time at +100 mV SCE for stainless steel 254 SMO, titanium and platinum in nearly stagnant sea water and at temperature 9°.

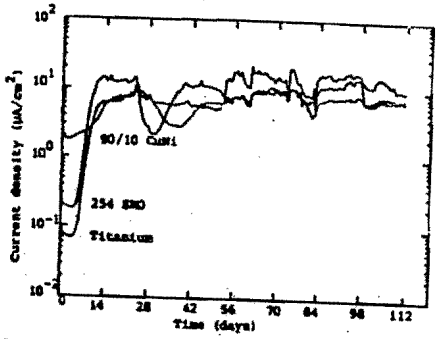

FIGURE 5 - Current density as a function of time at -300 mV SCE for samples of stainless steel 254 SMO, titanium and 90/10 CuNi in nearly stagnant sea water at temperature 9°C.

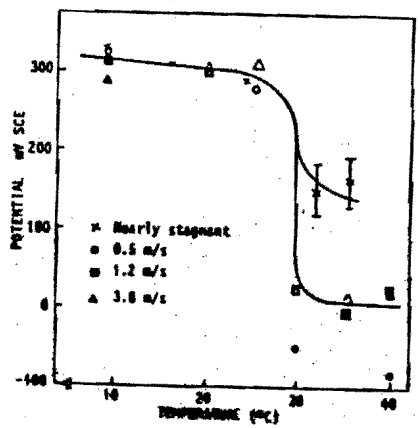

FIGURE 6 - The [illegible] potential of [illegible] after 30 days of [illegible] as a function of temperature at [illegible] flow rates.

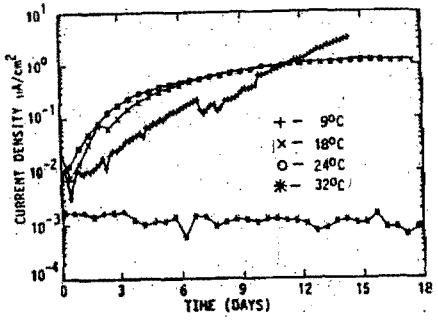

FIGURE 7 - The development of cathodic CD on stainless steel 254 SMO at +100 mV SCE (0 mV at 32°C). Preexposed for 14 days of free corrosion potential. At nearly stagnant conditions and 4 different temperatures.

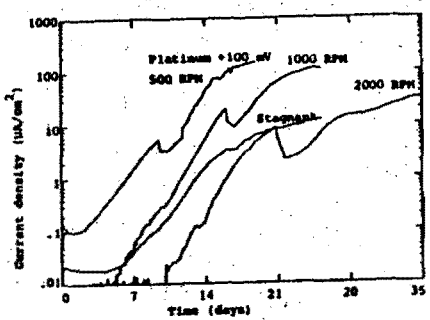

FIGURE 8 - Evolution of CD for RDE samples of 254 SMO polarised to -100 mV SCE at rotation rates 0, 1000 and 2000 rpm and platinum sample at +100 mV and rotation rate 500 rpm.

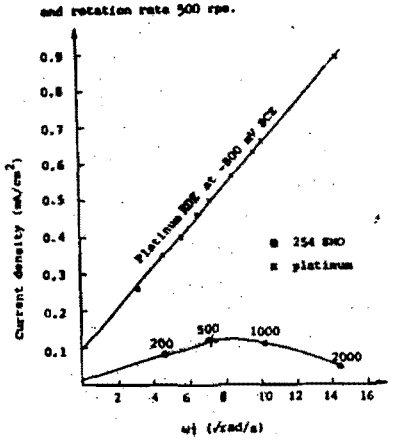

FIGURE 9 - CD as a function of $\omega^{1/2}$ for a platinum RDE sample polarized to -800 mV SCE compared to the

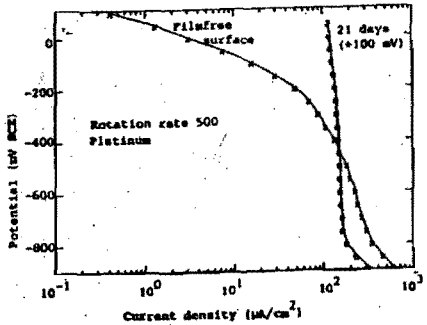

FIGURE 10 - Potentiodynamic curves for platinum samples with (after 21 days at +100 mV, see Fig. 7) and without biofilm.

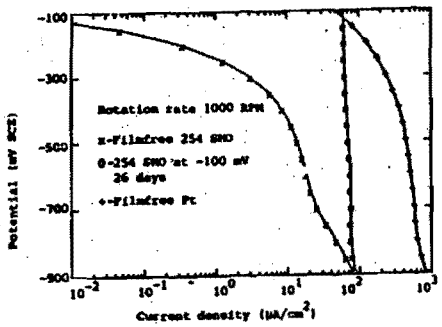

FIGURE 11 - Potentiodynamic curves for samples of 254 SMO with (after 26 days at -100 mV, see Fig. 7) and without biofilm.

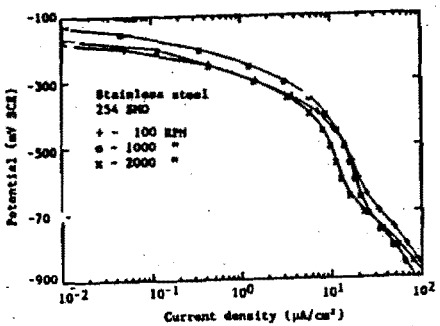

FIGURE 12 - Potentiodynamic curves for samples of 254 SMO at different rotation rates.

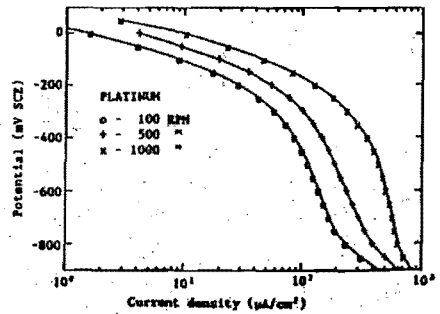

FIGURE 13 - Potentiodynamic curves for samples of platinum at different rotation rates.

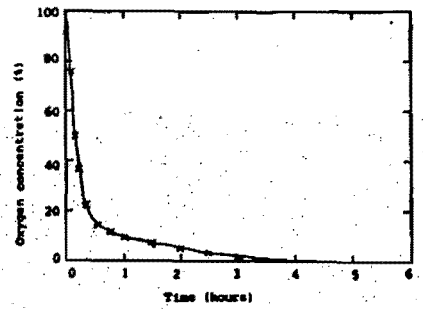

FIGURE 15 - Oxygen concentration during the first 12 hours of purging nitrogen through a closed cell for experiments shown in Figs. 15 and 16.

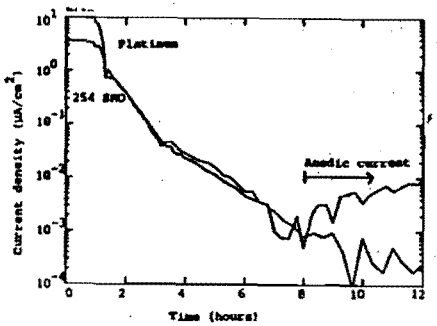

FIGURE 16 - Effect on CD of removing oxygen from sea water according to Fig. 15 for samples of platinum and 254 SMO preexposed in 3 weeks in sea water

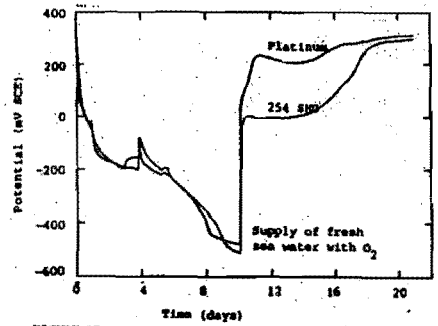

FIGURE 17 - Potential during oxygen removal for samples of platinum and 254 SMO preexposed at free corrosion potential for 3 weeks.

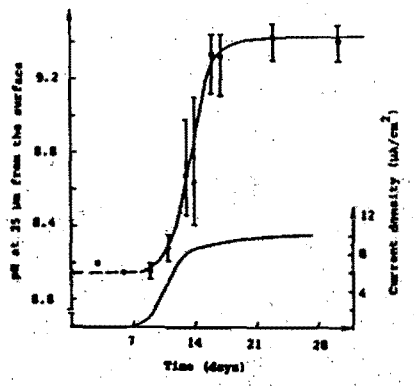

FIGURE 14 - pH measured at 25 μm distance from surface of stainless steel 254 SMO polarised to -100 mV SCE as a function of time. At the right y-axis the CD as a function of time for the same sample.

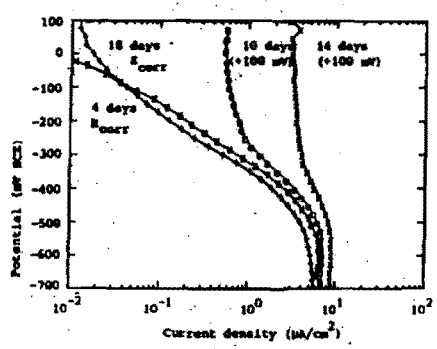

FIGURE 18 - Potentiodynamic curves on 254 SMO steel recorded after 1 and 18 days of free exposure and at 10 and 14 days at +100 mV SCE respec-

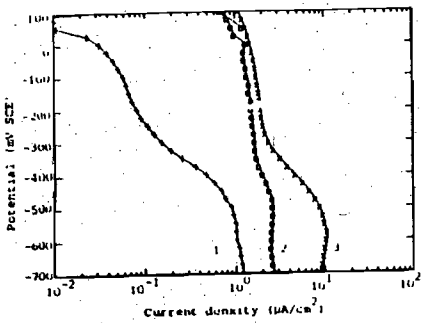

FIGURE 19 - Potaniodynamic curves on 254 SMO exposed at different conditions

1) Free exposure for 24 hours. O_2 concentration 10 %
2) Preexposodd at +100 mV for 2 weeks. O_2 concentration 10 %
3) Preexposed at +100 mV for 2 weeks. O_2 concentration 100 %

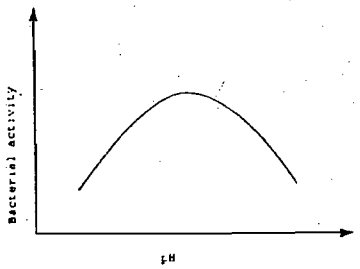

FIGURE 20 - Schematic illustration of bacterial activity as a function of pH.

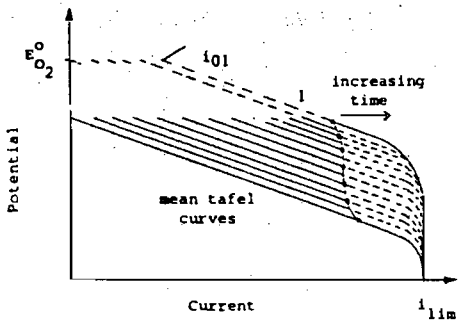

FIGURE 21 - Schematic illustration of the situation during potentiodynamic polarization of a sample pre-exposed at $E < E_{corr}$ with pH limiting current as described in the text.

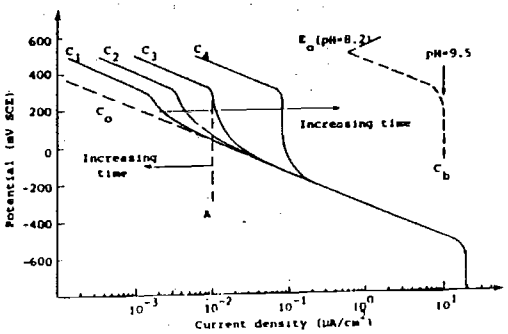

FIGURE 22 - Schematic illustration of the changes in the cathodic polarization curve due to an increased relative area of super active micro-cathodes with the time.

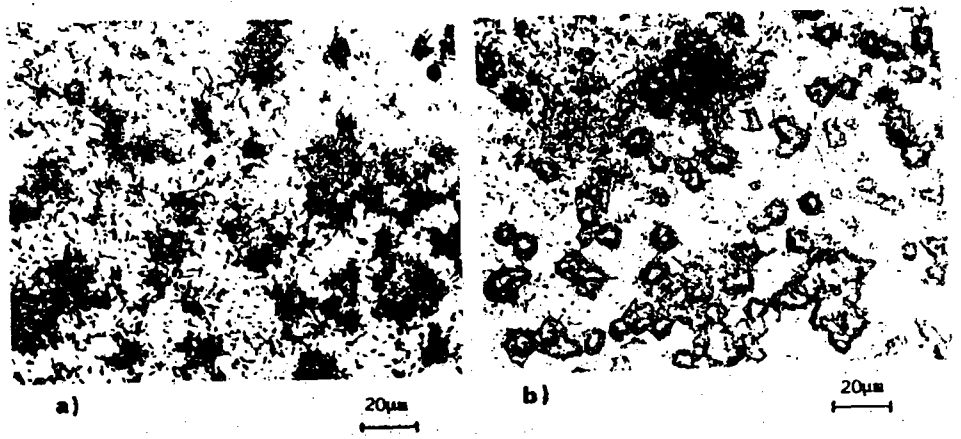

FIGURE 23 - Optical micrographs of bacteria colonies on surface of stainless steel after 26 days of exposure at -100 mV in sea water.

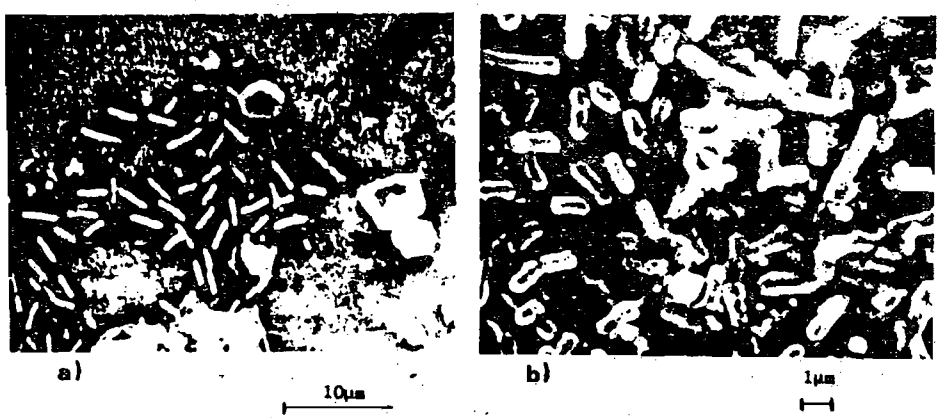

FIGURE 24 - SEM micrographs of bacteria colonies on surface of stainless steel at two different magnifications.

CORROSION OF THE BRAZED JOINT BETWEEN Cu90Ni10Fe PIPES

P. Vassiliou[1] and V. J. Papazoglou[2]
National Technical University of Athens
[1] Department of Chemical Engineering, Section of Material Science and Engineering, Laboratory of Physical Chemistry and Applied Electrochemistry
[2] Department of Naval Architecture and Marine Engineering, Laboratory of Shipbuilding Technology

ABSTRACT

The corrosion behaviour of brazed Cu90Ni10Fe pipes with circulation of 3.5% NaCl solution was investigated in laboratory conditions at 30±2 °C and at a Reynolds Number of 17900. The brazed joint was also examined under the metallographic microscope. The corrosion rate equation obtained is compared with the corrosion rates of non-brazed pipes and of pipes which underwent the same thermal treatment as the brazed ones. Metallographic photographs of the joint before and after the exposure are presented and analyzed. Significant differences were found in the corrosion rates of the cases considered.

GENERAL

The family of CuNiFe alloys has been in use for the last forty or so years under conditions of severe sea water corrosion, because of their resistance in pitting corrosion. Several researchers have studied the seawater resistance of CuNiFe alloy pipes under various flow conditions (1-3). All the above researchers have studied extensively the conditions for the formation of the protective film, since the excellent corrosion resistance of the alloy is based on this film, a phenomenon that is more pronounced when the alloy contains a small amount of iron. IJsseling (2) presents data that indicate corrosion rates equal to 50-250 μm/yr during film formation, 5-20 μm/yr after film formation, and 1-2 μm/yr after an exposure of 10-14 yrs, as these were measured by other authors (4,5). Other data existing in the literature, concerning exposure in seawater under stagnant conditions (6), indicate corrosion rates for the 706 Alloy between 0.3 and 1.1 mpy for an exposure period between 181 and 608 days. Similarly, for the 962 Cast Alloy corrosion rates fluctuate from 0.9 to 1.1 mpy for an exposure period between 181 and 366 days. Finally, data presented by other authors for the 706 Alloy (7) give a corrosion rate of 0.02 mm/yr.

In this work, an investigation is made on the corrosion behaviour of brazed Cu90Ni10Fe pipes, and a mathematical expression, derived from short term experimental data, is presented for the corrosion equation of brazed pipes.

EXPERIMENTAL PROCEDURE

The specimens used were pieces of pipes made of Cu90Ni10Fe alloy used in standard naval applications, with an internal diameter of 2.14 cm and an external diameter of 2.53 cm. The length of each piece was approximately equal to 10 cm. The nominal composition of the alloy was Cu: 87.3%, Ni: 10%, Fe: 1.7%, and Mn: 1%, and its specific gravity was 8.94 g/cm^3.

The specimens used were cut from long pipes, their edges were smoothed out with emery paper and they were subsequently degreased in petroleum ether and acetone to remove the protective oil of the factory. The specimens were cleaned from the oxides with inhibited hydrochloric acid, washed with water and dried in alcohol and acetone. The inhibitor was then removed with steel wool. The specimens were subsequently weighed and properly marked for identification purposes.

All specimens were torch brazed using the silver alloy filler metal BS AG5, in the form of a ring, with the following nominal composition: Ag 42-44 %, Cu 36-38 %, Zn 18.5-20.5 %. The internal diameter of the ring was 2 mm smaller than the external diameter of the specimens. The ring was placed over both pieces that were to be joined together. Melting of the filler metal was accomplished using an oxygen flame for a period of 3 min, the resulting temperatures being in the order of 650-700 °C. Simultaneously with the brazing operation, cleaning of the inside and outside specimen surfaces was performed using borax

powder ($No_2B_4O_7.10H_2O$). By brazing two pieces of pipe of approximately 5 cm long each, the final length was close to 10 cm. For each experiment three specimens were used for reasons of reproducibility.

For comparison purposes, the same thermal treatment was performed on pieces of pipe that had not been brazed. More specifically, this treatment consisted of heating the pipe pieces at approximately 700 °C with an oxygen torch for the same length of time as for the brazing (approximately 3 min), and then letting the pipes to cool down at a slow rate.

To conduct the experiments, the specimens were connected to a pump with pieces of a plastic reinforced pipe of approximately 15 cm long. The circulating conditions were on a fully recirculating stream with periodical change of the solution every 48 hours. Thus the solid influence on the film formation were kept to a minimum. The corrosive environment that circulated through the specimens was a 3.5 % NaCl solution. All experiments were performed at 30±2 °C. At prespecified time intervals the exposed specimens were removed, washed, cleaned with inhibited hydrochloric acid, dried and weighed for loss of weight due to corrosion. Curves were thus produced of weight loss versus time. The weight loss method was employed as the most direct method for determining the corrosion rate, assuming that the flow velocity is very low, and hence that there is no erosion involved. For this short exposure period it was assumed that a more or less uniform corrosion occured, since there were no pits formed on the internal surface of the pipes.

Note that the pump operated at a 12.91 liters/min load, thus producing a corrosive fluid velocity equal to 0.6 m/sec, corresponding to a Reynolds Number equal to 17900.

RESULTS AND DISCUSSION

All results presented in this section correspond to a continuous flow of 3.5% NaCl solution inside the pipes, but differ in the exposure conditions of the outside surface of the pipes, which are described separately for each case.

The results from the experiments with the reference pipes, namely with pipes that were neither brazed nor heat treated and whose outside surface was exposed to a dry atmosphere, are shown in Figure 1. The resulting mathematical equation for the corrosion rate, derived by least square approximation techniques, is:

$$y = 3.90*10^{-4}*t^{0.197} \qquad (1)$$

For the thermally treated specimens, exposed on the outside surface in a dry atmosphere, the experimental results are shown in Figure 2, whereas the corrosion rate equation was found to be:

$$y = 6.31*10^{-4}*t^{0.167} \qquad (2)$$

The brazed specimens, exposed on the outside surface also in a dry atmosphere, gave the results shown in Figure 3 and the following corrosion rate equation:

$$y = 8.17*10^{-4}*t^{0.171} \qquad (3)$$

When the brazed specimens had their outside surface exposed in an equilibrium atmosphere over a 3.5% NaCl solution at 30 °C, they gave the results of Figure 4 and the following equation:

$$y = 10.73*10^{-4}*t^{0.140} \qquad (4)$$

The exposed in the flowing solution of 3.5% NaCl surface of the brazed joint was observed under the metallographic microscope, before and after the exposure (see Figures 5 and 6). The edges of the grains were etched with an attack by a saturated solution of $(NH_4)_2S_2O_8$ at 40 °C and were observed under a microscope with a magnification of 150. A diffusion of copper ions in the silver brazing is observed, which appears to lessen in amount after the exposure, as shown in the photographs. The presence of silver creates anodic conditions that enhance the corrosion of copper due to galvanic action. It thus appears that the corrosion rate of the brazed pipes results from two simultaneous processes. The one is the anodization of the CuNi alloy due to the presence of silver, and the other is the effect of the thermal treatment of the pipe during the brazing process. This latter effect is

also evident from the results obtained in the thermally treated specimens (see eq. 2), and from the similarity of the rate constants in eqns (2) and (3).

The resulting mathematical equations (1) to (4) show that there is a tendency for higher corrosion rates for the thermally treated and the brazed Cu90Ni10Fe pipe, as expected. Furthermore, the equations show a high corrosion tendency for the pipe specimens exposed simultaneously to the NaCl environment on the outside and to the saline water on the inside.

It can, thus, be concluded that when designing a heat exchanger, or any other system for that matter, using Cu90Ni10Fe, one should take under consideration the equations for the brazed specimens in order to predict the longevity of the system.

ACKNOWLEDGEMENTS

Part of the work reported has been performed as part of Mr. N. Papayoannou's diploma thesis in the Dept. of Naval Arch. and Marine Engineering. The authors wish to thank the Hellenic Shipyards, Scaramangas, Greece for kindly providing all the material required for the specimens.

REFERENCES

(1) F. P. IJsseling, L. P. Drolenga and B. H. Kolsker, Brit. Corrosion J., 1982, 17(4), p. 162.
(2) F. P. IJsseling, Reviews on coatings and corrosion, Vol. IV, no. 3, 1981, p. 269.
(3) F. P. IJsseling, J. M. Krougman,and L. J. P. Drolenga, Proc. 5th Intern. Congress on Corrosion and Fouling, Barcelona, Spain, 1980.
(4) J. M. Popplewell, Paper No. 21, NACE Corr. Conf., Houston, 1978.
(5) K. D. Efird and D. B. Anderson, Materials Performance, 14 (11), 1975, p.37.
(6) M. Schumacher (ed.), Seawater Corrosion Handbook, Noyes Data Corp., N. Jersey, U.S.A., 1979.
(7) I. R. Scoles, J. C. Rowlands, Proc. 6th European Cong. Met. Corrosion, London, England, Sept. 1977.

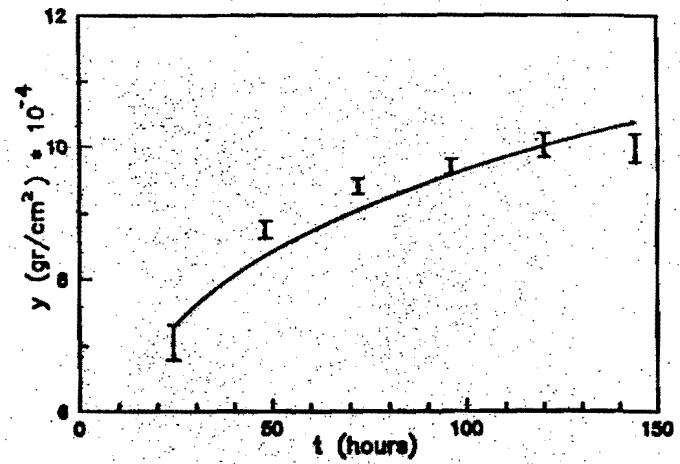

Fig. 1 Corrosion rate for reference CuNiFe pipes under flow conditions of 3.5% NaCl solution

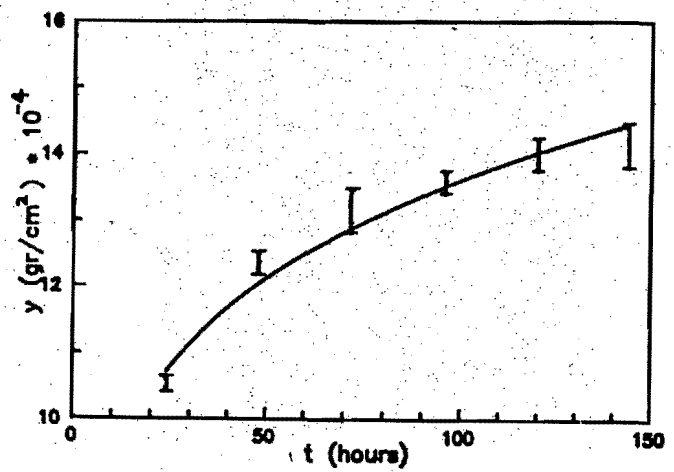

Fig. 2 Corrosion rate for thermally treated CuNiFe pipes under flow conditions of 3.5% NaCl solution

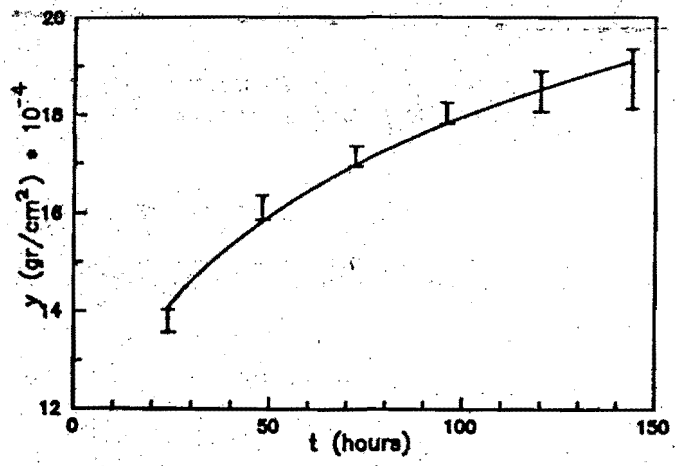

Fig. 3 Corrosion rate for brazed CuNiFe pipes under flowing conditions of 3.5% NaCl solution

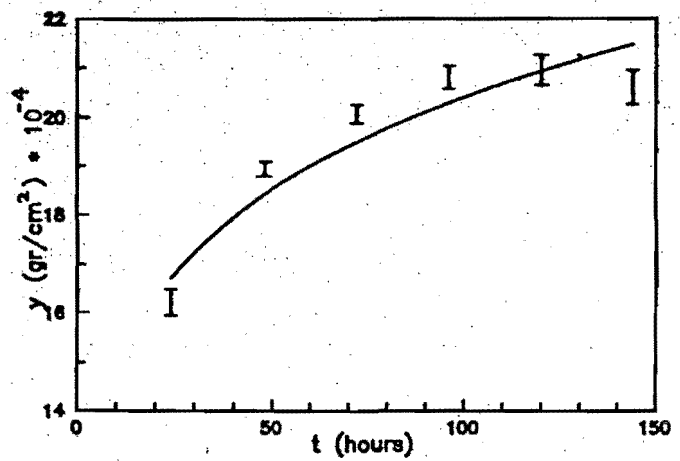

Fig. 4 Corrosion rate for brazed CuNiFe pipes under flowing conditions of 3.5% NaCl solution with simultaneous exposure in a saturated atmosphere over the NaCl solution

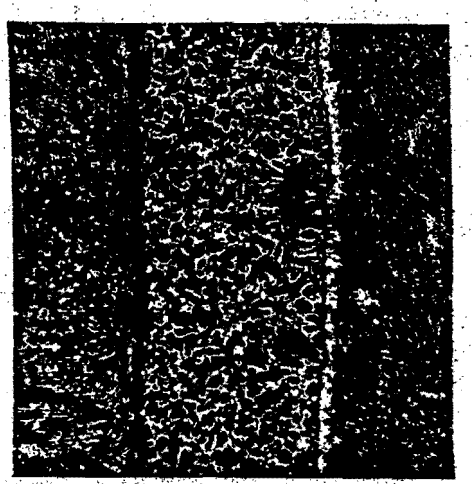

Fig. 5 Microphotograph of the brazing before the corrosion exposure (150 enlargement)

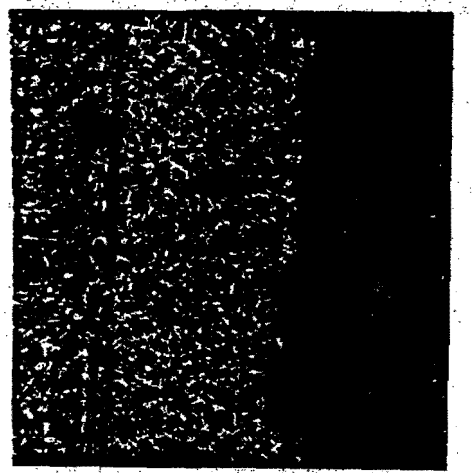

Fig. 6 Microphotograph of the brazing after the corrosion exposure (150 enlargement)

CATHODIC PROTECTION OF STEEL IN PURE CULTURES OF THE MARINE BACTERIA VIBRIO NATRIEGENS

L. FIKSDAL (1) and J. GUEZENNEC (2)

(1) N.T.H University of Trondheim (NORWAY)
(2) IFREMER Centre de Brest BP 70 29263 PLOUZANE

ABSTRACT

Stainless steel has been exposed to enriched natural seawater with or without the marine bacteria *Vibrio natriegens* in short term laboratory experiments. Specimens were freely exposed or polarized to potentials from -700 to -900 mv SCE. At the end of the exposure period polarisation curves and AC-impedance diagrams were determined. Due to the presence of bacteria, current density demand increased during cathodic polarization of specimens to -800 and -900 mv SCE, precipitation of Mg- and Ca-compounds on the metal surface decreased as did also the charge transfer resistance value measured during AC-impedance analysis.

INTRODUCTION

Cathodic protection of steel constructions exposed to sea water is widely used to prevent corrosion. The presence of bacterial films on the metal surface is demonstrated to increase the free potential and to change the current density requirement during cathodic protection (Mollica et al., 1984, Johnsen and Bardal, 1986). These results are obtained with biofilms in nonsterile environment where the biofilm contains a mixture of naturally ocurring bacterial species.
Biofilms may have an influence on electrochemical reactions on the metal surface in different ways: The physical presence of a biofilm can create differential aeration cells, and metabolic activities such as production of extracellular enzymes, organic acids, polysaccharides etc. may have an effect on surface reactions by decreasing

activation energy, changing pH or creating differential aeration cells. It is suggested that biofilms in natural sea water modify the activation controlled part of cathodic oxygen reaction but the exact mechanism is not known (Johnsen and Bardal, 1985, Scotto et al., 1985). Studies of monobacterial biofilms may be helpful in understanding the mechanism, because growth and metabolism of this type of biofilm can be more easily controlled and changed than with a multibacterial biofilm.

The objective of the present study was to investigate the influence of a single bacterial species, *Vibrio natriegens*, on electrochemical surface reactions and current density demand during cathodic protection of steel in sea water. The results obtained can be useful in evaluating the role of *V.natriegens* in natural biofilms that modify metal surface activities, and could also be important for understanding the mechanism by which the biofilm interfer with reactions on the metal surface.

EXPERIMENTAL PROCEDURE

Coupons. 17 C-steel plates (Table 1), approximately 2x4.5cm², were polished with decreasing grain size, from 120 to 1000 mesh, and rinsed with acetone.

Experimental system and medium. The coupons were placed in a glass flask (Fig.1) which were autoclaved (15 min at 120°C) and filled with ca.800 ml sterile, modified Oppenheimer-Zobell (1952) medium: 1 mg/l pepton (Difco), 0.2 mg/l liver extract (Difco), 0.01 mg/l glucose, in natural sea water. The glucose was sterilized separately and added after the medium had cooled. The experiments were done at 21-23°C and with stirring at 500 rpm.

Organism. *Vibrio natriegens*, ATCC 14048, DSM 759, were received from Deutsche Sammlung von Microorganismen. Cultures in the experimental system were inoculated to approximately 10^6 cells/ml using 8 ml from organisms grown in test tubes for 48 hrs (stationary phase organisms). Stocks were maintained on agar slants at 4° C. Culture purity was followed microscopically and by colony morphology.

Electrochemical measurements. 4 metal coupons were polarized to the same fixed potential (-900, -800 or -700 mv SCE) or freely exposed. The electric current supply to the polarized specimens was recorded as a potential drop over a 100 ohm resistor. The potential of freely exposed specimens was measured relative to a saturated calomel reference electrode.

At the end of each experiment, uptake of polarization curves was done with Solatron 1286 electrical interface controlled by a Olivetti computer, AC-impedance analysis was done with Solatron 1170 frequency analyzer through a Solatron interface.

Bacterial analyzes: During experiments, viable bacteria in the liquid phase were recovered on Oppenheimer-Zobell agar and counted after 2 days incubation at 25°C. Bacteria on the metal surfaces were coloured with acridine orange (0.01%) and counted with epifluorescense microscope at 1000 times magnification.

Chemical analyses. Lipid content of the biofilm was analyzed as described by White et al (1979) and Guezennec (1986) Ca- and Mg-concentrations on the metal surface were determined by atomic absorption spectroscopy after rincing of the coupons in phosphate buffered saline solution (pH 7.2) and dissolution of Ca- and Mg-compounds in 0.1 M acetic acid.
Oxygen in the liquid phase was measured using the Winkler method.

RESULTS AND DISCUSSION

After 12-24 hrs. of exposure, the current density demand of steel coupons polarized to -900 and -800 mv SCE in the presence of V.natriegens, increased as compared to sterile environment, but did not increase at -700 mv SCE (Fig. 2).

Enumeration of attached bacteria at the end of each experiment, demonstrated that when V.natriegens was present, the number of bacteria on metal surfaces was in the range of 10^6-10^7/cm² (Table 2), a density commonly found on metal surfaces after 1-6 days in natural sea water (Marzalek et al., 1979). Because bacterial numbers remained approximately the same at all potentials, other factors than number of attached cells seemed also to be important in determining the influence of V.natriegens on current density demand of coupons polarized to constant potential in the present study.

Some attached bacteria were also found on coupon surfaces in sterile environments (Table 2). These bacteria may have originated from the natural sea water used in the medium. They were killed during the sterilization of the medium, as indicated by the zero colony forming unit counts of environments without V. natriegens (Table 3).

Analysis of fatty acids on coupon surfaces demonstrated the presence of fatty acids characteristical of bacterial membranes, as cis vaccenic acid (C18:1w7c), cis palmitoleic acid (C16:1w7) and branched pentadecanoic (C15:0) and heptadecanoic acid (C17:0) in environment with V. natriegens.
Lipid phosphate is often used as measure of viable biomass, and in many bacterial strains the average content is 50 µmol lipid-P/g dry weight (White et al., 1979). By using a fatty acid to phosphate molar ratio of 2: 1, we calculated bacterial densities on surfaces exposed to different potentials to be in the range of $3x10^7$ to $7x10^7$ cells/cm². The cell numbers calculated from lipid analysis seem to confirm that bacterial attachment was not influenced by the potential level of coupons.

Changes in pH and production of H_2O_2 at the metal surface are suggested as reasons for changes in absorption of bacteria on metal during cathodic protection (Dhar, 1986, Gordon et al., 1981). The relatively high and constant attached cell numbers which were found at all imposed potentials in the present study, may indicate that H_2O_2-production and/or pH- changes at the metal surfaces, were not sufficiently significant to reduce bacterial absorption.
Measurements of pH and oxygen showed for all potentials the same pH(8.4±0.1) and aerobic conditions in the liquid phase at the end of the experiments (Table 3).

The polarization behaviour of steel coupons which have been kept 68 hrs at -800 mv SCE and 42 hrs at free potential, in environments with and without V.natriegens, is shown in Fig. 3. For coupons kept at -800 mv and at -900 (not shown in the figure), the cathodic polarization curve moved to the right when bacteria were present, while the curves were less different for coupons kept at free potential. The results obtained in the presence of V.natriegens seem to be in accordance with data from previous work where a change of cathodic properties of stainless steel was observed when biofilm developed on polarized specimens in natural seawater (Mollica et al., 1984; Johnsen and Bardal, 1985).

As a result of pH-increase during cathodic polarisation in sea water, calcium carbonate and magnesium hydroxide may precipitate as a deposit on the metal surface. Analysis of Ca and Mg demonstrated that these elements were present on the surface when metal coupons were polarized to -700 mv SCE or lower potentials (Table 4) in solutions with and without V.natriegens. Presence of bacteria did, however, decrease the precipitation. This decrease may be related to a lower interface pH caused by bacterial production of organic acids. Analysis of acetate demonstrated that volatile fatty acids were produced in the liquid phase, in the presence of bacteria (data not shown). In sterile solution, at -900 mv SCE, the Ca/Mg (w/w) ratio was ca.1. This ratio incrased when bacteria were present on the surface.

AC-impedance analyses performed after removing the cathodic potential and allowing samples to return to free potential, showed that for all potentials, the complex plane diagrams exhibited single depressed capacitive loops with centers below the real axis as demonstrated by examples in Fig. 4. Double layer capacitance varied in the range of 0.1-0.2 mF / cm² in solutions with and without bacteria. Without V.natriegens on the surface, the charge transfer resistance, Rt, varied in the range of 55-65 kohm.cm², with the unexpected exception of the high value 153 kohm.cm² obtained at -700 mv SCE. Bacterial attachment decreased Rt -values from 58, 153, 60, 65 kohm.cm² to 31, 125, 32, 53 k ohm.cm² at free potential, -700, -800, -900 mv SCE respectively. This decrease in charge transfer resistance indicate a higher corrosion current density due to the presence of the the biofilm.

CONCLUSIONS

Attachment of the marine bacteria V.natriegens to 17 C steel coupons polarized to -800 and -900 mv SCE increased the current density demand compared to sterile controls.

Presence of V. natriegens on metal surfaces, polarized to potentials below -700mv SCE, moved cathodic polarisation curves to the right as compared to controls. This may indicate that V.natriegens participate in increasing the cathodic reaction efficiency during cathodic polarization of steel in natural sea water.

AC-impedance analysis demonstrated that presence of V. natriegens decreased the charge resistance value thus indicating higher corrosion current density than in environment without V. natriegens.

Mg-and Ca-compounds were precipitated on polarized metal surfaces, but presence of V.natriegens decreased the precipitation.

ACKNOWLEDGEMENTS

The authors are extremely grateful for the financial support provided as fellowships to L.F. by the Royal Norwegian Council for Scientific and Industrial Research (NTNF) and by Elf Aquitaine. We would also like to thank Jean-Pierre LE ROUX and Max CONTE for their invaluable technical assistance.

REFERENCES

Dhar, H.P. (1986). Electrochemical methods for the prevention of microbial fouling. in Modern Bioelectrochemistry. eds. F. Gutmann and H. Keyzer. Plenum Press, New York.

Guezennec, J. (1986). La colonisation bactérienne des surfaces métalliques exposées en milieu marin. Utilisation des lipides bactériens. Thèse de Doctorat Université Paris VI.

Gordon, A.S., Gerchakov, S.M. and Udey, L.R. (1981). The effect of polarization on the attachment of marine bacteria to copper and platinum surface. Can. J. Microbiol. 27, pp. 698-703.

Johnsen, R. and Bardal, E. (1985). Cathodic properties of different stainless steels in natural sea water. Corrosion 41, pp. 296-302.

Johnsen, R. and Bardal, E. (1986). The effect of a microbiological slime layer on stainless steel in natural sea water. Proc. Corrosion/86 NACE, Houston, Texas.

Marszalek, D.S., Gerchakov, S.M. and Udey, L.R. (1979). Influence of substrate composition on marine microfouling. Appl.Environ. Microbiol. 38, pp. 987-995.

Mollica, A., Trevis, A., Traverso, E., Ventura, G., Scotto, V., Arabiso, G., Marcenaro, G., Montini, U., De Carolis, G. and Dellepiane, R. (1984). Interaction between biofouling and oxygen reduction rate on stainless steel in sea water. Proc. 6th Int. Congr. on Marine Corrosion and Fouling, Athens, Greece.

Oppenheimer, C.H. and Zobell, C.E. (1952). The growth and viability of sixty three species of marine bacteria as influenced by hydrostatic pressure. J. Mar. Res. 11, pp. 10-12.

Scotto, V., Di Cintio, R. and Marcenaro, G. (1985). The influence of marine aerobic biofilm on stainless steel corrosion behaviour. Corros. Sci. 25, pp. 185.194.

White, D.C., Bobbie, R.J., Herron, J.S., King, J.S., and Morrison, S.J. (1979). Biochemical measurements of microbial mass and activity from environmental samples. In : J.W. Costerton and R.R. Colwell (Eds), Native Aquatic Bacteria : Enumeration, Activity and Ecology. ASTM STP 695, American Society for Testing and Materials, Philadelphia, p.p. 69-81.

Table 1. Chemical composition of the alloy 17 C (wt %)

C	Cr	Ni	Mo	Cu	Mn	Si	P	S
0.013	17.66	11.54	2.15	0.35	1.37	0.52	0.0027	0.0013

Table 2. Numbers of bacteria on steel (17 C) coupons polarized to different potentials in environment with (+) and without (-) V. natriegens.

potential (mv SCE)	attached bacteria (cells/cm²) -	+
-900	1.3 10^4	4.6 10^6
-800	2.5 10^3	2.9 10^6
-700	4.5 10^3	1.2 10^6
Free pot.	2.0 10^3	6.4 10^6

Table 3. Measurement of pH, O_2 and viable bacteria in the liquid phase at the end of polarization of steel (17 C) coupons to constant potential in environment with (+) and without (-) V. natriegens.

Potential (mv SCE)	O_2 (mg/l) -	+	pH -	+	bacteria (CFU/ml) -	+
-900	6.7	5.4	8.6	8.4	0	7.5 10^9
-800	6.7	5.3	8.6	8.5	0	2.6 10^9
-700	6.1	5.1	8.4	8.3	0	5.6 10^8
free pot.	6.1	5.2	8.5	8.3	0	3.3 10^8

1) CFU = colony forming units.

Table 4. Ca and Mg (ng/cm²) on coupon surface at the end of polarization of steel (17 C) coupons to constant potential in environment with or without V. natriegens.

Potential (mv SCE)	Without bacteria Ca	Mg	Ca/Mg (w/w)	With bacteria Ca	Mg	Ca/Mg (w/w)
-900	19.5	10.2	1.1	18.8	12.1	1.6
-800	17.8	8.9	2.0	13.7	4.8	2.9
-700	10.4	3.2	3.3	7.3	1.2	6.1
free pot.	2.3	0.5	4.6	1.9	0.1	19

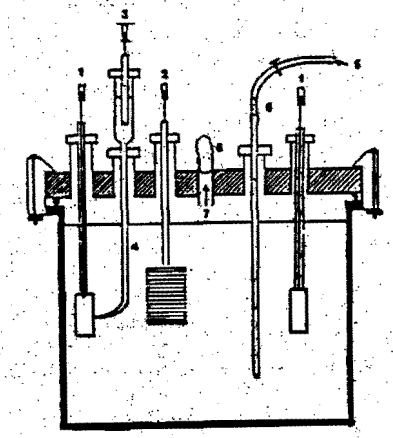

Figure 1. Schematic diagram of experimental system with steel coupons (1), counter electrode (Pt) (2), reference electrode (saturated KCl (3) in a tube with a glass frith in the end and filled with medium (4), air inlet (5), cotton plug (6) and air outlet (7).

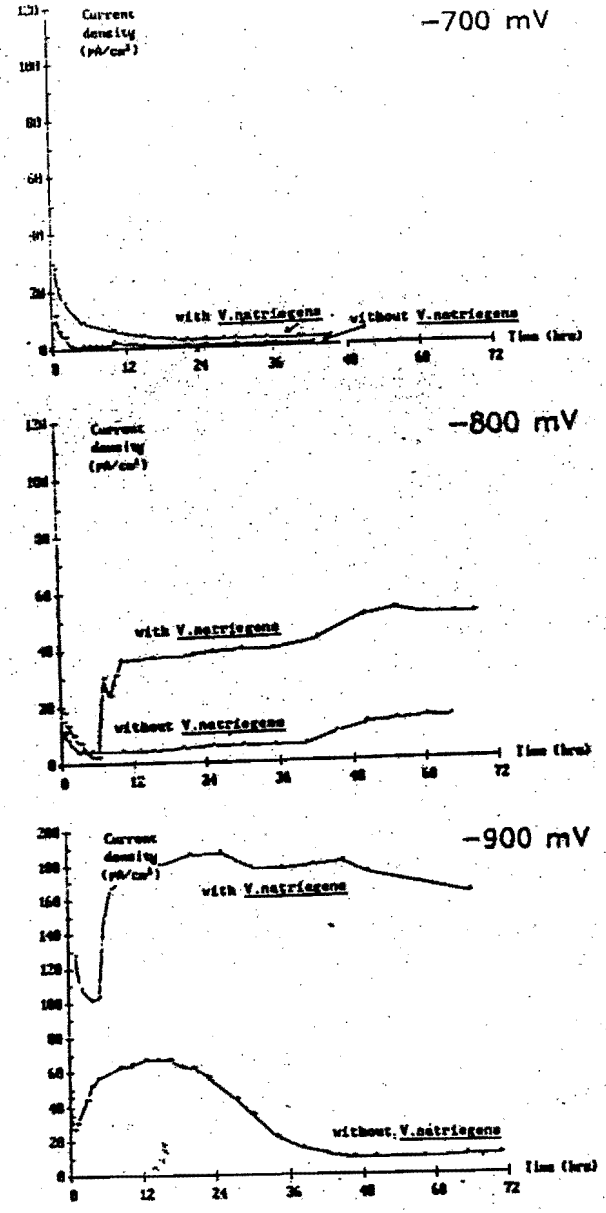

Figure 2. Cathodic current density demand of steel (17 C) coupons polarized to -700, -800 and -900 mv SCE in environment with and without V.natriegens.

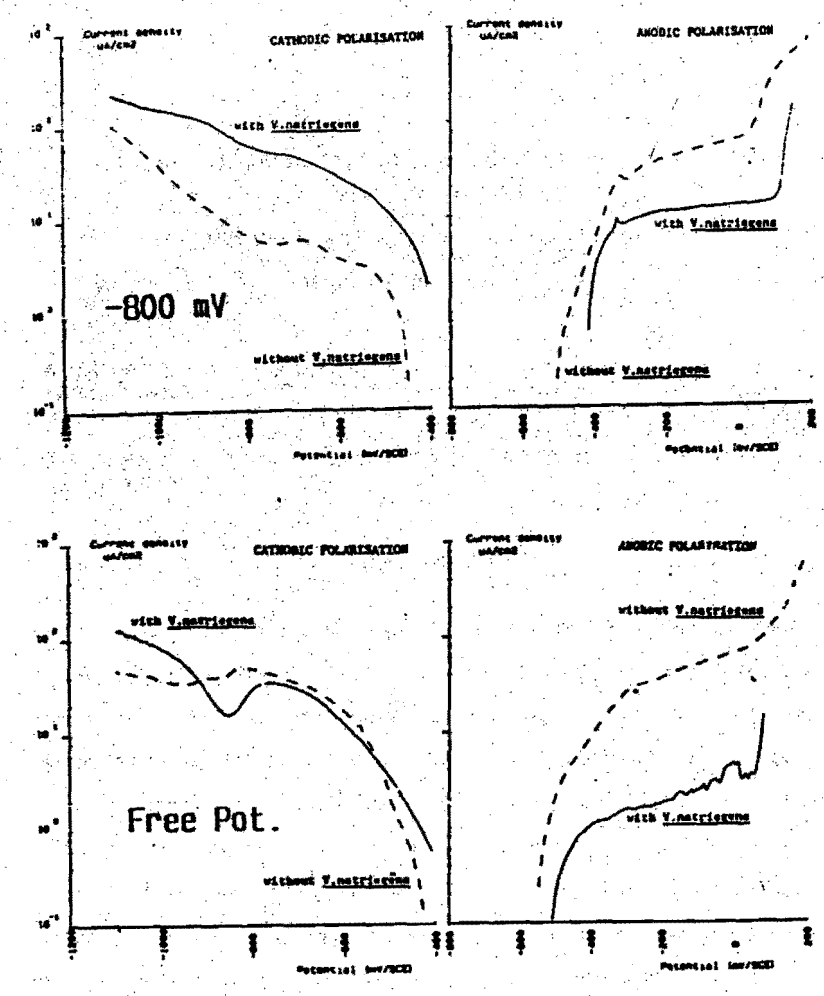

Figure 3. Cathodic and anodic polarization curves after 42 hrs exposure of steel (17 C) coupons at free potential and after 68 hrs exposure at -800 mv SCE in environment with and without V.natriegens.

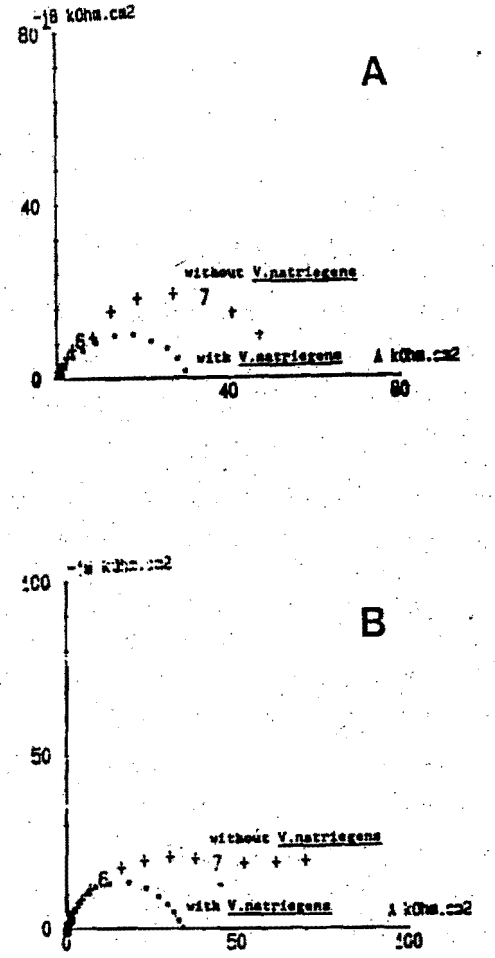

Figure 4. AC-impedance curves of steel (17 C) coupons after 42 hrs exposure at free potential (A) and 68 hrs exposure at -800 mv SCE (B), in environment with and without V. natriegens.

ON THE BARNACLE-INDUCED CREVICE CORROSION PHENOMENON IN STAINLESS STEEL

M.Eashwar, G.Subramanian and P.Chandrasekaran
Corrosion Research Centre, CECRI Unit,
Mandapam Camp - 623 519, India

ABSTRACT - Barnacles induce crevice corrosion in stainless steels which usually resemble the shape of the base of their shells. This investigation has been carried out to elucidate the most probable mechanism by which such crevices occur. Based on a series of experiments with 304 SS, a model is proposed on how crevices nucleate and propogate. The role of oxygen and bacteria are highlightened.

INTRODUCTION

Perhaps the most striking instance of biological corrosion in seawater is the attack influenced by barnacles in stainless steels and nickel alloys. LaQue (1948) has shown that weight losses were enormous for stainless steel specimens subjected to natural attachment of marine organisms, whereas, those held in a flume with seawater flowing fast enough to discourage marine growth, suffered little damage. Relini, et al., (1976), provide additional proof for the higher rates of attack induced by barnacles. These workers have compared corrosion losses of two sets of panels, one allowed to gather natural marine growth and the other protected from fouling using phyto or zoo-plankton nets. There have been a number of other instances (LaQue 1972, Degerbeck 1971, Rowlands 1976, King 1980, Pipe 1981, Ravindran & Pillai 1984, Eashwar et al., 1987a) where barnacle-induced attacks have been described as a characteristic phenomenon

in stainless steels occuring, primarily, beneath the shells of dead organisms. Also, Riumu, et al., (1984), have observed similar attacks on nickel alloys.

In spite of extensive marine corrosion research for decades, this phenomenon has been neglcted by scientists for its details such as why and how it occurs. This has been pointed out by LaQue (1982) who regards this area as a promising topic for research in marine corrosion.

This investigation has been taken up to elucidate the most probable mechanism by which crevice corrosion occurs on 304 stainless steel.

MATERIALS AND METHODS

Type 304 stainless steel (Nominal composition = Fe/Cr 18/Ni 8/C 0.07) was chosen for the present study. Sheets, 1.1 mm thick, were cut into panels of size 150 mm x 50 mm. They were then derusted in inhibited acid solution, polished, degreased and exposed to natural seawater in conventional wooden racks. Panels were retrieved to the laboratory after about 25 to 40 days allowing sufficient time for attachment and growth of barnacles. Such manner of seawater exposure and retrieval for experimentation under controlled laboratory conditions was done twice, during January-March 1987 and during the same period in 1988. This particular season coincides with the heaviest growth of barnacles, principally Balanus reticulatus, at a settlement density varying between 2×10^4 and 2.5×10^4 m^{-2} for a 30 days exposure period (Eashwar, et al., 1987b).

The panels, each holding about 100 barnacles, were subjected to various environmental conditions in the laboratory. Prior to this, panels were all checked for the activity of barnacles, using cirral beating as an indication. Any barnacle that was found dead on retrieval to laboratory was removed in order to eliminate error which could be created by an already initiated crevice. Following this, panels holding alive barnacles were immersed in a hot seawater bath at 70°C, twice, for about 15 minutes each time. This ensured killing of barnacles and attached bacteria. Transfers were then made to different conditions such as given below:

i) Natural seawater, unstirred

ii) Natural seawater, constantly aerated

iii) Deaerated (nitrogen sparged) natural seawater

iv) Deaerated, sterilized (autoclaved) seawater

v) Same as (iv) but a pure culture of sulphate-reducing bacteria inoculated.

In addition, certain other parameters were also analysed and will be dealt with in the text later.

Experiments were terminated about 15 to 20 days after commencement and this exposure time was found to be sufficient enough for positive and negative results to be considered genuine and reproducible. For each variable experimental, a minimum of 2 specimens, with at least 200 barnacles, were considered. On

termination of the experiments, the panels were cleaned, first by hand scrubbing and later in inhibited acid solution, and observed by naked eye for appearance of crevice.

RESULTS AND DISCUSSION

From a natural immersion test spanning 2 years, it was confirmed that all attacks occurred only beneath dead barnacles (Eashwar et al., 1987a). Three broad stages in barnacle's cycle, as relating to corrosion, could be identified. These can be observed in Fig.1 which implies that the flesh, after the organism's death, should remain inside the shell to initiate corrosion and that 'empty' shells - the resultant of predation by fishes or gastropods - do not produce any attack.

Results a series of laboratory tests are shown in Table-1. It can be seen that data collected during 1987 and 1988 agree well. Results indicate that in the absence of either oxygen or biological activity, crevices do not occur. Also, oxygen can be observed to increase, considerably, the percentage of attack in natural seawater. Some of the salient features observed in experiments pertaining to aerated, natural seawater were;

1) Red rust showed up along the edges of the shells of barnacles where crevices had begun.

2) Where corrosion occurred, barnacles could be uprooted easily. Observations showed that the bases of their shells were perforated at those places where the flesh of the animal rested (near the centre in most cases). The edges of the shell-bases, however, remained strong.

It needs mention, here, that the base of the barnacle shell is not uniform in thickness; it is weak at the spot where the organism rests. In some barnacles, the base is incomplete and the living organism contacts the substratum direcly (Balasubramanyan 1988).

3) Corrosion began along the edges of the shells. In all of the crevices, the centre region remained unattacked.

4) There was evidence for the presence of sulphides in the corrosion products.

Table-1 explains that in the absence of oxygen, biological factors (SRB) do not produce any significant effect. Where corrosion had occurred, in this case, it was not the characteristic crevice with an unaffected centre. It was, rather, a different pattern of attack with a deep pit at the centre. The bases of the rest of barnacles were in tact and were not perforated by sulphide accumulation.

Results of another series of experiments carried out during January-March 1988 are given in Table-2. Perforation of the shell-base, as it can be seen, appears to cause no effect in the absence of biots. Evidently, a corrosive product is required to penetrate the shell and dissolve the base. The second of this series of study shows that the oxidised product of sulphide is harmless in the absence of marine aerobic bacteria. The third trial reveals that exposure to aeroabic bacteria, following heavy H_2S accumulation within the shell, causes corrosion to occur. It can be argued that the corrodant formed upon the exposure to natural seawater should be a product of the sulphur cycle. This is because that the flesh of barnacle, prior to exposure to natural seawater, had already been acted upon, completely, by the SRB.

Test for thiobacilli

From the decay matter within the shell, tests were made for the presence of thiobacilli which are capable of oxidising sulphides to sulphuric acid. Samples were inoculated in the elemental sulphur medium (Booth 1971). A drop in pH from 7 to 3, within 5 days, indicated the presence of thiobacilli.

Thiobacilli are abundant in seawater and are most likely to occur in places where H_2S is produced or deposited such as in decaying turf within the barnacle shell. From the results of experiments, it appears, most likely, that thiobacilli are responsible for the production of acidic substance capable of penetrating the calcareous shell of barnacle. To suspect these organisms as the cause looks straight forward since they are, like SRB, widely distributed in the world ocean.

Also understood from the results is that killing of microbes thriving beneath the shell or those already present within the shell has not affected the crevice corrosion phenomenon. This also implies that bacteria responsible for this particular attack very abundant in natural seawater.

THE CREVICE-CORROSION MODEL AND CONCLUSIONS

In the organism considered for the present study, **Balanus reticulatus**, all attacks occurred beneath dead organisms.

As the first step, the flesh of the organism is acted upon by micro-organisms, chiefly SRB and thiobacilli. This results in lowering of pH within the shell.

The product formed as a result of putrefaction is an oxidised form of sulphide and appears to be sulphuric acid produced by the action of thio-bacilli.

The corrosive product perforate the shell at its weak centre and dissolve the base moving, at random, from the centre across the shell.

This establishes a corrosion cell between the completely exposed centre region and the adjacent crevice gap. Differential aeration and difference in pH between these two regions seem to be the factors influencing corrosion.

Corrosion, therefore, begins at areas nearer to the edge of the shell rather than at the centre where the products directly contact the metal surface.

Deepest pits, within a crevice, occur at areas where shell is adhered most firmly.

Creation of a deep pit at the centre, essentially, is due to the build-up of an almost completely an aerobic environment within the shell. Here corrosion is induced by the acidic product itself instead of differential aeration cells. This type of attack, however, is not very common.

Finally, it is worthwhile mentioning that more direct proof for this model would be given by careful and precise measurement of pH and oxygen levels within the shell.

Acknowledgement

The authors are thankful to Prof.K.I.Vasu, Director, CECRI, and Dr.K.Balakrishnan, Head Corrosion Division, CECRI, for encouragement and permission to communicate the paper.

REFERENCES

1. F.L.LaQue, in Corrosion Hand Book, H.H.Uhlig - Ed., John Wiley & Sons Inc., N.Y. (1948) p.413
2. G.Relini, et al., Proc. 4th Int'l Cong. Marine Corr. & Foul., France (1976) p.445
3. F.L.LaQue, Proc. 3rd Int'l Cong. Marine Corr. & Foul., USA (1972) p.2
4. J.Degerbeck, Proc. Scandinavian Corr. Congress (1971) 36

5. J.C.Rowlands, Br. Corr. J., 11, 4 (1976) 195

6. R.A.King, One-day Seminar Organised by Oyez Business Limited, London (1981) pp.1-12

7. A.Pipe, Marine Corrosion on Offshore Structures, Soc. Chem. Industry, London (1981) pp.13-21

8. K.Ravindran and A.G.Pillai, Proc. 6th Int'l Cong. Marine Corr. and Foul., Greece (1984) p.282

9. M.Eashwar, et al., Proc. International Workshop on Marine Electrochemistry, Tuticorin (1987), Session-II, Paper-4

10. F.L.LaQue, Master Perform., 21, 10 (1982)

11. M.Eashwar et al., Proc. 10th ICMC, Madras (1987) p.3265

12. K.Balasubramanyan (1988) Personal Communication

13. G.H.Booth, Microbiological Corrosion, M and B Monographs, London (1971) p.15

Table 1 : Results of barnacle - induced corrosion under different environmental conditions in laboratory - I

	Environment/Variable	Percent attack *	
		1987 Test	1988 Test
1.	Natural seawater	17	20
2.	Natural seawater, constantly aerated	52	44
3.	Sterilized seawater	0	0
4.	Sterilized seawater, constantly aerated	0	0
5.	Natural seawater, deaerated	0	0.5
6.	Sterilized seawater, deaerated	0	0
7.	Sterilized seawater, deaerated + SRB culture	0.5	1

* Based on crevice attack beneath 200 barnacles or more

Table 2 : Results of barnacle - induced corrosion under different environmental conditions in laboratory - II

	Environment / Variable	Percent attack * (1988 test)
1.	Sterile seawater, aerated; Flesh of animal removed; Base of the shell perforated with a sterile needle.	0
2.	Sterilized seawater + SRB (pure culture) 10 days exposure; Subsequently sterile air sparged for 10 days	1
3.	Sterilized seawater + SRB (pure (culture) 10 days exposure; Subsequently exposed to natural seawater for 7 days	35

* Based on crevice attack beneath 225 barnacles or more.

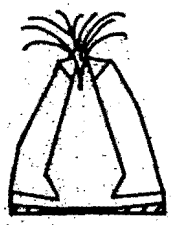

ACTIVE BARNACLE
NO CORROSION

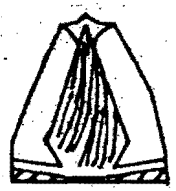

DEAD BARNACLE
FLESH RETAINED
PROBABLE CREVICE

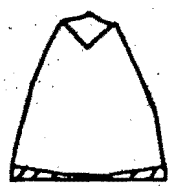

'EMPTY' SHELL
NO CORROSION

FIGURE 1. THREE BROAD STAGES OF BARNACLE IN RELATION TO CREVICE CORROSION

7.° CONGRESO INTERNACIONAL DE CORROSIÓN MARINA E INCRUSTACIONES

7th INTERNATIONAL CONGRESS ON MARINE CORROSION AND FOULING

7ème CONGRES INTERNATIONAL DE LA CORROSION MARINE ET DES SALISSURES

UNIVERSIDAD POLITÉCNICA
Valencia, 7-11 Noviembre, 1988
ESPAÑA

SECCIÓN II

Biología marina
Marine biology
Biologie marine

The unpublished manuscripts have been reproduced as received from the authors. The Scientific Committee takes not responsability for any - errer or omission

Las ponencias no han sido publicadas y están reproducidas tal y como se han recibido de sus autores. El Comité Científico no se responsabiliza de cualquier error u omisión.

SESSION II Marine Biology
Wednesday 9th November

A STUDY OF MARINE FOULING DIATOMS ON SHIPS IN THE NORTH ATLANTIC
D C Woods and R L Fletcher

MECHANISM OF CORROSION POTENTIAL ENNOBLEMENT BY MARINE BIOFILMS
Stephen C Dexter and Shiang-Ho Lin

ENHANCED CORROSION RATES OF AISI 316 STAINLESS STEEL WELDMENTS IN THE MARINE ENVIRONMENT DUE TO BACTERIA
N J E Dowling, C Lundin, C H Lee, M Franklin and D C White

SYNERGISTIC ACTION OF BACTERIA ON THE CORROSION OF MILD STEEL IN A MARINE MEDIUM
Christine C Gaylarde

BACTERIAL ATTACHMENT ON Cu/Ni ALLOYS AND ITS RELATION WITH CORROSION
S G Gomez de Saravia, M F L de Mele, H A Videla and E Erauskin

MICROBIAL INTERVENTION IN COPPER CORROSION
Brenda J Little

A STUDY OF MARINE FOULING DIATOMS ON SHIPS IN THE NORTH ATLANTIC

D.C. Woods and R.L. Fletcher

Portsmouth Polytechnic, School of Biological Sciences, The Marine Laboratory, Ferry Road, Hayling Island, Hampshire, PO11 0DG, U.K.

Abstract

Diatoms were found to be the most significant contributors to the 'slime' forming, microfouling communities present on the hulls of a wide range of in-service vessels which were dry-docked in the British Isles. A total of 207 diatom species/subspecies, distributed in 44 genera, were identified, although only a small number of these were persistently abundant; the latter included Amphora coffeaeformis var. perpusilla, Navicula carynhosa, Berkeleya rutilans, Licmophora gracilis var. anglica, Navicula ramosissima and Stauroneis decipiens. Marked differences were observed in the floristic composition on vessels with different modes of operation, whilst the local distribution of diatoms observed on each ship's hull appeared to be largely dictated by hydrodynamic forces.

Introduction

The importance of microfouling films composed of unicellular organisms and their exudates was first recorded by Harris (1943) who identified that they represented the early stages of biofouling development. The most common and economically important fouling organisms at this time, however, were animals such as barnacles and tube worms which were considered to have the greatest influence on the skin frictional resistance of ships' hulls (Bishop et al., 1949). As a result of advances in antifouling technology during the 1970's and 1980's more recent surveys of ship fouling have revealed slime forming microfouling communities, particularly comprising diatoms, to be playing a much more dominant role (Sims & Denham, 1971; Fletcher & Chamberlain, 1975; Christie et al., 1976; Denham, 1978; Denham & Bellinger, 1979; Gunn et al., 1986; Woods et al., 1987); Denham (1978), for example, described diatom and bacteria based slimes to be approximately three times more important as the next group (Balanus). In addition, an increasing number of studies are revealing that these diatom slimes, although microscopic in proportion, can significantly effect the operational efficiency of these vessels (Christie et al., 1976; Characklis 1981; Clitheroe, 1983; Baciocco, 1984; Lauthwaite et al., 1985; French & Evans 1986).

Despite the economic importance of these diatom dominated slimes a dearth of information exists on aspects of their ecology and biology. Except for a small number of field studies in which species of the genera Achnanthes and Amphora have been identified as the dominant fouling organisms on ships' hulls (Bishop & Sims, 1969; Bishop et al., 1972; Christie et al., 1976; Daniels & Chamberlain, 1981; Daniels et al., 1982), detailed considerations of diatom fouling communities are restricted to the work of Fyne (1987). In addition, although much information can be obtained from general studies on the colonisation of toxic paint surfaces using raft trials, it is still vital that studies are continued on the fouling of in-service shipping as these are subject to much greater variation in the environmental conditions which influence the rate and characteristics of biofilm development (Fyne 1987).

The present paper is, therefore, concerned with a detailed study of diatom fouling of in-service vessels, with particular respect to the identification of the major contributors and their distribution in relation to the operational characteristics of the vessels, e.g. routes, antifouling paint formulation and hull design.

Materials and Methods

Samples of microfouling films were collected from a range of hull sites on 15 in-service coastal or oceanic vessels during dry dockings

in England. Where possible, collection was from sites at the same draft level along the length of the hull. The procedure used corresponds with the sampling method employed by Benhem (1978); samples were obtained by scraping the hull surface with a razor blade in regions where it could be reached from the floor of the dry dock, or with a dutch hoe for sample sites at, or near, the waterline. All samples were collected by scraping an area in excess of 15 x 15 cm to ensure a sufficient sample size.

General observations were made on the samples by light microscopy prior to acid treatment according to the method of Haste & Fryxell (1970). For each sample the prevalence of each diatom species was recorded using an arbitrary scale whereby species constituting 10-25% of a population were denoted as common (C), 25-50% as frequent (F) and over 50% as abundant (A). Additionally the relative percentage occurrence of the six main species and seven major genera was recorded. For each sample site the total number of taxa i.e. individual species plus additional varieties, and for each vessel the total numbers of genera, species and varieties were recorded.

Results

Taxonomic studies on the diatom content of the microfouling samples obtained from the 15 ships revealed a total of 44 genera and 197 species plus 10 additional varieties (i.e. total taxa = 207) identified as fouling organisms. By far the most well represented genus observed on these vessels was *Navicula*, for which 41 species (total taxa = 44) were recorded. Other prevalent genera included Cocconeis and Nitzschia, each with 15 species (total taxa = 16) and Amphora with 13 species (total taxa = 15). Eighty seven of the overall species total were, therefore, confined to only four genera. Individual vessels, however, exhibited considerable variation in the number of fouling diatoms recorded, ranging from 35 to 120 taxa (see Table 1).

It is also noteworthy in Table 1 that vessels operating over oceanic routes generally supported a lower diversity of diatoms compared to that of vessels with a coastal mode of operation.

Despite the diverse range of species identified, only a small number were found to constitute over 10% of the diatom population at one or more of the sample sites (Table 2). Among these, the two species Amphora coffeaeformis var. perpusilla and Navicula corymbosa, emerged as being by far the most prevalent fouling diatoms. The former species constituted over 10% of the diatom population at 63 of the 116 sample sites and over 50% at 14 sites. Both species were observed to have a procumbent attachment morphology and were enveloped in large quantities of extracellular mucilage. Other genera which were recorded as prevalent at a number of sites included Berkeleya rutilans, Licmophora gracilis var. anglica, Navicula ramosissima and Stauroneis decipiens (Table 2). It is clear from this study, therefore, that it is the small procumbent species (i.e. A.coffeaeformis and N.corymbosa) which represent the major diatom contributors to biofilm development on these vessels.

Tables 3-5 show the relative percentage occurrence of diatoms on three of the vessels studied. They demonstrate that the proportions of the main diatoms contributing to the microfouling communities varies according to the hull site. Diatom fouling on vessel II shows both a horizontal and vertical transition with erect forms being more abundant in the forward and waterline regions, and smaller procumbent

forms being more abundant in the aft region and at the lower draft levels on the hull. For example, there appears to be a transition in dominance from L.gracilis var.anglica in the forward region, to A.coffeaeformis var.perpusilla and N.corymbosa in the midship and aft regions. Additionally the relative occurrence of the Licmophora species was greater at or near the waterline than at the corresponding 120 cm sites in each region.

A similar study of vessel III showed that, in the forward region, all three main species observed on vessel II were abundant. In the midship region, however, the abundance of the erect species, L.gracilis, was reduced whilst in the aft region both this species and N.corymbosa were less evident and A.coffeaeformis was the dominant species.

The occurrence data results show that, in addition to its dominance at the waterline site, there was an increase in the presence of A.parvula at the 90 cm and 120 cm sites. This indicates a marked preference by this species for the higher draft level regions of this vessel. Generally, however, fouling was dominated by N.corymbosa in the forward region, but by A.coffeaeformis and Navicula sp in the midships region.

Discussion

It is evident from these results that all the ships examined, the majority of which were protected by modern antifouling paints, supported microfouling communities dominated by a wide range of diatom species. Of the ships examined in this investigation, only one of these, vessel IX, had the fouling growth dominated by organisms other than diatoms. It is notable that the total number of species identified from these vessels was 197, but that most vessels supported between 41 and 72 species, whilst individual sample sites rarely supported more than a third of the vessel total. This indicates that the majority of diatom species occurred only occasionally and sporadically. This is in agreement with the results of Pyne (1987) who similarly identified a large number of species from in-service ships but found that only a limited number were prevalent and persistent colonisers. A similar situation has also been observed for microfouling of antifouled static panels (Hendey, 1951; Callow, 1984, 1986; Robinson et al., 1985).

In the present study, only nineteen species were recorded as major fouling organisms on the vessels in that they constituted more than 10% of the diatom population at a sample site. Within this group, the most abundant and frequently recorded species were Amphora coffeaeformis (primarily var.perpusilla) and, to a lesser extent, Navicula corymbosa. It is interesting to note that both species are small, procumbent forms that were observed to produce large quantities of extracellular mucilage. Amphora coffeaeformis has previously been shown to be a common fouling organism on antifouling paints from in-service ships (Bishop & Silva, 1969; Bishop et al., 1972; Daniel et al., 1980; Pyne, 1987) and from static panels (Hendey, 1951; Callow, 1984, 1986; Robinson et al., 1985). Significantly, N.corymbosa has not previously been recorded as a major fouling organism on either static or in-service antifouling paint samples. It is, however, a small species with a morphology similar to a number of other naviculoid diatoms and may have been overlooked and/or incorrectly identified in previous investigations. Additionally, members of the

genus Achnanthes were not found to be as abundant as recorded previously on antifouled panels (Callow et al., 1978; Callow, 1984, 1986). This is in agreement with the results of Pyne (1987) who rarely observed Achnanthes spp. to be dominant microfouling organisms on in-service vessels but found members of the genus Licmophora to be the more abundant stalk forms.

The variation in the biofouling observed for individual vessels can be attributed to differences in the wide range of environmental parameters to which the colonising organisms were exposed. The results show, for example, that there appear to be fewer diatom species on ocean going vessels (eg Vessels IV, XI and XII) compared to those operating in coastal waters. This is probably the result of more severe changes in temperature due to movement between polar, temperate and tropical regions and to the lower nutrient availability of oceanic waters compared to coastal waters. The operational speeds of the ocean going ships were not significantly greater than many of the coastal vessels and was not, therefore, likely to be the major cause of reduced diatom diversity on these vessels.

The formulation of the antifouling paints appeared to have little significant effect on the diatom composition of the microfouling films on the vessels. It is noteworthy, however, that two vessels protected by paints containing only cuprous oxide as the biocide exhibited fouling almost entirely dominated by Amphora coffeaeformis (vessel I), and A.coffeaeformis and Stauroneis decipiens (vessel V). Conversely two vessels coated with paints containing a particularly high organotin loading, eg vessels VI and XII, tended to exhibit an increased prevalence by other species, primarily N.corymbosa, at the expense of A.coffeaeformis. Variations in biofilm composition on different paint formulations has previosly been demonstrated in other investigations (Callow, 1984, 1986; Pyne, 1987). For the majority of vessels, however, no such relationship was found and any possible variation in the diatom composition caused by the different toxic paints applied to the vessels studied was likely to have been masked by those caused by differences in other environmental conditions to which the fouling organisms were subjected.

In addition to inter-vessel variation in microfouling composition there were significant horizontal and vertical variations in the different regions of the ships investigated. For a number of vessels (II, III, VIII, X, XII, XIV and XV) the results showed an increase in the occurrence of erect stalked species of genera such as Achnanthes and Licmophora and/or mucous tube producing colonial species such as Berkeleya rutilans and Navicula ramosissima at or near the waterline compared to lower draft levels. In this respect it is interesting to note that depth of immersion and light intensity have been show to influence both the total biomass (Round, 1961) and diversity of diatom colonisation (Bacon & Taylor, 1976; Stupak et al., 1976; Hudon & Bourget, 1983; Pyne, 1987) on a range of substrata including antifouling paints. More generally, vertical zonation of fouling organisms was also observed on in-service ships by Benham (1978) and Benham and Bellinger (1979). It is notable, however, that on a number of vessels (III, IV, IX, X, XII, XIII, XIV and XV) the major fouling species, Amphora coffeaeformis and Navicula corymbosa, were more abundant between approximately 30 cm and 300 cm below the waterline. Correspondingly these species generally exhibited a reduced abundance weighting for sites at the waterline and at the lower draft levels.

To some extent, the vertical variations on these vessels tended

to be masked by far more marked horizontal variations which are caused by the action of fluid shear forces on the attached fouling organisms. The major fouling diatom genera exhibit a wide range of morphologies and attachment mechanisms which afford varying strengths of adhesion under the influence of shear forces which in themselves alter in nature and severity along the length of a moving vessel. Horizontal variation in the diatom composition of microfouling films was observed on vessels I, II, III, IV, V, VI, XI, XII and XIV, usually as a change in the abundance of dominance of the different species. Microfouling films on the majority of these vessels were dominated by Amphora coffeaeformis and Navicula corymbosa, but their relative occurrence was greatest in regions where the influence of shear forces were minimal. For example A.coffeaeformis was recorded as 'frequent' or 'abundant' in the forward region on vessel 1, 'common' in the midship region and 'common' or 'present' in the aft region. This type of decline in the abundance of the only extensively recorded species on this vessel can be correlated with the character of flow pattern about the hull, specifically the increase in flow turbulence along the length of the hull. On the hull of vessel II the same type of flow characteristics produced a transition in the abundance of the main species. Microfouling in the forward regions, where flow tended to be laminar, was thicker and dominated by the erect, stalked species Licmophora gracilis var.anglica whilst in the midship and aft regions the dominant forms were the small, low profile, procumbent species, A.coffeaeformis var.perpusilla and N.corymbosa. It would appear that the smaller procumbent species, particularly A.coffeaeformis var.perpusilla, which have been shown experimentally to exhibit greater attachment strength than Achnanthes and Licmophora spp (Pyne et al., 1984) were better able to remain attached to these surfaces under turbulent flow conditions.

It has also been observed (Woods & Fletcher, unpublished) that the comparative strength of attachment of the four main fouling diatoms observed in the present study correlated closely with their relative abundance in the fouling samples collected from in-service ships. The most abundant species, Amphora coffeaeformis var.perpusilla, exhibited the strongest initial attachment strength and the most rapid increase in adhesion. Navicula corymbosa which was far more abundant than Achnanthes spp and Licmophora spp, but less than Amphora spp., was characterised by a high initial level and rate of increase in attachment strength. The two stalk forming species which were markedly less abundant in the microfouling samples, showed much lower attachment strength than the procumbent Amphora and Navicula species. They also exhibited relatively little increase in the initial attachment strength between one and 24 hours. As most diatom settlement on ships' hulls must necessarily take place whilst the vessels are stationary the first 24 hours are critical in the successful settlement on these surfaces.

Acknowledgements

We would like to thank the Research Organisation of Ships Compositions Manufacturers (R.O.S.C.M.) for financial support (awarded to Professor E.B.Gareth Jones) and, in particular, Drs O.P.Morris and K. Borer for helpful discussions.

Hendey, N.I., 1951. Littoral diatoms of Chichester Harbour with special reference to fouling. J.R.Microsc.Soc., 71: 1-86.

Hudon, C.& Bourget, E., 1981. Initial colonisation of artificial substrata: community development and structure studied by SEM. Can.J.Fish.Aquat.Sci., 38: 1371-1385.

Lewthwaite, J.C., Molland, A.F.& Thomas, K.W., 1985. An investigation into the variation of ship skin frictional resistance with fouling. Roy.Inst.Naval Arch.Suppl. paper, 127: 269-284.

Pyne, S., 1987. Studies on microbial slime formation on toxic and non toxic surfaces with particular reference to diatom fouling of in-service shipping. PhD Thesis, Portsmouth Polytechnic.

Pyne, S., Fletcher, R.L.& Jonas, E.B.G., 1984. Attachment studies on three common fouling diatoms. In: Proc.Sixth Int.Congr.Mar.Corrosion & Fouling pp.99-112, Athens.

Robinson, M.G., Hall, B.D.& Voltolina, D., 1985. Slime films on antifouling paints. Short-term indicators of long-term effectiveness. J.Coatings Technol., 57: 35-41.

Sims, R.E.& Benham, B.R., 1971. A study of the marine fouling organisms. Br.Ship Res.Assoc.Rep., 305: 1-32.

Stupak, M.E., Bastida, R.& Arias, P.J., 1976. The biological incrustations of the port of Mar del Plata. CIDEPINT ANALES, II: 175-232.

Woods, D.C., Fletcher, R.L.& Jones, E.B.G., 1988. Diatom fouling of in-service shipping with particular reference to the influence of hydrodynamic forces. In: Proc.Ninth Int.Symp.On Living and Fossil Diatoms. In pres.

Table 1. The relative distribution of diatom taxa on in-service vessels

Mode of Operation	Vessel	No.Genera	No. Species	Total Taxa
Coastal	I	22	62	67
Coastal	II	25	57	59
Coastal	III	24	58	63
Coastal/Oceanic	IV	21	47	51
Coastal	V	25	63	69
"	VI	26	53	57
"	VII	37	113	120
"	VIII	30	72	76
"	IX	25	72	76
"	X	30	66	73
Oceanic	XI	17	30	35
"	XII	19	51	55
Coastal	XIII	16	41	43
"	XIV	25	66	70
"	XV	25	59	63

Table 4. Relative Percentage Occurrence of the Main Fouling Diatom Species/Genera Identified from Vessel III

	Sample site (cm below waterline (W/L) and occurrence (%)							
	Forward		Midships			Aft		
Species	W/L	150	W/L	60	150	W/L	90	150
Amphora coffeaeformis	100	100	100	94	100	98	100	100
Berkeleya rutilans	36	64	58	66	0	6	50	28
Licmophora gracilis var. anglica	100	28	70	98	34	100	64	32
Navicula corymbosa	100	100	100	100	98	70	26	74
N. pseudocomoides	6	88	0	4	2	24	2	8
Synedra fasciculata	4	4	0	4	2	4	4	16
Genera								
Achnanthes	2	0	2	2	2	6	0	22
Amphora	100	100	100	94	100	98	100	100
Cocconeis	4	2	0	0	8	0	2	0
Licmophora	100	28	70	96	34	100	64	32
Navicula	100	100	100	100	98	76	28	74
Nitschia	2	0	0	0	4	0	0	2
Synedra	4	4	0	4	2	6	4	16
Others	44	74	62	66	8	66	62	28

Table 5. Relative Percentage Occurrence of the Main Fouling Diatom Species/Genera Identified from Vessel XII

	Sample site (cm below waterline (W/L) and occurrence (%)									
	Forward			F/M		Midship		Aft		
Species	90	270	390	W/L	120	360	450	450*	540	600
Achnanthes parvula	74	0		100	74	0	0			
Amphora coffeaeformis	90	38		92	100	100	100			
Berkeleya rutilans	40	44		40	100	24	56			
Navicula sp	18	72		10	78	100	100			
N. corymbosa	100	100		94	100	46	40			
N. pseudocomoides	68	4		46	20	2	2			
Genera										
Achnanthes	90	0		100	74	0	0			
Amphora	96	48		92	100	100	100			
Cocconeis	8	6		10	2	6	12			
Licmophora	2	0		16	0	0	0			
Navicula	100	100		96	100	100	100			
Nitzschia	10	0		10	0	2	2			
Synedra	12	0		10	4	0	0			
Others	60	48		48	100	18	57			

* = Sample site on flat bottom of vessel

MECHANISM OF CORROSION POTENTIAL ENNOBLEMENT BY MARINE BIOFILMS

Stephen C. Dexter and Shiang-Ho Lin

College of Marine Studies
University of Delaware
Lewes, DE 19958 USA

ABSTRACT

Corrosion potentials of stainless alloys and platinum are shown to become more noble with formation of a microbial film in natural seawater, while the potentials of the same metals in filtered seawater remains unchanged. These results show that potential ennoblement can be achieved without a supply of heavy metal ions from the alloy surface. A mechanism for ennoblement that does not rely on the catalytic effect of such heavy metal-exopolymer complexes is suggested.

INTRODUCTION

It has been well documented that the formation of primary microbiological films on the surface of metals and alloys immersed in natural seawater has an important effect on the corrosion behavior of those alloys[1-8]. Those results have shown that the corrosion potential of passive alloys becomes more noble (positive), and the corrosion rate of active alloys increases in the presence of the biofilm.

Such results have been used to explain why natural seawater tends to be more aggressive than are the sodium chloride and artificial seawater solutions often used to study marine corrosion in the laboratory. It has been pointed out previously[3-8] that the consequences of a more noble corrosion potential in natural as opposed to artificial seawater are 1) a greater tendency for localized corrosion initiation, or an increase in cathodic protection current density for preventing localized corrosion, and 2) an increase in the severity of biofilmed stainless alloys as the cathodes of galvanic couples.

A proposed mechanism for corrosion potential ennoblement[3,5,8,9] involves catalytic enhancement of the oxygen reduction reaction by heavy metal complexes of Fe, Cr, Ni or Mn from the alloy and extra- cellular polymers produced during microbial metabolism. The purpose of the work reported in this paper was to investigate the validity of that mechanism by studying the effect of microbial films on the potential of platinum, which does not contain the necessary heavy metals.

EXPERIMENTAL TECHNIQUES

The three alloys used in this study were AISI Type 316 stainless steel, stainless alloy C-276 and platinum. The nominal compositions and suppliers of these metals are shown in Table 1. Type 316 and alloy C-276 samples were cut from 1.6 mm thick sheet and measured 2 cm by 4 cm and 2 cm by 2 cm respectively, each with a thin stem 2 cm long coated with an insulating lacquer. Upon immersion, the stem passed up through the air/water interface, and a length of nickel wire spot welded to the stem provided an electrical lead. All stainless type samples were surface ground through 600 grit silicon carbide metallurgical paper, degreased in acetone and rinsed in distilled water immediately before exposure.

Platinum samples were 1.5 cm by 2.5 cm, cut from 0.08 mm thick foil. On these samples, an electrical lead was provided by spot welding a platinum wire directly to the sample. Platinum electrodes were not surface ground, but were degreased and rinsed as above.

Natural seawater exposures were done in a gently flowing, once through, seawater trough at the College of Marine Studies facilities. Water is pumped directly into the lab from Roosevelt Inlet on the southern shore of lower Delaware Bay about 1.5 miles from the open Atlantic Ocean. This location is well flushed by tidal currents, and the water during the summer months has a temperature of 21 to 26° C, salinity of 23 to 31 parts per thousand (ppt), pH of 7.8 to 7.9 and 5 to 7 ppm dissolved oxygen. The trough was placed in a darkened room to minimize growth of photosynthetic algae.

During the winter months exposures were done in the corrosion laboratory using water from the 8,000 gallon capacity recirculating seawater system in the Cannon Marine Studies Laboratory. The water in that system is refreshed twice weekly, being brought to the lab in a fiberglass tank truck from the Indian River Inlet, 28.5 km south of the mouth of Delaware Bay. Water is collected on the incoming tide, and it is typically air saturated with a pH of 7.9 to 8.1 and a salinity of 32 to 35 ppt.

Filtered seawater was made by passing the raw water through a 0.2 micron Millipore membrane filter. This treatment did not sterilize the water, but removed most suspended particulates and all but the smallest spherical bacteria. Preparation of the filtered water in this way prevented primary bacterial film formation on our samples over the two to four week period of these experiments. Moreover, this technique leaves the water unaltered chemically as compared to water that has been sterilized by photooxidation. Exposures in filtered seawater were done in a two liter beaker, in which the water was replaced with freshly filtered seawater once a day.

Sodium azide solutions were made from purified grade Fisher reagent in fresh water prepared by passing through a Millipore Milli-RHO/Milli-Q system with supplemental Organix cartridge. That water typically tests at 18 meg-ohms. Glutaraldehyde solutions were made from the Fisher Reagent grade chemical and Milli-Q water.

Electrochemical potential measurements were made on the saturated calomel scale using a series of commercial calomel electrodes intercalibrated with each other and a high impedance digital voltmeter or a Princeton Applied Research Model 173 potentiostat with the Model 276 computer interface. Corrosion potential monitoring was done by hand once or twice a day for the long term exposures in natural seawater, or once every half hour by computer in filtered seawater.

RESULTS

The corrosion potentials of AISI Type 316 stainless steel, stainless alloy C-276 and platinum in natural and filtered seawaters are shown in Figures 1 to 3. All corrosion potentials in the natural seawater were shifted in the noble direction by the build up of a microbiological film on the surface of the metal. In contrast, the potentials measured in filtered seawater stayed relatively steady over the same time period.

On Type 316 stainless steel (see Fig. 1), the potential in the natural water shifted about 330 mV in the noble direction within the first 5 days of immersion, recovered most of that noble shift by day 6, and then continued a slow and somewhat erratic noble drift over the next two weeks. In the filtered seawater, the corrosion potential was also erratic but it never reached the noble value it did in the natural

water. This behavior is consistent with our previously published results on this alloy[5], and it can be linked to the relative instability of the passive film on Type 316 stainless steel in chloride bearing solutions such as seawater, and to the consequent initiation and repassivation of localized corrosion events.

The corrosion potentials of stainless alloy C-276 and platinum, shown in Figures 2 and 3 respectively are steadier than those on the stainless steel. Both C-276 and platinum show a rapid ennoblement of the corrosion potential in the natural seawater over the first 8 to 10 days of exposure. Their passive films are stable enough, however, to withstand quite noble potentials without the initiation of localized corrosion. Thus, their corrosion potentials became steady with time at noble values of +300 to +400 mV SCE. The potentials recorded in filtered seawater in Figures 2 and 3 remained steady at -230 +/-30 mV for alloy C-276 and at +225 +/- 25 mV for platinum. The potential rise was 400 to 500 mV for alloy C-276 and 150 to 250 mV for platinum. The largest potential rise we have ever recorded was nearly 600 mV on alloy C-276. Regardless of the amount of potential rise, the most noble potential on a biofilmed electrode in this work and in that of other authors[1-8] appears to be about +410 mV SCE.

The existance of a biofilm on the samples from the natural seawater was verified by acridine orange staining and examination of the stained sample under the epi-fluorescence microscope. On all the samples, films that had been developing for two weeks or more were easily discernable by touch and were visible to the naked eye as a translucent brownish coating covering the entire sample and up to one millimeter in thickness.

Previous investigators had used sodium azide to show that the corrosion potential ennoblement is a function of microbial metabolism, rather than the mere physical presence of the film[2,7]. In order to demonstrate that this was also true for the ennoblement shown for platinum in Figure 3, we removed a biofilmed platinum electrode (after 26 days exposure) from the exposure trough along with 1.5 liters of seawater. A fresh, bare platinum electrode was also inserted into the same volume of water, and the corrosion potentials of both electrodes were monitored for one day as shown in Figure 4.

The biofilm on the 26 day platinum electrode was similar to that described above. It is probable that the "bare" platinum electrode that had been exposed to seawater for 24 hours also had a bacterial film. Although this 24 hour film was not specifically analyzed, a comparison of Figures 3 and 4 reveals that the corrosion potential of the "bare" platinum electrode in Figure 4 is nearly the same as that of the platinum electrode exposed to the filtered seawater in Figure 3. Thus, this 24 hour biofilm had not yet had a measurable effect on the corrosion potential of the "bare" electrode. At the one day exposure point, indicated by the first of the three dashed vertical lines on the Figure, 20 ml of 0.1 M sodium azide were added to the seawater. This addition produced no measurable effect on either the dissolved oxygen concentration or the pH of the seawater.

The corrosion potentials of both electrodes decreased rapidly as shown, by 80 mV for the filmed electrode and 40 mV for the bare platinum. At the beginning of day 2, another 20 ml of the sodium azide solution were added. The corrosion potential of the bare electrode immediately decreased another 20 mV but then remained steady. In

contrast, the potential of the biofilmed electrode decreased another 75 to 80 mV gradually over the next two days. A final addition of 20 ml of the sodium azide solution at day 5 produced no effect on the bare electrode and very little effect (perhaps a slight potential increase) on the filmed electrode.

A similar set of experiments was done using 500 ppm glutaraldehyde instead of sodium azide. The results were inconsistent. Sometimes the potential of a bare electrode was unaffected, and at other times it was shifted as much as 40 mV in the active direction. Similarly, the potential of a filmed electrode was sometimes unaffected by glutaraldehyde additions, while at other times the same active shift was observed as with sodium azide.

DISCUSSION

The results presented here confirm those of earlier investigators that the growth of a microbiological film on stainless alloy surfaces immersed in natural seawater causes the corrosion potential of the metal to shift in the noble direction[1-8]. These results also confirm that such a noble shift does not happen when the same alloys are exposed in seawater from which the microorganisms have been removed[5], or otherwise rendered inactive[6].

In the present set of experiments, the control waters were not artificial seawater, but rather natural seawater in which the population of microorganisms had been reduced by filtration. This process leaves the control water with the same organic and inorganic chemistry as that of the natural water. Moreover, the filtration process does not sterilize the water but leaves it with a greatly reduced bacterial population. This shows that the corrosion potential ennoblement is not due to a difference in the organic or inorganic chemistry between natural and artificial seawaters. It also shows that the control water need not be sterile in order to demonstrate the difference a biofilm makes on the corrosion potential.

Other investigators have treated biofilmed electrodes with sodium azide to show that the potential returns to that of the unfilmed metal when the bacterial respiration is inhibited[2,7]. The inference of such experiments is that the corrosion potential ennoblement is somehow tied to the metabolic activity of the organisms, rather than to their physical presence. In this paper we have shown in Figure 4 that addition of sodium azide affects not only the potential of the filmed electrode, but also that of the "bare" electrode. This does not invalidate the results of the sodium azide experiments, but it does mean they should be interpreted cautiously. The most popular ennoblement theory is that exo-polymers produced during bacterial metabolism form complexes with heavy metal ions such as Fe, Cr, Ni and Mn from the metal surface[3-5]. These heavy metal complexes are then proposed to catalyze the conventional cathodic reduction of oxygen to OH^- in seawater[9]. If this is the only enhancement mechanism operative, one would expect there to be no ennoblement of the corrosion potential on metals such as platinum and titanium which do not contain those metal ions. The data in Figure 3, however, show that there is an ennoblement on platinum. Others have shown similar results for platinum[8] and titanium[7,8]. Thus, while the catalytic enhancement mechanism may contribute to the observed ennoblement, it cannot be the only contributor.

In addition, it is well documented that sulfate reducing bacteria contribute to corrosion under mature biofilms on a number of alloys in both fresh and sea water systems[10]. Since the SRB are obligate anaerobes, it is apparent that the biofilm may create anaerobic conditions (oxygen concentration = 0) at the metal-film interface[11]. If there is no oxygen present, then the catalytic enhancement mechanism cannot be operative. Thus, it is difficult to see how that mechanism could account for sustained ennoblement under a mature biofilm where the oxygen concentration is likely to be low or even zero.

We would like to suggest another mechanism that may also contribute to the observed ennoblement phenomenon. We propose that the predominant cathodic reduction reaction at the metal-film interface may change as the metabolism of the organisms causes a change in the chemistry of the water incorporated into the film. Consider, for instance the change in pH under an aerobic biofilm in which the organisms are producing H^+, CO_2 and perhaps acetic acid[12]. It is considered likely that the pH within such a biofilm could decrease to 5 or even lower, and that the dissolved oxygen concentration could drop to one tenth or less of that in aerated seawater. Let us then compare the equilibrium potential for the oxygen electrode under ambient aerated seawater conditions (pH 8, oxygen partial pressure 0.2 atm) with that under the biofilm at pH 5 and 0.02 atm oxygen. In ambient seawater the oxygen reduction reaction is usually taken to be:

$$O2 + 2H2O + 4e^- \longleftrightarrow 4OH^- \qquad E^o = -0.401 \text{ V SHE} \qquad (1)$$

Using the Nernst equation, and accounting for the activity coefficient of H^+ in seawater, one calculates an equilibrium potential of +392 mV SCE under ambient seawater conditions and +566 mV at pH 5 and DO 0.02 atm under the film. This more noble potential under the film is due mostly to the decrease in pH. That same decrease in pH, however, probably means that the form of the cathodic oxygen reaction changes from that shown above to:

$$O_2 + 4H^+ + 4e^- \longleftrightarrow 2H_2O \qquad E^o = -1.229 \text{ V SHE} \qquad (2)$$

The Nernst equation gives a value of +688 mV SCE for the equilibrium potential of this reaction under the biofilm at pH 5 and oxygen 0.02 atm. Moreover, at pH 3, this potential becomes +804 mV SCE.

Returning now to Figure 3 for the platinum electrode, our data show an ennoblement of about 150 mV in the presence of the biofilm. If the platinum sample in this case is acting as a pseudo-equilibrium oxygen electrode, then its potential is governed mostly by thermodynamics, and the potential rise of 174 mV calculated above upon going from pH 8 with no film to pH 5 under the film, is alone enough to account for the data in Figure 3. Note that all the potentials in Figure 3 are less noble than the calculated values. This is to be expected since the oxygen electrode on platinum in seawater is not strictly at equilibrium. Nevertheless the calculated difference in potential is sufficient to account for the observed data.

The interpretation of the data for alloy C-276 in Figure 2 is less straight forward. In this case, one is not dealing with just the oxygen electrode, but rather with a mixed potential system. A pseudo-equilibrium oxygen electrode provides the cathode reaction, while the metal itself, in the process of maintaining its passive film, provides the anode reaction. Thus, considering Figure 5, we see that the shift in the oxygen potential alone from that at pH 8 to that at pH 3 could produce about half of the observed corrosion potential ennoblement.

Sources for the other half could include an increase in the exchange current density due to the catalytic enhancement mechanism as shown, or under anaerobic conditions, the introduction of some new cathodic reaction producing a sufficiently large reduction current at a potential of +400 mV SCE under the conditions produced by the organisms. Alternatively, the oxygen reaction might still be involved if there were a biochemical mechanism for electron transport across the anaerobic portion of the biofilm.

CONCLUSIONS

1. Corrosion potential ennoblement in the presence of a marine microbial film occurs not only on iron and nickel based stainless alloys, but also on platinum.

2. Another ennoblement mechanism besides the catalytic enhancement of oxygen reduction is needed to account for the results on platinum.

3. The calculated change in oxygen potential with decreasing pH, coupled with a change in the oxygen reaction itself can account for the observations on platinum and about half of the observed ennoblement on stainless alloy C-276.

4. Sustained ennoblement under a mature biofilm where the conditions become anaerobic will probably require a change in the predominant cathodic reaction to one not involving oxygen.

ACKNOWLEDGEMENTS

This work was supported by NOAA Office of Sea Grant, U.S. Department of Commerce under Grant No. NA 81 AA-D-0006 and by the Office of Naval Research under Contract No. N00014-87-K-0108.

REFERENCES

1. Mollica, A. and A. Trevis, In: Proc. 4th Intl. Congr. on Marine Corrosion and Fouling, Juan-Les-Pins, Anitbes, France, June, 1976, p. 351.

2. Scotto, V., R.D. Cintio and G. Marcenaro, Corrosion Science, Vol. 25, No. 3, 1985, p. 185.

3. Johnsen, R. and E. Bardal, Corrosion Journal, Vol. 41, No. 5, 1985, p. 296.

4. Johnsen, R. and E. Bardal, The Effect of Microbiological Slime Layer on Stainless Steel in Natural Seawater, NACE Paper No. 227 presented at CORROSION/86, Houston, TX, March 1986.

5. Dexter, S.C. and G.Y. Gao, Effect of Seawater Biofilms on Corrosion Potential and Oxygen Reduction of Stainless Steel, NACE Paper No. 377 presented at CORROSION/87, San Francisco, CA, March, 1987.

6. Mollica, A., A. Trevis, E. Traverso, G. Ventura, G. De Carolis and R. Dellepiane, Cathodic Performance of Stainless Steels in Natural Seawater as a function of Microorganisms Settlement and Temperature, Unpublished Manuscript.

7. Mollica A., G. Ventura, E. Traverso and V. Scotto, Cathodic Behavior of Nickel and Titanium in Natural Seawater, Presented at 7th Intl. Biodeterioration Symposium, September, 1987, Cambridge, UK.

8. Holthe, R., E. Bardal and P.O. Gartland, Time Dependence of Cathodic Properties of Stainless Steels, Titanium, Platinum and 90-10 CuNi in Sea Water, NACE Paper No. 393 presented at CORROSION/88, St. Louis, MO, March, 1988.

9. Van den Bring, F., E. Barendrecht and W. Visscher, Rec. Trav. Chim. Pays-Bas, Vol. 99, 1980, p. 253.

10. Biologically Induced Corrosion, Proceedings of the Intl. Conf., S.C. Dexter, Ed., Gaithersburg, MD, June, 1985, National Association of Corrosion Engineers, Houston, TX, NACE-8, 1986.

11. Lewandowski, Z., W.C. Lee and W.G. Characklis, Dissolved Oxygen and pH Microelectrode Measurements at Water Immersed Metal Surfaces, NACE Paper No. 93 presented at CORROSION/88, St. Louis, MO. March, 1988.

12. Pope, D.H., T.P. Zintel, A.K. Kuruvilla and O.W. Siebert, Organic Acid Corrosion of Carbon Steel: A Mechanism of Microbiologically Influenced Corrosion, NACE Paper No. 79 presented at CORROSION/88,

TABLE 1. Nominal Compositions of Materials Used.

Material	Nominal Composition	Supplier
AISI Type 316	0.08 C, 16-18 Cr, 10-14 Ni, 2-3 Mo, 2 Mn, 1.0 Si, Bal Fe	Allegheny-Ludlum Co. Brackenridge, PA
Alloy C-276	0.02 C, 16 Cr, 55 Ni, 16 Mo, 6 Fe, 4 W, 2 Co, 1 Mn	Huntington Alloys Huntington, WV
Platinum	99.99%	Fisher Scientific Co.

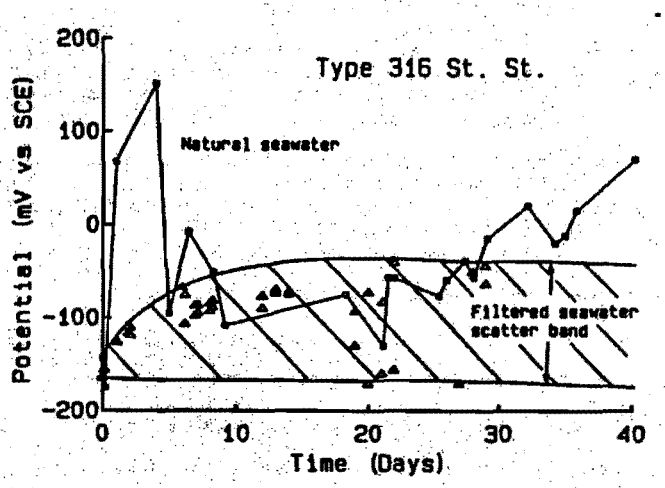

Figure 1. Corrosion potential of Type 316 stainless steel as a function of time in natural and filtered seawaters.

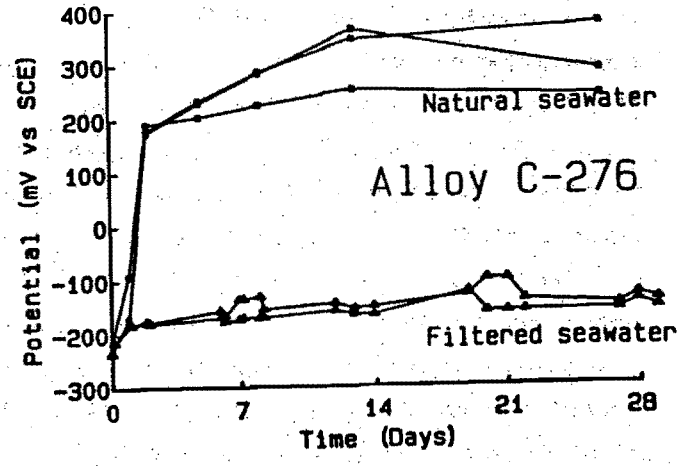

Figure 2. Corrosion potential of stainless alloy C-276 as a function of time in natural and filtered seawaters.

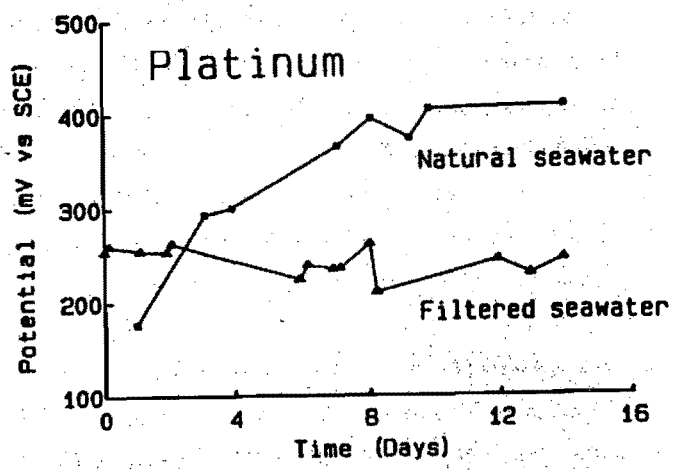

Figure 3. Potential of the oxygen electrode on platinum as a function of time in natural and filtered seawaters.

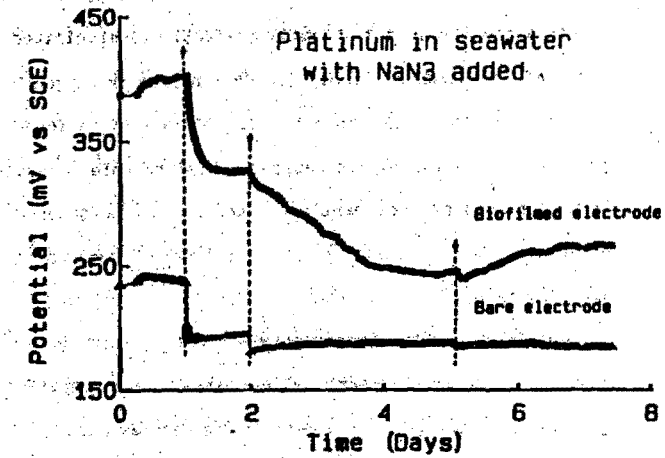

Figure 4. Effect of sodium azide additions on the potential of bare and biofilmed platinum electrodes in seawater.

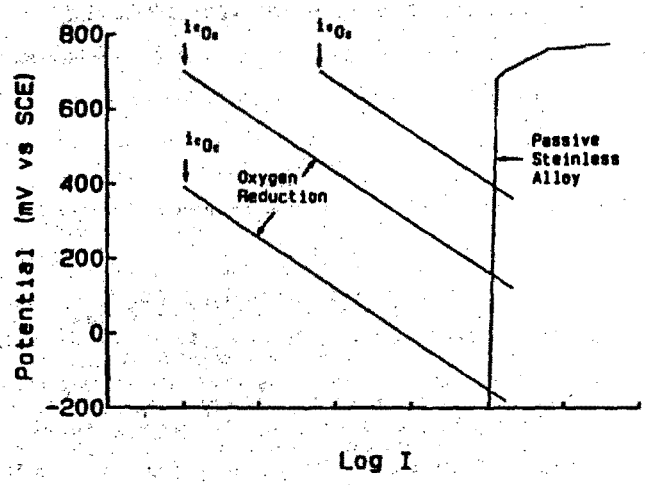

Figure 5. Schematic mixed potential diagram showing the effects of oxygen potential and exchange current density on the mixed potential of a filmed stainless alloy electrode.

ENHANCED CORROSION RATES OF AISI 316 STAINLESS STEEL WELDMENTS IN THE MARINE ENVIRONMENT DUE TO BACTERIA.

Dowling, N.J.E.[1], Lundin, C.[2], Lee, C.H.[2],

Franklin, M.[1], and White, D.C.[1]

1: Institute for Applied Microbiology, University of Tennessee at Knoxville, TN 37932, USA.
2: Materials Science and Engineering Dept., University of Tennessee at Knoxville, TN, USA.

ABSTRACT

Stainless steel coupons of various types, including autogenous weldments, were subjected to bacterial attack in artificial seawater and monitored using electrochemical impedance and small amplitude cyclic voltammetry. Unpolished coupons with a heat-affected zone (HAZ) were attacked first and appeared to be the most susceptible. The corrosion mechanisms of the different coupon-types were shown to be very different in nature.

INTRODUCTION

Serious failures of several alloys due to microbiological attack have been observed in industries with exposure to untreated water. These have included both circulating supply and stagnating systems such as dead-ended emergency piping (Kobrin, 1976; Tatnall, 1981). No established, central hypothesis for the corrosion of metals by microbial consortia has yet been proposed and tested. Several models have, however, been suggested for individual genera (Pope et al.,1984). These suggestions have revolved mainly around the more traditional organisms such as sulphate-reducing bacteria (SRB), acid-producing fermenters, and iron-oxidizing thiobacilli etc.

Although corrosion due to individual strains is well established, the location and interaction of those strains within a biofilm is not. Hamilton (1985) has elucidated the model of SRB which are protected from oxygen by oxygen-respiring aerobes. Thus in a biofilm SRB are to be found associated with the oxygen depleted metal surface concealed by aerobes and aerotolerant fermenters. The corrosion produced by such a community therefore has as much to do with the aerobes as the SRB.

Corrosion due to microorganisms tends to occur at discreet sites and "generalized corrosion", as exemplified by alloys in low pH environments, is a rare event. Particularly prominant among the site-specific failures have been weldments. In this article we report the rapid deterioration of some autogenous welds (without filler metal) in contact with a mixture of marine microrganisms from sediment.

EXPERIMENTAL

Several stainless steel coupons were fabricated for trial against unselected marine bacteria. These coupons were of 316L Nuclear Grade material : C 0.016%, Mn 1.66%, P 0.024%, S 0.011%, Si 0.47%, Cr 16.3%, Ni 10.13%, Cu 0.18%, Mo 2.11%, Co 0.2%, N 0.054%. The alloy sheet was obtained from Eastern Stainless Steel Co., Pittsburgh, PA., USA. The types of coupons tested included autogenous welds in the

as-welded condition (AW: unpolished weld), polished (600 grit) autogenous welds, and polished base metal. Samples were welded with the gas tungsten-arc process (GTAW). The ferrite content in the fused zone was 3.8 ferrite number (FN) measured by Magne-Gage.

The 2x2 cm^2 coupons were embedded in epoxide resin and placed in the bottom wall of two (15 cm i.d., 1 m L) polypropylene pipes. The coupon surfaces were made flush with the inside wall of the pipes. Titanium counter electrodes and calomel reference electrodes were provided for each coupon (figure 1). In all, 18 coupons were exposed, in the two pipes with three replicates for each condition (see above), to either sterile or inoculated media. The pipes were monitored during a fourteen day exposure period for pH, organic acid content (volatile fatty acids) and numbers of suspended cells. The coupons were periodically examined by open-cell potential, electrochemical impedance spectroscopy (EIS), and small amplitude cyclic veltammetry (SACV). Finally, some of the coupons were subjected to cathodic polarizations to obtain values for Icorr and cathodic Tafel parameter. The remainder were available for surface analysis.

Electrochemical impedance analysis was carried out using a Solartron 1250 frequency response analyser and 1286 potentiostat controlled by a Hewlett-Packard 310

microcomputor. Frequencies between 10 KHz and 3 mHz were selected with an interval of 5 or 10/decade. Signal amplitude was set at 5 mV rms. SACV measurements were carried out galvanostatically with a maximum sweep of $\pm$1E-8 Amps. at 0.2 mV/sec (equivalent for the system). Cathodic polarization sweeps started at the open-cell potential and proceeded at 0.2 mV/sec to -0.8 V.

The media consisted of the following (g/L distilled water): fibrous cellulose 2, cellobiose 1, chitin 0.125, yeast extract 0.1, starch 0.5, "Instant Ocean" (Aquarium systems, Ohio) 30, complex vitamins (Dowling et al., 1988a) and trace elements (Pfennig et al., 1981). After separate autoclaving in large glass vessels, the pH of the cooled media was adjusted to 7.5 with sterile Na_2CO_3.

Inoculation was of the organisms that grew from an inoculum of 10 mls of black sulphide-rich marine sediment in a test-tube of cellulose/chitin media.

Organic volatile fatty acids produced by the microbiota were monitored by packed column gas chromatography using a Schimadzu GC-9A with SP-1220 packing (Supelco, Bellafonte, PA).

The system was sterilized with 4 % formaldehyde after which the interiors were washed with sterile distilled water. Sterility was maintained in the control pipe by introducing 5 mM sodium azide.

RESULTS

The fluctuations in open cell potential are recorded in figure 2. Notably, by day 3, the potential of all the inoculated coupons fell to around -0.48 V/SCE, and stayed in this region for the duration of the experiment, while the sterile coupons remained at approximately -0.05 V/SCE. While the potential of the as-welded coupons exposed to bacteria decreased to -0.51 V/SCE within the first 24 hours, the potentials of the the polished coupons did not achieve those low potentials for a further 24 hours in the case of the polished welds and 48 hours for the base metal.

A summary of the evolution of the polarization resistance (Rp) of the coupons is presented in table 1. Figures 3a and 3b show the differences observed in impedance for the different coupons exposed to the microorganisms at days 1 and 8. Figure 4 compares the impedance of the polished base metal in sterile and inoculated conditions at day 12. After eight days exposure to the artificial seawater, high frequency capacitive loops were observed in all the coupons exposed (figure 5). Rp for the sterile coupons were only obtained by SACV due to the very large reactance of the corrosion cell and the difficulties in using extremely low frequencies (< 0.003 Hz). The Rp values for the as-welded coupons in the presence of the microbes

showed a rapid decrease (increase in corrosion rate) mimicked to a lesser extent by the polished coupons (days 1 and 2). After 3 days however, the polished coupons appeared to have uniformly lower values for Rp than the as-welded coupons. In all cases the small values for Rp indicated that the corrosion rate was faster for the inoculated than the sterile coupons.

Organic acid analysis showed that acetic acid and butyric acid were produced by the bacteria during the experiment in the following quantities and low pH :

DAY	Acetic (mM)	Butyric (mM)	pH
2	ND	ND	4.73
8	2.5	1.6	4.03
12	2.7	3.7	3.83
14	3.5	4.7	3.86

Analysis of the sterile system showed no detectable volatile fatty acids and a pH maintained at 6.8.

Microscopical observation of the inoculated media (day 14) by phase contrast using a Petroff-Hausser counting chamber showed 6.6×10^9 cells/ml. The surface of the coupons were inspected at 100X and 200X after removal from the pipes. Several globular type oxide deposits were observed along the fusion line in the as-welded coupons. Careful microscopical examination revealed that some of the oxides were attacked, resulting in hemispherical pits (figure 6). More of these oxide-depleted pits were observed on the coupons exposed to the bacteria than those in sterile

conditions. No such failures were seen on any of the polished coupons.

DISCUSSION

Failure of welds in raw water systems due to microbiological deterioration is a considerable problem. Unfortunately little work has focused upon this area and most of that has been in the nature of a case study (Kobrin, 1976; Tatnall, 1981). Metallurgical analyses show that austenitic (face-centred cubic) stainless steels are "sensitized" to some degree depending on the variables (peak temperature, base metal composition, and rate of cooling etc.) used in the welding process (Lundin et al., 1986). Weld sensitization is particularly associated with the heat affected zone (HAZ) which was present in the welded samples of this study.

In order to observe corrosion by microbial consortia, complex, insoluble carbon sources were used (eg. cellulose and chitin). These substrates were allowed to accumulate at the bottom of the pipes during the experiment as they might when a pipe is allowed to fall stagnant. In such a condition, welds tend to corrode rapidly at the bottom. Thus "suspended" particles may well exacerbate corrosion problems after falling out of suspension.

The evolution of the open-cell potential (OCP) in all

coupons (figure 2) showed that the presence of the bacteria decreased the potential in all cases to around -0.48 mV/SCE while that of the sterile coupons remained relatively constant over the 14 days. The OCP of the as-welded coupons changed within the first 24 hours which indicates that it was more susceptible to initiation of corrosion than the polished welds or base metal.

EIS confirmed that the AW coupons were attacked during the first two days by the bacteria by showing a smaller Rp value. After this initial period the average corrosion rates of the polished surface coupons (both welded and base metal) were higher probably due to the larger area unprotected by chromium oxides (mostly Cr_2O_3) tints which were observed in the HAZ. These tints covered a significant proportion of the surface area of the as-welded coupons and have been shown to affect the corrosion behaviour of various austenitic steels (Kearns, 1985). EIS measurements agreed well with those obtained by SACV at low reactances, however at very high reactances there are discrepancies between the two techniques and more reliance was placed on SACV (MacDonald, 1987). Average corrosion rates showed that the coupons in the sterile pipe corroded slowly compared to those exposed to bacteria (table 1). Examination of the EIS diagrams showed several consistant differences between the coupons. All of the sterile coupons had extremely high

reactances, providing only a small section of the theoretical semicircle obtained by complex plane plot (Dowling, 1988b). These could not be extrapolated to the real axis due to the high error involved and values for Rp were thus unobtainable by EIS (table 1). In contrast, the corrosion rates in the inoculated coupons were high enough so extrapolation was possible and a reasonable value for Rp obtained. Figure 4 shows the contrast between polished base metal tested in sterile and inoculated conditions. The numbers on the diagram show that without the bacteria the reactance is very high even at high frequencies such as 1.0 Hz. The inoculated coupons however provide sufficiently low reactance to obtain an accurate extrapolation for Rp, moreover it is possible to observe that the corrosion mechanism is considerably more complex than just a single capacitive loop. The lower portion of a second capacitive loop with higher reactance than that associated with the double layer capacitance and polarization resistance appears at frequencies less than 0.1 Hz. This may be due to adsorbed corrosion products, however no such capacitive loop appears to be associated with the as-welded coupons (figure 3B).

It seems likely that the electrochemical phenomena and impedance diagrams associated with the double-layer capacitance and charge transfer in the as-welded coupons

were affected by other events such as oxide tinting of the surface and some galvanic corrosion due to microsegregation. These and other differences with the polished coupons undoubtedly contribute to a significantly different impedance diagram.

After 8 days a high frequency loop was observed (figure 5) with capacitance of approximately 10 uF/cm^2. This capacitive loop occurred in all the coupons examined and may have been due to a film formation and appeared to be independant of microbiological effect.

Examination of the as-welded coupons by incident-light microscopy showed the presence of oxide deposits in the fused zone which may have been excavated by bacteria (figure 6). These deposits were produced during the welding process (Heiple, 1986) as slag and acted as pit initiation sites for the bacteria. The deposits occurring on the coupons exposed to the bacteria occupied hemispherical depressions underneath which a pit had formed.

This work shows that the presence of bacteria significantly increased the corrosion rates of 316L stainless steel coupons. The major corrosion mechanisms may be related to the production of acetic and butyric acids which would lower the local pH. The results demonstrate important and reproducible differences in corrosion mechanisms, the true nature of which cannot be deduced from

this data. Further experimentation must be carried out in less complex systems to identify and explain the different electrochemical phenomena observed.

Acknowledgements

The authors would like to thank David Ringleberg for help with the diagrams and Dr.Ray Buchanan for discussions on the nature of corrosion. The US Navy is thanked for generous funding via the Office of Naval Research grant N00014-86-K-0275.

LITERATURE CITED

Dowling, N.J.E., Nichols, P.D. and White, D.C. (1988a). FEMS Microbial Ecol. Accepted for publication. Characterization of a sulphate-reducing consortium with phospholipid fatty acids and infra-red spectroscopy.

Dowling, N.J.E., Guezennec, J., Lemoine, M.L., Tunlid, A., and White, D.C. (1988b). Corrosion (NACE). Accepted for publication. Corrosion analysis of carbon steels affected by bacteria using electrochemical impedance and DC techniques.

Hamilton, W.A. (1985). Ann.Revs.Micro. 39, 195. Sulphate-reducing bacteria and anaerobic corrosion.

Heiple, C.R. (1986). Proceedings of the conference on progress in resolving undesirable trace element effects on the weldability of steels. Rockwell International, Golden, Colorado 80401.

Kearns, J.R. (1985). Corrosion '85 (NACE). Paper No. 50. The corrosion of heat-tinted austenitic stainless alloys.

Kobrin, G. (1976). Mats. Perf. 15(17), 38. Corrosion by microbiological organisms in natural waters.

Lundin, C.D., Lee, C.H., Menon, R., and Stansbury, E.E. (1986). Welding Research Council (USA) Bullitin No. 319. Sensitization of austenitic stainless steels; Effect of welding variables on HAZ sensitization of AISI 304 and HAZ behaviour of BWR alternative alloys 316 NG and 347.

MacDonald, J.R. (1987). Impedance spectroscopy: Emphasizing solid materials and systems. J.Wiley & Sons Inc. Canada.

Pfennig, N., Widdel, F., Truper, H.G. (1981). The dissimilatory sulphate-reducing bacteria. In: The prokaryotes. Vol. 1, pp926-940. Eds. Starr, M.P., Stolp, H., Truper, H.G., Balows, A., and Schlegel, H.G. Springer-Verlag, Berlin & New York.

Pope, D.H., Duquette, D.J., and Johannes, A.H. (1984). Mats.Perf. 24, 14-18. Microbially influenced corrosion of industrial alloys.

Tatnall, R. (1981). Mats.Perf. 19(8), 41-48. Case histories: Bacteria induced corrosion.

Table 1: Summary of the values for the polarization resistance (Rp) in ohms (for 4cm2 coupons) obtained by electrochemical impedance spectroscopy (EIS) or small amplitude cyclic voltammetry (SACV) over two weeks exposure.

DAYS	Sterile			Inoculated		
	316B	AW	PW	316B	AW	PW
1	U	U	U	180000	30000	180000
2	U	U	U	9000	30000	8000
5	U	U	U	1750	10000	1750
6	17076	11833	14000	1464	3592	1499
7	ND	ND	ND	2000	9000	2000
8	U	U	U	1400	ND	1800
12	U	U	U	1400	2000	2000
13	29590	19766	23240	1800	4597	1971
14*	1E-7A 40 mV	1E-7A 98 mV	2E-8A 100 mV	3E-6A 120 mV	1E-6A 80 mV	3E-6A 100 mV

U: Unobtainable due to insufficiently low frequency.
ND:Not determined. 316B: Polished base metal.
AW: As-welded. PW: Polished weld
*: Cathodic polarization to determine Icorr. and Tafel parameter.

FIGURE 1

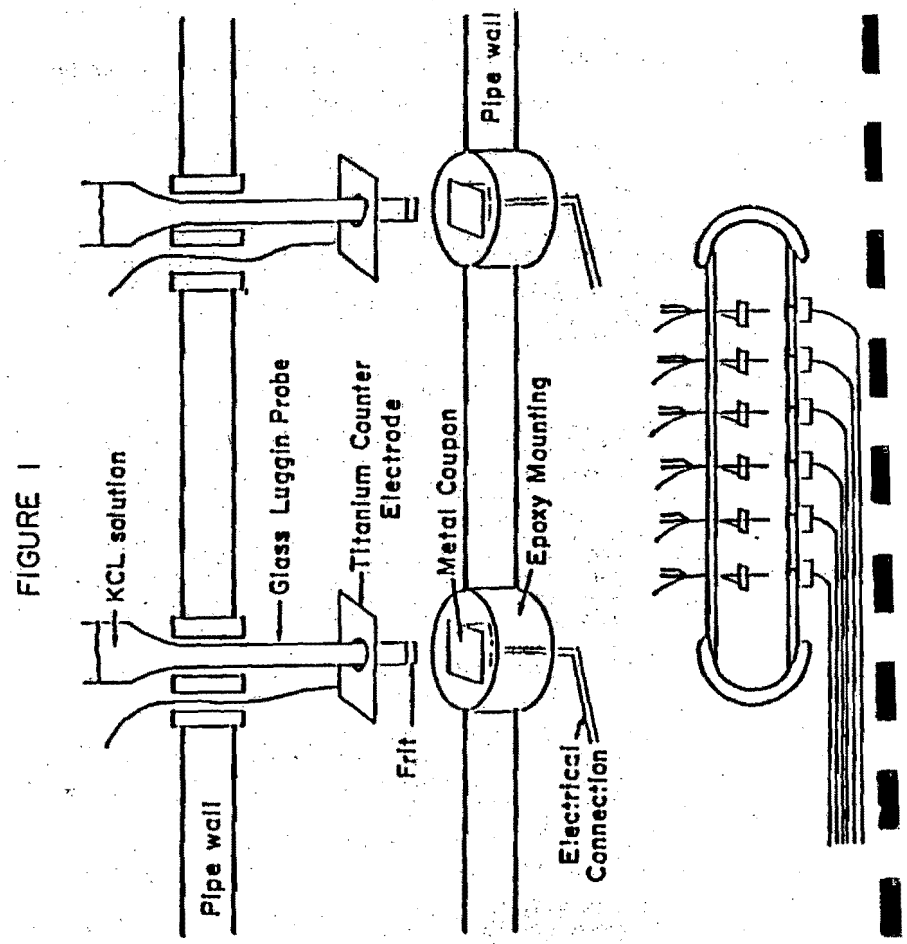

FIGURE 2.

Open-Cell Potential of Coupons Over Two Weeks

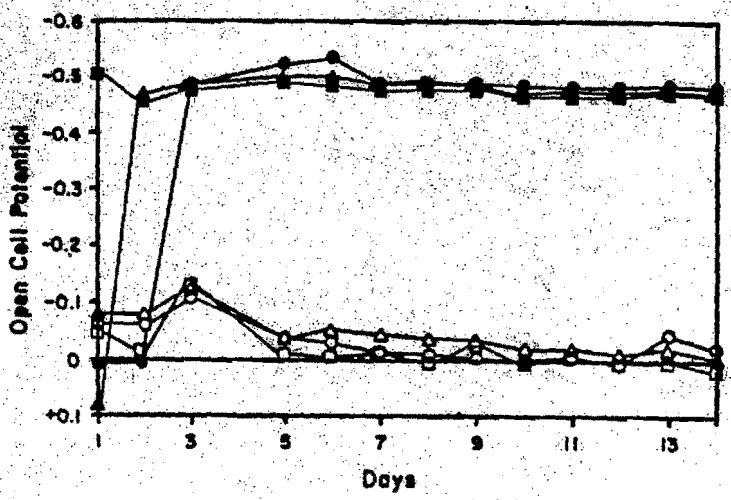

○ POLISHED BASE METAL, STERILE
● " " " , INOCULATED
□ AS-WELDED STERILE
■ " INOCULATED
△ POLISHED WELDED STERILE
▲ " " INOCULATED

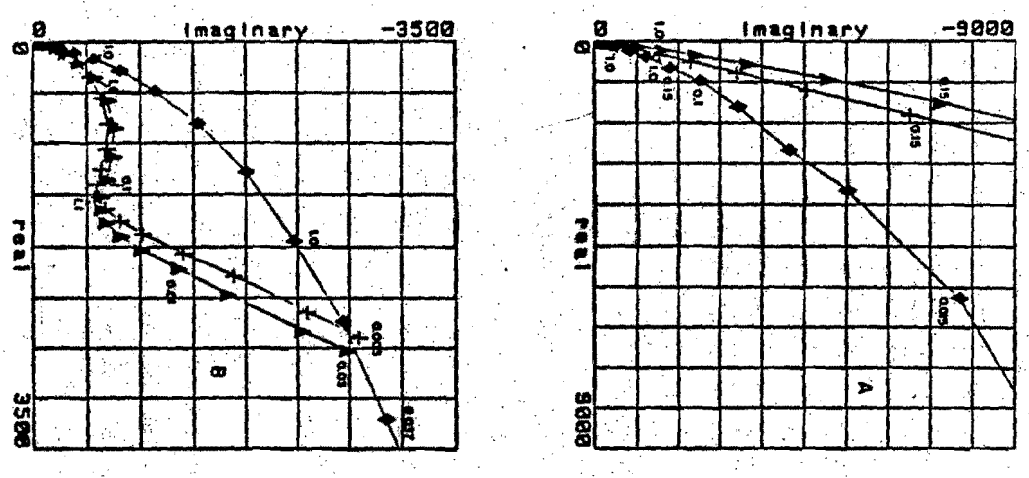

Figure 3: Coupons exposed to bacterial attack after 24 hrs (A) and 8 days (B). ◆ As-welded ▲ polished weld, and + base metal.

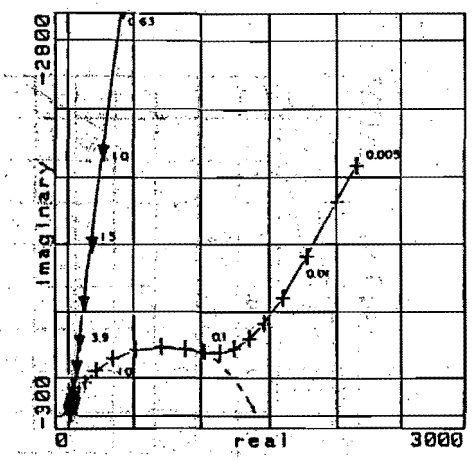

Figure 4: Base metal exposed to sterile ▼ , and inoculated + conditions after 12 days.

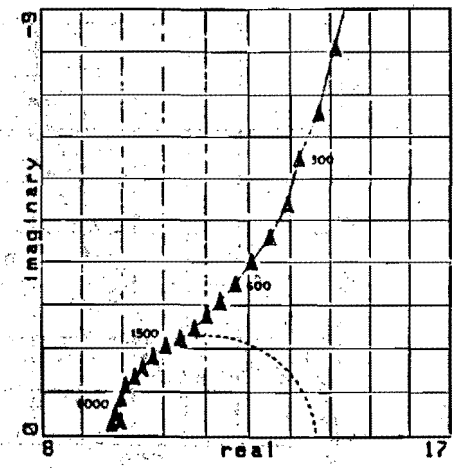

Figure 5: High frequency capacitive loop observed after 8 days in all conditions.

Figure 6: Attacked globular oxides observed at the edge of the fused zone in a small depression. The

SYNERGISTIC ACTION OF BACTERIA ON THE CORROSION OF MILD STEEL IN A MARINE MEDIUM

Christine C. Gaylarde

Department of Biological Sciences, City of London Polytechnic, Old Castle Street, London E1 7NT, U.K.

Hector A. Videla

Bioelectrochemistry Section, INIFTA, Faculty of Pure Sciences, University of La Plata, C.C. 16 Suc. 4, (1900) La Plata, Argentina.

ABSTRACT

The role of a marine vibrio in association with sulphate-reducing bacteria in the corrosion of mild steel in a saline medium is studied in the laboratory by means of electrochemical techniques complemented with scanning electron microscope observations and EDAX analysis of the corrosion products.

Dramatic differences in localised corrosion of mild steel coupons occurs when *Vibrio alginolyticus* colonises the metal surface alone or in association with sulphate-reducers. A preferential attack beneath microbial colonies can be observed by SEM. The iron reducing capacity of *Vibrio*, confirmed in laboratory experiments, suggests a possible mechanism of passivity breakdown through the removal of passive films by bacterial action.

INTRODUCTION

The active interaction between microorganisms and metal surfaces involves adhesion which is often facilitated by extracellular polymeric substances (EPS). The adhesion processes and subsequent EPS production lead to an important modification of the metal/solution interface, which becomes partially or totally covered by strongly adherent biofilms forming a barrier to the exchange of elements between the metal and the aqueous environment (Characklis, 1981). Reactions between the metal and metabolites derived from bacterial cells will take place within the biofilm. The products of these reactions will add to the corrosion products which are formed as soon as a metal such as mild steel comes into contact with a saline solution like sea water. As corrosion and microbial fouling in the marine environment occur in the same time scale, a new metal/solution interface, mainly formed by a complex layered structure of corrosion products, EPS and bacterial cells, will be produced (Videla, 1988) The growth of microorganisms of different species within adherent biofilms facilitates the development of structured consortia that enhance the microbial effects on metal corrosion (Costerton & Geesey, 1986).

The importance of microbial consortia in biologically induced corrosion (BIC) is increasingly recognised and previous workers have referred to the facilitating action of other microorganisms on the corrosion of mild steel by sulphate-reducing bacteria (SRB). These papers centre around the use of saline media like injection waters used in oil production (Westlake et al., 1986), estuarine waters (Gaylarde & Johnston, 1982), or laboratory media supplemented with sodium chloride (Gaylarde & Videla, 1987). In the last publication, evidence is provided from electrochemical measurements and SEM

observations showing that a marine strain of *Vibrio alginolyticus* is able to promote chemical or SRB-induced corrosion. This effect is suggested to occur through the removal of passive films (mainly ferric oxides) from the metal allowing aggressive species like sulphides and chlorides to have direct contact with the metal surface.

In this present paper new experimental evidence is presented to support the synergistic action of two microbial species (*Vibrio* and SRB) in the MIC of mild steel in marine media. Potentiodynamic polarisation experiments complemented with SEM observation of biological and inorganic deposits on the metal surface are used. EDAX or electron microprobe analysis are also employed to determine the nature of these deposits.

EXPERIMENTAL

V. alginolyticus was isolated from water collected from the port of Mar del Plata, Argentina and was kindly supplied by Dr. Luis Monticelli (INIDEP, Mar del Plata). Purity was checked periodically by plating on nutrient agar containing 10% sodium chloride and the identity was confirmed by biochemical tests. The ability of the cells to reduce iron(III) was determined by growth on Medium B (Westlake et al., 1986).

SRB were maintained in Postgate C (Postgate, 1984) solidified with 1.5% agar and incubated in anaerobic jars (Anaerocult, Merck, Darmstadt). Identity was verified by the desulfoviridin test (Postgate, 1964) and purity was checked at intervals throughout the experiments.

Vibrio was grown as batch cultures at 30 C in a LEH fermentor unit using a five litre vessel with automatic pH control at 7.8 by the addition of 0.5M sulphuric acid. Dissolved oxygen was monitored continuously using a LEH 1601/261 oxygen probe. Redox potential measurements were also made at intervals. Postgate C medium supplemented with 3% sodium chloride in the fermentor vessel was inoculated with a 24h culture of *V. alginolyticus* in 200ml of the same medium. Growth in the fermentor was monitored either by the consumption of sulphuric acid required to maintain the pH or by optical density measurements. Thirty minutes after inoculation the oxygen concentration in the medium was nil and the redox potential was -0.060V. A 96h culture of SRB in 200ml Postgate C was added to the *Vibrio* culture after 48-72h of incubation in the fermentor. Several mild steel specimens were included in the vessel and removed in pairs at intervals during incubation. One specimen was used for electrochemical polarisation experiments and the other for observation of corrosion products or biofilms using either a JEOL JSM35CF or a Philips 505 scanning electron microscope. Occasionally EDAX analysis of the corrosion products was made. Electron microprobe analysis was also used on occasions to confirm the nature of some deposits. For biofilm examination fixation of the specimens was made in 2.5% glutaraldehyde in phosphate buffer for 24-48h followed by washing in phosphate buffer and then dehydration through an acetone series to 100% and critical point drying.

Electrochemical measurements were made in a conventional single compartment glass cell. The temperature was 30 C + 0.1 and the potential of the working electrode was referred to a standard calomel electrode (SCE) through a Luggin capillary. The counter electrode was a platinum wire. Potentiodynamic sweeps were run from -0.80V at a low sweep rate (0.010V/min) to evaluate the corresponding breakdown potential (Eb). Electrodes used were SAE 1020 steel rods of about 5mm diameter embedded in an epoxy resin to give an exposed metal surface of 0.2cm2. Before use, the

metal surface was polished with several fine-grained emery papers and finally with alumina paste (1um). Postgate C without iron(II) sulphate (to avoid interference in the electrochemical experiments) and with 3% sodium chloride was used as electrolyte.

RESULTS

Vibrio alginolyticus produces typical orange iron-reducing bacterial colonies on Medium B both when incubated aerobically and when incubated in an anaerobic cabinet.

The appearance of mild steel electrodes immersed for several hours in a culture of Vibrio in saline Postgate C varies markedly with time. During the early hours before inoculation, the mild steel surface is covered by an homogeneous layer of oxide beneath overlying corrosion products (Gaylarde & Videla, 1987). Several hours after inoculation isolated *Vibrio* cells can be seen randomly dispersed over the cracked layer of corrosion products (Figure 1).

As incubation time progresses, some areas of the metal surface become covered by groups of bacterial cells with no evident EPS (Figure 2). Later, groups of cells resembling colonies can be seen on the surface even at low magnification (Figure 3). The interior of these colonies is composed of *Vibrio* cells and small amounts of corrosion products entrapped by EPS (Figure 4). Although the time necessary to allow the colony formation varies with the inoculum and the fermentation process, the metal colonisation generally takes place within 24h of inoculation. At this time dissolved oxygen in the medium is nil and redox potential values usually range from -0.040 to -0.060V. Occasionally, when some of the colonies slough off, a dense layer of lenticular blades of haematite (Fe_2O_3) lining the cavity below the colony can be observed (Figures 5 and 6). No bacterial cells can be seen over or among the inorganic formation. After cleaning the metal surface, it is apparent that intense localised attack has occurred beneath the areas where the colonies were seen (Figure 7).

SRB addition to the culture was made after 48 to 72h of incubation, after the *Vibrio* colonisation process has taken place. At this time, the oxygen concentration and redox potential in the medium are suitably low to allow SRB growth. Also at this time, many areas of the mild steel surface appear densely covered by layers of corrosion products preventing easy visualisation of microorganisms. Many of these corrosion products correspond to spherules of dense metallocolloidal goethite (Figure 8) and tabular haematite crystals. SRB colonies can be seen, with difficulty, between these inorganic deposits as sparsely dispersed colonies protected by the crystal formations (Figures 9 and 10). Apparently pure SRB cells can be seen at higher magnifications (Figure 11). In certain areas microbial consortia of *V. alginolyticus* and SRB mixed with amorphous corrosion products and EPS are evident (Figure 12).

The Eh values obtained from the polarisation experiments made in *V. alginolyticus* culture and *Vibrio* plus SRB culture are summarised in Table 1. Redox potentials are also shown to illustrate the oxidising conditions of the medium.

TABLE 1

Eh and redox potential values in saline Postgate C with or without bacteria.

Conditions	Eh(V)	Eh(V)
Sterile medium	-0.37	NT
24h *Vibrio* culture	-0.46	-0.044
Vibrio plus SRB (48h after SRB addition)	-0.75	-0.120

DISCUSSION

One important fact, generally not taken into account in the literature in mechanistic explanations of the anaerobic corrosion of iron, is that in practical situations metal surfaces are rarely free from various deposits. Inorganic deposits are usually oxides of different types, hydroxides and, mainly in the presence of SRB, sulphides. Organic deposits are due to the process of bacterial attachment and colonisation of any metal surface immersed in a marine environment. It is widely accepted that the attachment of living organisms is preceded by the formation of a thin film of organic macromolecules that alters the electrostatic charge and wetting properties of the metal surface (Dexter et al., 1975; Loeb & Neihof, 1977). The later bacterial settlement results in the development of a biofilm usually known in this initial stage as microfouling. A series of factors such as the nature and characterisitics of the metal surface, food supply from sea water (related to its degree of pollution), pH, temperature and ionic composition are assumed to influence the initial bacterial attachment (Videla et al., 1987).

The observation of microfouling is more easily made on less corrodible surfaces such as stainless steel or titanium. Mild steel surfaces are rapidly covered, after immersion in sea water, by several layers of corrosion products which can differ on unprotected and cathodically protected structures (Edyvean, 1984). Once bacterial settlement is in progress, EPS and bacterial cells increase biofilm thickness forming a diffusion barrier to the exchange of elements between the metal and the solution (Characklis, 1984).

Biofilms affect the behaviour of the metal by a) hindering the transport of chemical species necessary for passivation of the metal surface; b) facilitating the removal of passive layers as biofilm detachment occurs; c) leading to formation of differential aeration cells as a result of patchy distribution of the biofilm; d) altering oxygen concentration gradients by acting as a diffusion barrier or through the direct utilisation of oxygen in bacterial respiration (Videla et al., 1988). Alterations in the local environment at the metal/solution interface, induced by biofilms, can be due to enzymic action alone (Scotto et al., 1985) or to the formation of adherent microcolonies (Gaylarde & Videla, 1987). Physiologically cooperative cells may be recruited by specific metal adhesion to produce a functional consortium (Costerton et al., 1985). Generally the effect of binding bacteria to a metal surface increases the corrosion risk.

In the controlled experimental conditions used in this paper it is noticed that *Vibrio* growth facilitates SRB growth through a drastic reduction of the oxygen concentration and redox conditions of the medium. Mild steel in these experiments will be conditioned prior to SRB addition by the double action of *Vibrio* and the saline environment. After 24 to 48h the mild steel surface densely covered by amorphous and crystalline iron oxides is very different from the surface initially colonised by Vibrio (Figure 8). According to previous results (Gaylarde & Videla, 1987), *V. alginolyticus* is able to cause a slight corrosion of mild steel in a saline environment. This effect was demonstrated by the slight decrease in Eh potential, corroborated in this paper (see Table 1) and by SEM observations of the close relation between colony formation and metal attack. When SRB are added to the environment, as in the present work, biogenic sulphides and other electrochemically active intermediate metabolites such as thiosulphates (Newman et al., 1989) are formed. These can only interact directly with the metal where *Vibrio* colonies have "cleaned" the surface by their iron(III)-reducing activity. Such activity can aid in the removal of the iron oxides and hydroxides formed as a result of the initial chemical reactions within the medium.

Beneath the biofilm shown in Figures 4 to 6, a rather homogeneous mass of lenticular blades of haematite can be found (Figures 5 and 6). A generalised attack and micropitting reproducing the colony profile can be seen after cleaning off this inorganic layer. SRB colonies formed at protected sites of the surface (among crystalline deposits) can interact with the *Vibrio*-conditioned mild steel surface and higher levels of corrosion can be produced (Table 1). The presence of consortia at other sites of the metal surface is also observed (Figure 12).

The results presented here give additional support to the earlier findings of one of the authors (Gaylarde & Johnston, 1988; 1989) and extend the conclusions formulated recently (Gaylarde & Videla, 1987). Moreover, other communications presented at this meeting (Gomez de Saravia et al.; de Mele et al., 1988), referring to the effect of bacterial settlement on the corrosion behaviour of copper/nickel alloys, validate and extend the assumptions of this paper. Biological corrosion beneath biofilms is then a complex procedure, involving electrochemical processes of passivity breakdown assisted by biogenic effects due to bacteria within biofilms. These effects are probably present at all metal surfaces immersed in sea water although affecting the corrosion process to different degrees according to the nature of the metal substrate.

CONCLUSIONS

a) Present results validate previous findings on the action of a marine vibrio on the corrosion behaviour of mild steel in a saline environment. *V. alginolyticus* is able to promote a slight corrosion of mild steel coupons by altering the chemical composition of the passivating films and physicochemical conditions of the environment.

b) These effects are experimentally followed by electrochemical measurements (Eh, Ecorr, pH) and SEM observations.

c) The chemical alteration of passive films by microbial reduction of iron(III) species corroborates results previously reported by other authors for mild steel in the presence of different bacteria (Wentlake et al., 1986).

d) SRB added to a medium previously conditioned by *Vibrio* interact with the now unprotected metal surface causing higher localised corrosion than that observed with pure *Vibrio* (this paper) or SRB (Videla 1986) separately.

e) Present results confirm the importance of biofilm interactions, microcolony formation and microbial consortia on the corrosion behaviour of metals in saline environments.

Acknowledgement

The authors would like to express their acknowledgements to the Royal Society of Great Britain and the Consejo Nacional de Investigaciones Cientificas y Tecnicas of Argentina for the support given to this research through their cooperation programme. The laboratory assistance of Eng. Claudia Urtiz and Mr. Oscar E. Pardini is also gratefully acknowledged. H.A. Videla would like to express his recognition to Merck Quimica Argentina for the supply of analytical reagents and culture media used in this work.

REFERENCES

Costerton JW, Geesey GG, Cheng KJ (1978) How bacteria stick. Scientific American 238, 86-95.

Costerton JW, Marrie TJ, Cheng KJ (1985) Phenomena of bacterial adhesion. In Bacterial Adhesion (Eds. Savage DC, Fletcher M) Plenum Press, New York, pp. 3-43.

Costerton JW, Geesey GG (1986) The microbial ecology of surface colonisation and of consequent corrosion. In Biologically Induced Corrosion. NACE-8, International Corrosion Conference Series, NACE, Houston, Texas. pp. 223-232.

Characklis WG (1984) Biofilm development: a process analysis. In Microbial Adhesion and Aggregation (Ed. Marshall KC) Springer-Verlag, Berlin. pp. 137-157.

Baxter BC, Sullivan JB Jr., Williams J III, Vatsun SV (1975) Influence of substrate wettability on the attachment of marine bacteria to various surfaces. App. Microbiol. 30, 298-308.

de Mele MFL, Bronkovich G, Videla HA (1986) A comparative study of the Cu/Ni 30 Fe alloy electrochemical behaviour in sea water and different chloride saline solutions to assess the effect of microfouling settlement. Paper presented at this conference.

Edyvean RGJ (1984) Interactions between microfouling and the calcarious deposit formed on cathodically protected steel in seawater. In Marine Biology, Proc. 6th Int. Congress on Marine Corrosion & Fouling, Athens, Greece. pp. 469-483.

Gaylarde CC, Johnston JH (1982) The effect of *Vibrio anguillarum* on the anaerobic corrosion of mild steel by *Desulfovibrio vulgaris*. Int. Biodet. Bull. 18, 111-116.

Gaylarde CC, Johnston JH (1986) Anaerobic metal corrosion in cultures of bacteria from estuarine sediments. In Biologically Induced Corrosion, NACE-8, Int. Corrosion Conference Series, NACE, Houston, Texas. pp. 137-143.

Gaylarde CC, Videla HA (1987) Localised corrosion induced by a marine vibrio. Int. Biodet. 23, 91-104.

Gomez de Saravia SG, de Mele MF, Videla HA, Brauzkia E (1988) Bacterial attachment on Cu/Ni alloys and its relation with corrosion. Paper presented at this conference.

Loeb GI, Neihoff RA (1977) Adsorption of an organic film at the platinum-seawater interface. J. marine Res. 5, 283-291.

Postgate JR (1984) The sulphate-reducing Bacteria. Cambridge University Press, Cambridge.

Scotto V, Di Cintio R, Marcenaro G (1985) The influence of marine aerobic microbial film on stainless steel corrosion behaviour. Corr. Sci., 25, 185-194.

Videla HA (1986) Corrosion of mild steel induced by sulphate-reducing bacteria - a study of passivity breakdown by biogenic sulphides. In Biologically Induced Corrosion, NACE-8, Int. Corrosion Conference Series, NACE, Houston, Texas. pp. 162-170.

Videla HA (1988) Electrochemical interpretation of the role of microorganisms in corrosion. In Biodeterioration 7 (Eds. Houghton D, Smith RN, Eggins HOW), Elsevier, Barking, Essex. In press.

Videla HA, de Mele MFL, Brankevich G (1988) Assessment of corrosion and microfouling of several metals in polluted sea water. Corrosion. In press.

Westlake DWS, Semple KR, Obuekwe CO (1986) Corrosion by ferric iron reducing bacteria isolated from oil production systems. In Biologically Induced Corrosion. NACE-8, Int. Corrosion Conference Series, NACE, Houston, Texas. pp. 195-200.

CAPTIONS FOR FIGURES

Fig. 1 Scanning electron micrograph of metal surface showing cracked surface film and isolated *Vibrio* cells among amorphous corrosion products. Mag. X4000

Fig. 2 Scanning electron micrograph showing groups of *Vibrio* cells on the metal surface. Mag. X4000

Fig. 3 Scanning electron micrograph showing colonies of *V. alginolyticus* on the metal surface. Areas between colonies are similar to the surface seen in Fig. 1. Mag. X60

Fig. 4 Scanning electron micrograph of the interior of a colony of *V. alginolyticus* on the metal surface Mag. X4800

Fig. 5 Scanning electron micrograph of the metal surface beneath a sloughed off colony of *V. alginolyticus*. A rather homogeneous layer of lenticular blades of haematite can be seen in the cavity. Amorphous corrosion products and bacterial cells surround the former colony areas. Mag. X312

Fig. 6 Scanning electron micrograph of lenticular blades of haematite crystals layering on the metal surface beneath a *V. alginolyticus* colony. Mag. X 5000

Fig. 7 Scanning electron micrograph showing mild steel surface beneath microbial colony after cleaning. Generalised attack and micropitting are found under the *V. alginolyticus* colonies. Mag. X240

Fig. 8 Scanning electron micrograph of mild steel surface after 48h of immersion in a saline Postgate C medium with *Vibrio* and SRB. Dense groups of tabular haematite crystals and spherules of dense metallocolloidal goethite can be seen on the metal surface. Mag. X160

Fig. 9 Scanning electron micrograph of SRB colonies located on the mild steel surface between different groups of crystalline and amorphous corrosion products. Mag. X905

Fig. 10 Scanning electron micrograph showing one of the SRB colonies seen in Fig. 9. SRB cells are located between accumulations of lenticular blades of haematite crystals. Mag. X2500

Fig. 11 Scanning electron micrograph of the SRB colony shown in Fig.10. Cells of SRB can be seen without any evident EPS. Mag. X6500

Fig. 12 Scanning electron micrograph of a microbial consortium of *V. alginolyticus* and SRB cells on the metal surface. Mag. X10000

Fig. 1

Fig. 2

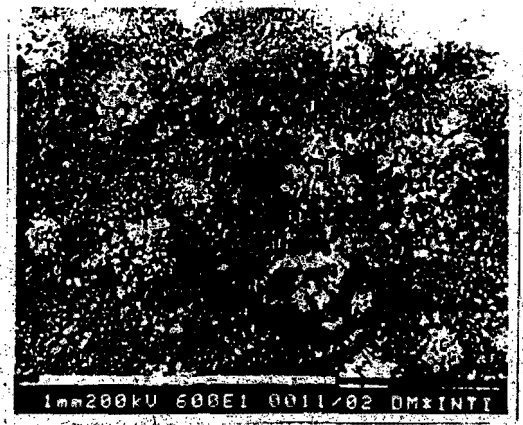

Fig. 3

Fig. 4

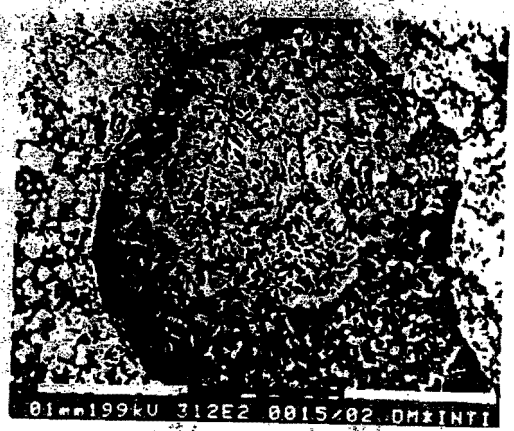

Fig. 5

Fig. 6

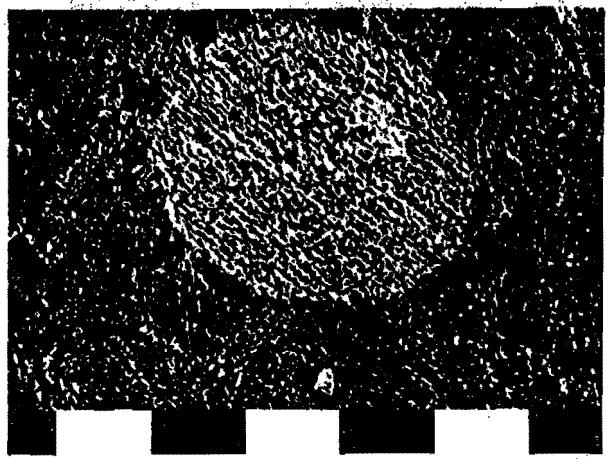

Fig. 7

Fig. 9

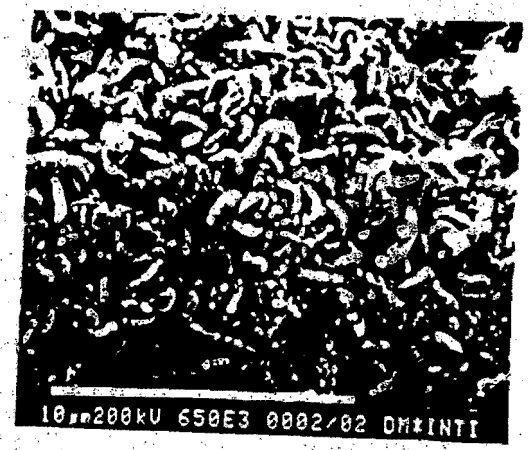

Fig. 11

Fig. 12

BACTERIAL ATTACHMENT ON Cu/Ni ALLOYS AND ITS RELATION WITH CORROSION

S.G. Gómez de Saravia, M.F.L. de Mele, H.A. Videla and E. Erauskin*

Bioelectrochemistry Section - INIFTA - Facultad de Ciencias Exactas, Universidad Nacional de La Plata - C.C. 16, Suc. 4 - (1900) La Plata Argentina

* Corrosion Section INASMET - B. Igara s/n 2009 San Sebastián, Spain

ABSTRACT

Bacterial settlement on 70/30 and 90/10 copper-nickel alloys specimens was followed by SEM using chloride solutions. Two different strains of bacteria (Pseudomonas sp. and Vibrio alginolyticus) isolated from harbour sea water were used. The corrosion behaviour of the alloy was studied through corrosion potentials measurements made in sterile and contaminated sea water. Well definite microbial colonies were seen by SEM after 24 hs of exposure. Corrosion attack seems to be closely related to the passive film modification by the bacterial settlement and to the nature of each alloy.

INTRODUCTION

Copper is extensively used in the marine environment as an antifouling agent due to its biocidal properties. In its alloy form with nickel (particularly 90/10 and 70/30 cupro-nickel) it offers an increased corrosion resistance and good antifouling properties due to copper ions leaching from the surface.

Microfouling is easily initiated in corrosion resistant metal surfaces whereas corrodable surfaces offer a complex behaviour with respect to bacterial attachment according to the physicochemical, structural and toxical properties of the corrosion products formed after the metal immersion in sea water (1).

Bacteria and diatoms can be present in large numbers very soon after immersion of a metal surface in sea water producing a slime film due to the production of extracellular polymeric substances (EPS). The first bacterial colonizers are usually reported to be predominantly gram negative rod-shaped bacteria such as species of the genera Pseudomonas, Vibrio, Flavobacterium and Achromobacter (2).

The aim of this work is to study the influence of microfouling formation on the corrosion of 90/10 and 70/30 copper-nickel alloys. With this purpose chlorine solutions contaminated with two bacteria strains isolated from harbour sea water were used. Corrosion potential variations were analysed together with SEM observation of the metal samples.

MATERIALS AND METHODS

Two different strains of microorganisms isolated from polluted harbour sea water were used: Pseudomonas sp. and Vibrio alginolyticus. They were kindly supplied by Dr. Luis Monticelli, INIDEP, Mar del Plata. Both strains were maintained in nutrient agar plus 3% sodium chloride. Purity was checked at intervals by plating on nutrient agar plus 10% sodium chloride for the Vibrio and through biochemical tests for Pseudomonas.

Laboratory experiments were made using artificial sea water according to a simplified Lymann and Fleming formula supplemented with 1 g/l of yeast extract and Postgate C medium added with 3% NaCl. All chemicals used for artificial sea water preparation were analytical grade (Merck Darmstadt). The initial pH of the solution was adjusted to 7.5 by addition of NaOH.

Bacteria were grown in 500 ml erlenmeyer flasks containing 200ml of artificial sea water. After inoculation the flasks were kept for three hours in a rotary shaker. Thereafter static conditions were chosen for microbial growth. Inocula were prepared by suspending agar slants cultures in equal volumes of 2 ml artificial sea water. The incubation temperature was 28°C. Growth in the flasks was monitored by determination of optical density at 610 nm.

Metal specimens used to assess microbial colonization and corrosion were 70/30 copper nickel disks of 15 mm and 7 mm diameter and 90/10 copper nickel square plates of 5 mm x 5 mm embedded in an epoxy resin. Each flask was provided with 6 metal probes, three of them to be used for microfouling observations and the other three were provided with electrical contacts to measure corrosion potential. Additionally, redox potential measurements were made in each culture. Both potentials were referred to standard calomel electrodes. "In situ" measurements of corrosion potential were made with samples placed in natural sea water at the Mar del Plata harbour, Argentina (38°08'15"S; 57°31'18"W).

Before using, metal samples were prepared by polishing through different grits of silicon carbide metallurgical paper (320, 600 and 1200) and finally, with alumina paste (1 µm grain size).

Metal probes were taken out of the flasks for SEM observations after different exposure times ranging from 1 to 7 days. In order to preserve biological material specimens were successively fixed with 2% glutaraldehyde solution in phosphate buffer, disalted in distilled water, dehydrated through an acetone series to 100% and finally critical point dried. To observe metal attack after exposure, samples were polished with alumina (1 µm) for removing the biological and inorganic products from the surface. Later, samples were cleaned and degreased with acetone and finally rinsed with distilled sea water. SEM observations were made using a Philips 505 microscope.

RESULTS AND DISCUSSION

Corrosion potential measurements from both 70/30 and 90/10 copper-nickel specimens immersed in sterile artificial sea water showed potential values close to - 0.20 V (Table I). Conversely, corrosion potential measurements made on 70/30 copper-nickel samples incubated

separately during 7 days with cultures of Pseudomonas sp. in artificial sea water showed a wide range of scatter (Table II) when compared with the same alloy samples immersed in the sterile media.

Potential values recorded in the bacterial cultures oscillated between -0.27 V and -0.4 V. On the other hand, 90/10 copper-nickel corrosion potential values were nearly constant at c.a. = -0.24 V.

Through SEM examination of the metal samples, after one day of exposure in Pseudomonas sp. cultures, isolated colonies can be seen on the 70/30 Cu-Ni surface. After longer periods of exposure the number of bacteria attached increased mainly as round shaped colonies of c.a. 10 to 20 µm diameter (Fig. 1). In some areas bacterial cells appeared in a layered arrangement with the production of extracellular polimeric substances (EPS) (Fig. 2). The formation of the round shaped microbial colonies seem to be closely related to EPS production. When colonies were removed, darked areas without the outer layer of corrosion products were visible (Fig. 3). It has been reported that the sloughing off of the corrosion/slime layer may occur frequently on copper-nickel samples and thus, the film thickness may vary with time and with the metal/alloy exposed surface (3).

In the case of 90/10 copper-nickel specimens a great number of colonies can be observed (Fig. 4). Besides, large areas with cells entrapped in an EPS mucilage can be seen (Fig. 5).

The superficial appearance of the two alloys after immersion was very different. In the case of 70/30 copper-nickel alloy cracked corrosion products can be observed on the metal surface. The outer layer of corrosion products corresponding to 90/10 copper nickel specimens appeared detached as fine sheets (Fig. 4). Additionally, when the detatchment of a colony occurred at this alloy, the surface beneath the accumulation of EPS products looked darker, although with little difference in depth. The initial detatchment process of EPS could be observed in Fig. 6.

Copper-nickel samples exposed to V. alginolyticus cultures showed a similar appearance to that reported for samples exposed to Pseudomonas sp. cultures. Few incipient colonies formed mainly by EPS and bacterial cells are clearly visible on the surface after 24 hs of immersion (Fig. 7). Size of microbial colonies was similar although they were not uniform in shapes as they were Pseudomonas sp. colonies (c.a. 10-15 µm). A great amount of EPS linked bacterial cells (Fig. 8). Corrosion potential measurements show for both 90/10 and 70/30 Cu/Ni alloys high cathodic values (Table II). Thus, more negative corrosion potential values and a greater localized attack than in the case of Pseudomonas cultures were observed for V. alginolyticus cultures (Fig. 9). It has been recently reported for mild steel samples in V. alginolyticus cultures that this microorganism may promote chemical or biological induced corrosion by removing a passive film from the metal, allowing aggressive species present in the environment to affect the surface (4). The same type of microbial colonies present on copper-nickel were observed in mild steel samples immersed in laboratory cultures of V. alginolyticus. After cleaned, there was intense attack beneath those colonies.

Recently reported chemical and ESCA analyses of copper-nickel alloy made with metal samples stepped in the vecinity of the corrosion potential value showed a complex passive film mainly composed oxide and chloride and a porous outer layer formed by precipitated cuprous hydroxichloride (paratacamite) (5). During the first days of sea water immersion a porous and discontinuous layer of paratacamite can be formed on copper-nickel samples. Bacterial contamination could lead to the loss of passivation mainly through a modification of the rate of oxygen diffusion through the bacterial slime (6, 7). Additionally the layering distribution of cells and corrosion products could modify the passive film adhesion (3).

According to the present results corrosion potential values obtained in the culture media and "in situ" measurements (1) show similar tendencies to that obtained for stainless steel in the presence of localized attack (8). A decrease in the corrosion potential measured is due to polarizing currents supplied by the localized corrosion areas. These events are not observed in sterile sea water. SEM observations reveals a different passive film structure under the colonies in the case of samples exposed to culture media. A complex corrosion pattern can be expected for copper-nickel alloys in the presence of biofouling, mainly due to the presence of localized and generalized corrosion occurring simultaneously and presenting a more intrincate distribution of corrosion products layers.

Microbially-induced corrosion beneath biofilms involves electrochemical cell formation and the breakdown of passivity according to the sloughing off of the corrosion/slime layers. These effects are clearly evidenced through the highly variable corrosion potential obtained for 90/10 and 70/30 copper-nickel samples exposed to V. alginolyticus inoculated media, in contrast to similar measurements obtained with sterile controls.

In the case of media inoculated with Pseudomonas sp. and 70/30 copper-nickel samples, wider variation in potential values and more intensive attack than in the case of 90/10 copper-nickel alloy were obtained. Thus, the nature of the metal surface and the type of bacteria play a relevant role in the relation between biofilms and corrosion.

REFERENCES

1. H.A. Videla, M.F.L. de Mele and G. Brankevich, "Microfouling of several metal surfaces in polluted sea water and its relation with corrosion", Corrosion 87(NACE), San Francisco, Ca, paper No. 365 (1987).
2. J. Carson, D. Allsopp, "Composition of fouling bacterial films on submerged materials", In Barry S., Oxley T.A. (eds) Biodeterioration 5, John Wiley and Sons, Chichester, pp. 291 (1983).
3. G. Blunn, "Biological fouling of copper and copper alloys", In Barry S., Houghton D.R., Lewellyn G.C., O'Rear C.E. (eds.) Biodeterioration 6, CAB International, pp. 567 (1986).
4. C.C. Gaylarde and H.A. Videla, International Biodeterioration 23(2) 91 (1987).
5. C. Kato and H.W. Pickering, J. Electrochem. Soc. 131(6) 1219 (1985).
6. D.J. Schiffrin and S.R. de Sanchez, Corrosion 41(1) 31 (1985).
7. M.F.L. de Mele, H.A. Videla and G. Brankevich, Br. Corros. J. (in press).
8. S.C. Dexter and G.Y. Gao, "Effect of sea water biofilms on corro- [illegible] of stainless steel", Corrosion

TABLE I: Open circuit potential values corresponding to sterile media

Time/ hours	Open circuit potential/V		
	Artificial sea water	Postgate culture media + 3% NaCl	
	70/30 CuNi alloy	70/30 CuNi alloy	90/10 CuNi alloy
0	- 0.197	- 0.242	- 0.257
3	- 0.198	- 0.246	- 0.256
13	- 0.220	- 0.245	- 0.255
17	- 0.222	- 0.240	- 0.247
23	- 0.225	- 0.239	- 0.243
37	- 0.227	- 0.237	- 0.237
45	- 0.227	- 0.236	- 0.229
51	- 0.199	- 0.236	- 0.226
60	- 0.207	- 0.238	- 0.223
75	- 0.220	- 0.244	- 0.222
81	- 0.220	- 0.243	- 0.227
85	- 0.222	-	-
147	- 0.225	- 0.239	- 0.217

TABLE II: Open circuit potential values corresponding to inoculated media

Time/ hours	Open circuit potential/V			
	Artificial sea water inoculated with:			Postgate C culture media + 3% NaCl inoculated with:
	Pseudomonas sp.		V.alginolyticus	V. alginolyticus
	70/30 CuNi alloy	90/10 CuNi alloy	70/30 CuNi alloy	90/10 CuNi alloys
0	- 0.207	- 0.240	- 0.230	- 0.274
14	- 0.196	- 0.236	- 0.465	- 0.364
20	- 0.236	- 0.234	- 0.242	- 0.429
24	- 0.366	- 0.236	- 0.231	-
38	- 0.335	- 0.262	- 0.249	- 0.444
40	- 0.400	- 0.236	-	- 0.447
44	- 0.310	- 0.235	-	-
54	- 0.278	- 0.234	- 0.458	-
62	- 0.308	- 0.233	- 0.422	-
74	-	-	- 0.415	-
112	-	-	-	- 0.251
130	- 0.297	- 0.195	- 0.300	-

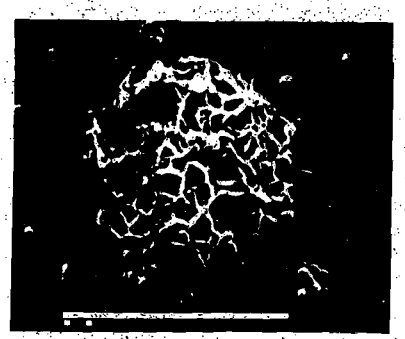

Fig. 1

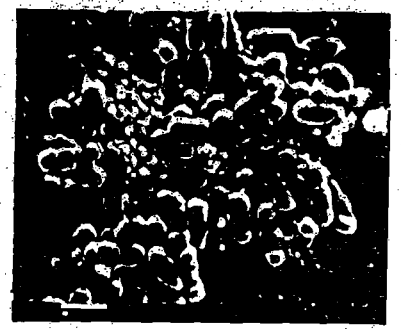

Fig. 2

Figs. 1 and 2: SEM microphotographs corresponding to 70/30 copper-nickel alloy specimens after 3 days of immersion in a Pseudomonas sp culture (7000 X and 15000 X, respectively).

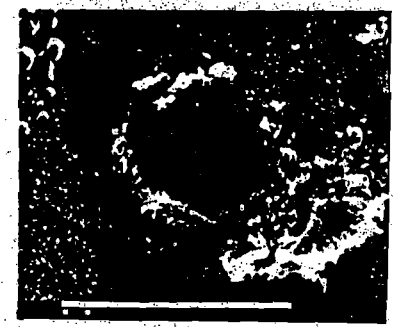

Fig. 3: SEM microphotograph corresponding to 70/30 copper-nickel alloy specimens after 3 days of immersion in a Pseudomonas sp. culture. Bacterial colony was removed (7000 X).

Fig. 4: SEM microphotograph corresponding to a 90/10 copper-nickel alloy specimen after 3 days of immersion in a Pseudomonas sp culture (2000 X).

Fig. 5: SEM microphotograph corresponding to a 70/30 copper-nickel alloy specimen after 3 days of immersion in a Pseudomonas sp culture (4500 X).

Fig. 6: SEM microphotograph corresponding to a 90/10 copper-nickel alloy specimen after 1 day of immersion in a Pseudomonas sp culture (3500 X).

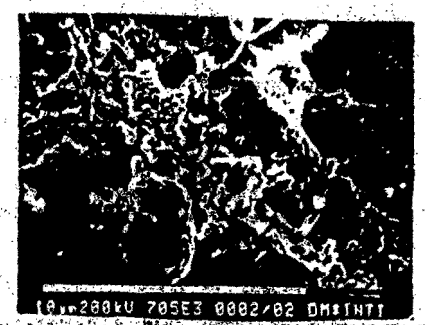

Fig. 7: SEM microphotograph corresponding to a 70/30 copper-nickel alloy specimen after 1 day of immersion in a V. alginolyticus culture (7000 X).

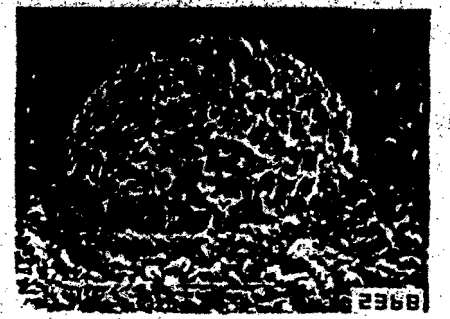

Fig. 8: SEM microphotograph corresponding to a 90/10 copper-nickel alloy specimen after 3 days of immersion in a V. alginolyticus culture (7500 X).

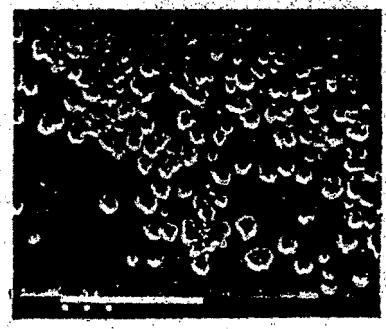

Fig. 9: SEM microphotograph corresponding to a 70/30 copper-nickel alloy specimen after 7 days of immersion in a V. alginolyticus culture. Bacterial colonies were removed (450 X).

MICROBIAL INTERVENTION IN COPPER CORROSION

Brenda J. Little
Patricia Wagner
Naval Ocean Research and Development Activity
NSTL, MS U.S.A. 39529-5004

ABSTRACT

A marine bacterium isolated from a copper-coated metal surface demonstrated the ability to oxidize/reduce copper under suitable conditions and to alter the corrosion of copper in a seawater medium. Proposed electron transport mechanisms are consistent with these observations.

INTRODUCTION

Microbial films develop on all solid surfaces placed into naturally occurring marine environments.[1] Bacteria are usually the first organisms to attach. On most engineering surfaces a diverse periphytic community develops, which includes diatoms, filamentous algae, ciliated protozoa, and other microbial species. In contrast, surfaces of copper-based alloys or surfaces painted with copper-containing paints, when exposed under the same conditions, develop less diverse communities composed primarily of bacteria.[2]

Numerous mechanisms have been proposed for the impact of bacteria on the corrosion of copper. These typically include differential aeration,[3,4] acid production,[5] and sulfide production.[6,7,8,9] Geesey et al.[10] recently reported that the exopolymer isolated from a freshwater bacterium promoted the deterioration of copper foil. In this paper we will demonstrate that the mechanism for the corrosion of copper can be altered by the presence of microorganisms and that microbially mediated electron transfers between copper species can impact corrosion.

METHODS AND MATERIALS

Bacteria

A gram-negative rod-shaped bacterium was isolated from a surface painted with a coating containing cuprous oxide and tributyl tin oxide. The surface had been exposed to the marine environment of Key Biscayne, Florida, for a period of 6 months. The microorganism permeated the coating and could be found on the surface of the paint, as well as in blisters beneath the paint. The organism was isolated and cultured using standard microbiological techniques. The growth medium was sterilized Gulf Stream water (3.5 w/o Cl) augmented with 1.2×10^{-4} M ammonium added as NH_4Cl and 1×10^{-5} M phosphate added as $N_a H_2 PO_4$, 70 ppm Cu (II) added as $CuSo_4$, and 1×10^{-2} M of either glucose or glutamate as a sole carbon source. Organisms that attached to metal surfaces were selected by providing copper discs in the culture tube with culture medium. Gulf Stream water was sterilized using a combination of pasteurization (70°C for 2 hours), and filtration (0.45 um pore size prefilter and 0.1 um pore size filter).[11]

Corrosion Experiments

Corrosion experiments were conducted in 500 ml magnetically stirred, continuous-flow culture vessels containing about 300 ml of media with a flow rate of ca. 20 ml/h. A copper electrode was cut from a polycrystalline rod stock (99% pure Hartz grade) embedded in epoxy to

expose 1.34 cm^2 uninsulated area. The electrode was placed in the center of the vessel with a saturated calomel reference electrode (SCE) and platinum auxiliary electrodes. Corrosion experiments were conducted under sterile conditions for 145 days, and then maintained as a pure culture for an additional 183 days. Quadruplicate sets of polarization resistance data were collected at 3-day intervals with a high impedance potentiostat. Measurements were made in the mixed potential region, i.e., in the vicinity of the corrosion potential. Polarization resistance data were analyzed by POLCURR to provide anodic and cathodic Tafel slopes, as well as corrosion current.[12]

Additional corrosion measurements were made using a 2-compartment corrosion cell, that has been described elsewhere,[13] and galvanically coupled copper electrodes. The system can be used to evaluate the electrochemical impact of microbiological species and individual abiotic chemical perturbations on metal electrodes. It consists of two compartments (electrolytically continuous but biologically isolated) externally connected to a zero resistance ammeter (ZRA). When either of the compartments is perturbed, biologically or abiotically, anodic and cathodic currents are established. An anodic current indicates oxidation; cathodic current, reduction. The extent of the impact is reflected in the magnitude of the observed current. Microorganisms were allowed to colonize the electrode in one of the compartments, and the electrochemical impact of their colonization measured using glucose-enriched media and glutamate-enriched media. Aerobic conditions were maintained by bubbling air through the media. Microaerobic conditions were maintained by bubbling nitrogen through the electrolyte. At the conclusion, electrodes were examined using scanning electron microscopy.

Results

In either sterile or inoculated glucose-enriched seawater media, the copper electrode surface exhibited a reddish color characteristic of Cu_2O. The electrochemical parameters of the sterile seawater were essentially unchanged in the presence of $1x10^{-2}$ glucose (145 days). In the presence of glucose, the bacteria (183 days) increased the corrosion rate of copper as indicated by an anodic shift of corrosion potential values and decreased cathodic Tafel slope (Table 1). A thin film of bacteria was found on electrode surfaces at the conclusion of the glucose experiments.

With the addition of sterile glutamic acid to the seawater medium, the copper surfaces exhibited a black color, which is characteristic of CuO, and the electrochemical parameters changed significantly (Table 1). Corrosion current increased tenfold from 5 uA cm^{-2} to 52 uA cm^{-2}. After approximately 6 days, microorganisms colonized the copper electrode, the black color was converted to red, and the corrosion rate decreased to 3 uA cm^{-2}. Tafel slopes increased with the addition of glutamic acid and decreased after the colonization by microorganisms.

A cathodic corrosion current was measured when the bacteria were added to one compartment of the two-compartment cell with glutamic acid under microaerobic conditions. Corrosion currents were typically 5-8 uA cm^{-2}.

Several qualitative observations were made concerning the growth of the microorganism in glutamate-enhanced media. The microorganism could oxidize Cu(I) and reduce Cu(II) under appropriate conditions. The

organism had to be "primed" by growing under aerobic conditions before it could visibly reduce Cu(II) to Cu(I) when its growth was shifted to a microaerobic environment. Following this shift, the bacteria developed spherical bodies ("cuprosomes") associated with the cell wall. These bodies, which contain Cu(I), impart to the cell a deep red color. This ability to reduce Cu(II) after an anaerobic shift was independent of growth rate as determined by studies using continuous culture. Reduction of Cu(II) was not observed with stationary phase cells. Following a shift back to aerobic growth conditions, the cells readily reoxidized the copper (I) to copper (II). If, however, the cells were fixed in ethanol or maintained at temperatures below 4°C, the oxidation took place slowly, even in the presence of oxygen. Cuprosomes did not form anaerobically when the cells were grown in a medium containing nitrite as a terminal electron acceptor. The microorganism does not accumulate the red spheres when grown on glucose, however, it does appear to deposit highly refractile copper-containing material in or near the cell wall.

Discussion

Cuprous oxide, a corrosion product of copper alloys, is commonly used as an additive to antifouling paints because of its toxic properties to biological systems. Recently cuprous oxide paint formulations have been supplemented with tributyl tin to enhance the antifouling properties. However, the experimental surface described in this paper was covered with a luxuriant biofilm predominated by the isolated bacterium. The choice of copper-bearing alloys for marine service is not only due to its antifouling properties, but also because of its predictable corrosion behavior. Despite the understanding of copper-seawater reactions, the performance of copper-bearing alloys and coatings in seawater service has not been predictable. There have been numerous corrosion failures of copper seawater piping systems and some of those failures have been attributed to microbiologically induced corrosion. Generalized copper corrosion in saline solution is depicted in Figure 1. At anodic sites chloride adsorbs to form a surface complex, which releases electrons that are available to the cathodic sites. The follow-up, nonoxidizing reactions give rise to cuprous oxide, which is the major component of the pseudopassivation on copper corroding in seawater. At cathodic sites oxygen adsorbs and then is reduced by the electrons supplied by the anodic sites. The possible intermediates may give rise to other chemical reactions at the surface and in the solution. In general corrosion, anodic and cathodic sites are randomly distributed and are interchangeable over the copper surface. They are separated in Figure 1 only for the purpose of illustration.

Glucose and glutamate have been shown by other investigators[14,15] to contribute substantially to heterotrophic activity to coastal bacterial populations. For this reason, these two model carbon sources were chosen for continuous culture bacterial corrosion experiments. Because Gulf Stream seawater is depleted in NH_4^+ and PO^- relative to coastal waters, the sterilized seawater was supplemented with these two nutrients.

It is apparent that glucose and glutamate provide different environments for the microorganisms. Few microorganisms attached to the copper surfaces when grown on glucose. Thick biofilms formed on the copper surfaces in the glutamate medium. The impact of carbon sources

on microbial adhesion has been previously reported.[16] It is also apparent that the two carbon sources provide different corrosive environments for copper. Glucose, a reducing sugar, is capable of maintaining an intact cuprous oxide (Cu_2O) film. Glutamate, a chelating agent for copper, can dissolve such a film and enhance its oxidation to cupric oxide (CuO). Cupric oxide is less protective to corroding copper than is cuprous oxide. Glutamate in the sterile seawater medium enhanced the corrosion of copper, while glucose had no measurable electrochemical impact. In the presence of a biofilm, copper corrosion increased in glucose media and decreased in glutamate media. One interpretation of this result might be that the biofilm provided a diffusion barrier to glutamic acid and/or oxygen. However, the decreased anodic and cathodic Tafel slopes in the presence of the biofilm with both glucose and glutamate are not consistent with such an interpretation. They indicate decreased barriers to diffusion, i.e., increased corrosion. These two conflicting conclusions suggest a shift in the corrosion mechanism and a more complicated situation than that depicted in Figure 1. The presence of the microorganism either removed the barrier to oxygen diffusion to the corroding surface or changed the primary cathodic reaction making the presence of oxygen at the corroding surface unnecessary.

When cathodic and anodic sites on a corroding copper surface are not freely interchangeable (e.g., during microbial colonization) they can become "permanent." Using the two-electrode apparatus, it was demonstrated that the bacterial isolate was responsible for cathodic reactions at the electrode surface. These observations are summarized in Figure 2. Active metabolism is required for this microorganism to oxidize or reduce copper as demonstrated in the growth studies. Furthermore, cuprosomes did not form anaerobically when the cells were grown in a medium containing nitrite as the terminal electron acceptor. Nitrite can serve as the sink for electrons involved in the anaerobic oxidation of Cu(I) to Cu(II). This mechanism eliminates the requirement for oxygen in the cathodic corrosion reaction. This mechanism may be important in estuarine waters since bacteria can oxidize ammonia to nitrite. Atmospheric input may also be a source of nitrite. These qualitative data are consistent with the hypothesis that copper is being oxidized/reduced by the electron transport chain in one of the sites depicted in Figure 3.

Microorganisms have evolved elaborate systems of electron transport involving a variety of metals to serve energy manipulation requirements.[17,18] For example, iron-oxidizing bacteria derive energy by transferring electrons from ferrous iron to oxygen.[19] Sulfate-reducing bacteria obtain energy by transferring electrons from organic matter or hydrogen to sulfate as a terminal electron acceptor.[20] Both procaryotes and eucaryotes have copper-containing proteins that can serve in electron transport and in several redox reactions. Proteins that complex copper can serve as reversible electron donors/receptors in biochemical reactions and are intimately involved in cellular energy manipulations. Soluble Cu(II) or its bacterially derived complexes can serve as the electron acceptor for the cathodic corrosion reaction. In the presence of microorganisms, this process may involve soluble redox components and/or highly saturated copper biopolymeric complexes associated with charge transfer.

CONCLUSIONS

The data presented in this paper indicate that microorganisms attached to copper surfaces can alter the mechanism of corrosion. In oxygenated, aqueous electrolytes, the electron acceptors are usually H_3O^+ and dissolved oxygen. However, metal species such as Cu(II) and Fe(III) can serve as electron acceptors. The data presented in this paper indicate that microorganisms can mediate electron transport and impact corrosion.

ACKNOWLEDGMENTS

This work was planned and a portion of it completed by the late Dr. Sol M. Gerchakov, formerly with the University of Miami in Florida. Research was funded by NORDA program element 61153N in support of the Defense Research Sciences Program, Herbert C. Eppert, Jr., Program Manager. Contribution 88:025:333 from the Naval Ocean Research and Development Activity.

REFERENCES

1. W. A. Corpe, 1974. Periphytic marine bacteria and the formation of microbial films on solid surfaces. In Effect of the Ocean Environment on Microbial Activities. eds. R. R. Colwell and R. Y. Morita. pp. 394-417. Baltimore: University Press.

2. D. S. Marszalek, S. M. Gerchakov, and L. R. Udey, 1979. Influence of substrate composition of marine microfouling. Appl. Environ. Microbial. 38:987-995.

3. J. D. A. Miller, Ed., 1970. Microbial aspects of metallurgy, p. 113. American Elsevier Publishing Co., New York, New York.

4. B. C. Edwards, 1969. The protection of Cu-Ni condenser tubes with high molecular weight water-soluble polymers. Corrosion Science Vol. 9, pp. 395-404.

5. D. H. Pope, D. J. Duquette, A. H. Johannes, and P. C. Wayner, 1984. Microbiologically influenced corrosion of industrial alloys, Materials Performance, Vol. 23, No. 4, 14-18.

6. B. C. Syrett. The mechanism of accelerated corrosion of copper-nickel alloys in sulfide-polluted seawater. National Association of Corrosion Engineers Corrosion '80, Paper No. 33, Chicago, Illinois, 1980.

7. J. F. Bates and J. M. Popplewell. Corrosion of condenser tube alloys in sulfide contaminated brine. National Association of Corrosion Engineers Corrosion '74, Paper No. 100, Chicago, Illinois, 1974.

8. J. P. Gridas and H. P. Hack. Sulfide induced corrosion of copper nickel alloys. National Association of Corrosion Engineers Corrosion '77, San Francisco, California, 1977.

9. R. Tanka, 1965. Corrosion of condenser tubes with polluted water (Rep. 6), Mechanism of Corrosion by Sulfide Action. Sumitomo Light Metal Technical Reports, Vol. 6, No. 3.

10. G. G. Geesey, M. W. Mittelman, T. Iwaska, P. R. Griffeths, 1986. Role of bacterial exopolymers in the deterioration of metallic copper surfaces. Materials Performance. 25:37-40.

11. B. J. Little, S. M. Gerchakov, and L. R. Udey, 1987. A method for sterilization of natural seawater. J.M.M. 7:193-200.

12. S. M. Gerchakov, L. R. Udey, and F. Mansfeld, 1981. An improved method for analysis of polarization resistance data. Corrosion 37:696-700.

13. S. M. Gerchakov, B. J. Little, P. Wagner, 1986. Probing microbiologically induced corrosion. 42:689-692.

14. R. W. Morita and G. E. Buck, 1974. Low-Temperature Inhibition of Substrate Uptake. In Effect of the Ocean Environment on Microbial Activities. University Part Press, Baltimore, Maryland, pp. 125-129.

15. R. T. Wright and J. E. Hobbie, 1966. Use of glucose and acetate b bacteria and algae in aquatic ecosystems. Ecology 47:447-464.

16. S. McEdowney and M. Fletcher, 1986. J. of Gen. Micro. 132:513-523.

17. T. D. Brock, Biology of Microorganisms, Prentice-Hall Inc., Englewood Cliffs, New Jersey (1974).

18. H. L. Ehrlich, Manganese as an energy source for bacteria. In: Environmental Biogeochemistry, Ann Arbor Science Publishers Inc., Ann Arbor, Michigan, Vol. 2, pp. 633-644 (1976).

19. H. Hanert, Investigations on isolation physiology and morphology of Gallionella ferruginea, Ehrenberg. Arch. Microbiol. 60:348-376 (1968).

20. E. L. Magee, B. D. Ensley, and L. L. Barton, An assessment of growth yields and energy coupling in Desulfovibrio, Arch. Microbiol. 117:21-26 (1978).

Table 1. Median values of electrochemical parameters evaluated by POLCURR for glutamate media. B_a and B_c are the anodic and cathodic Tafel slopes, respectively. Icorr is the corrosion current and Øcorr is the corrosion potential.

	Sterile Seawater (20 days)	Sterile Seawater w/glutamate (145 days)	Seawater w/glutamate and bacteria (183 days)
B_a (mV/dec)	80	120	50
B_c (mV/dec)	50	100	60
Icorr (A/cm^2)	5	52	3
Øcorr (mV vs SCE)	-280	-266	-286

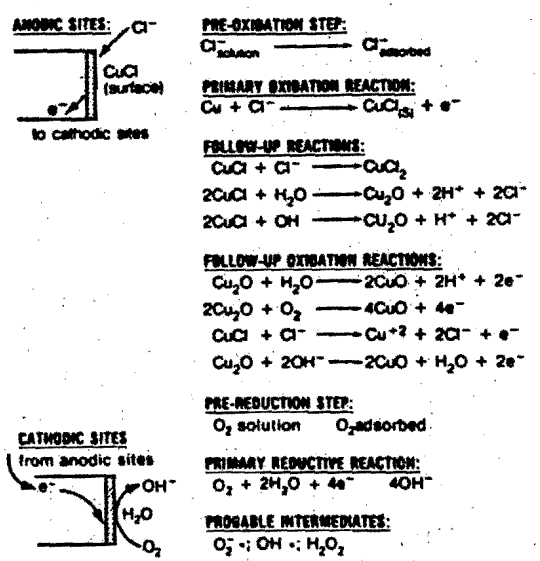

Figure 1. Generalized copper corrosion in saline solution.

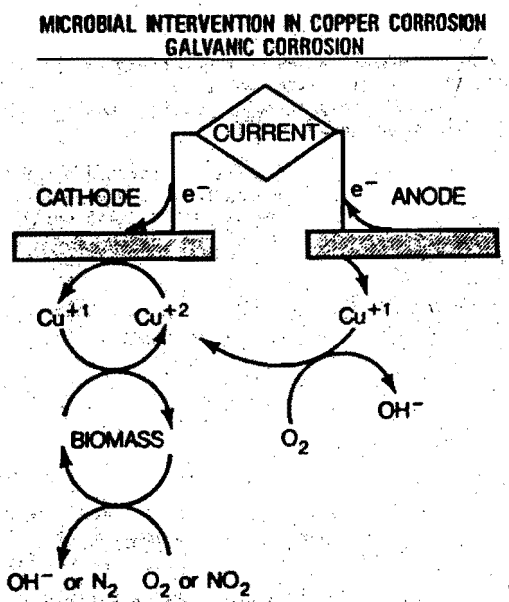

Figure 2. Localized copper corrosion mediated by bacteria.

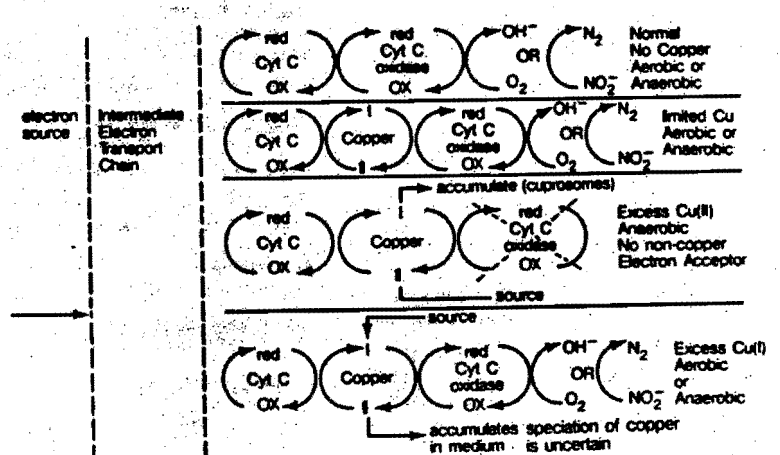

Figure 3. Electron transport chain for oxidation/reduction of copper species by bacteria.